



Università degli Studi di Ferrara

DOTTORATO DI RICERCA IN
SCIENZE DELL'INGEGNERIA

CICLO XXII

COORDINATORE Prof. STEFANO TRILLO

DUROTAXIS MODELLING FOR TISSUE ENGINEERING APPLICATIONS

Settore Scientifico Disciplinare ING/IND 22

Dottorando

Dott. STEFANONI FILIPPO

Tutore

Prof. MOLLICA FRANCESCO

Anni 2007/2009

To Cristina, I Ide and Bruna

"I know that I know nothing"
(Socrates)

PREFACE

This thesis comes from my three years PhD period at the University of Ferrara. I began to be a PhD student on January 2007 and I finished on December 2009. During these years a lot of events took place but now I remember when I was in Aachen for my abroad stage and Dragos, a Romanian PhD student working with me, told me: “When you start your PhD you are like a student, when you finished it, you are like a worker”. I think Dragos was right or at least, this happen to me during my PhD. Three years ago I was still a student trying to study something useful and not only to take an exam. Now I have changed my mind and I see things in a different way.

During these years I studied many subjects and problems on polymeric materials, biomaterials and not only, supervised by Professor (or Engineer as he prefers) Francesco Mollica.

I participated as a student at the following summer schools and lectures:

- **“Nonlinear Computational Solid and Structural Mechanics. Theoretical formulation, FEM technology and computations”**. IMATI-CNR, Università degli studi di Pavia. Pavia, 14-18 Maggio 2007.
- **“14th CIRMIB Biomaterials School”**. Ischia (NA). 9-13 Luglio 2007

I collaborated with the Dental Clinic Section and with the Orthodontic School of the University of Ferrara through Dr. Luca Lombardo and Dr. Nicola Mobilio supervising students in their thesis:

- Francesco Zampini (2007), Facoltà di Medicina e Chirurgia, Corso di Laurea in Odontoiatria e Protesi Dentaria, Tesi di laurea in Ortognatodonzia. **“Valutazione al FEM delle tensioni che si generano attorno ad una minivite ad ancoraggio osseo mono e bicorticale”**. Supervisor: Prof. Giuseppe Siciliani.
- Paolo Contiero (2008), Facoltà di Medicina e Chirurgia, Corso di Laurea in Odontoiatria e Protesi Dentaria, Tesi di laurea. **“Valutazione comparativa**

della distribuzione dei carichi masticatori su impianti in Titanio e Zirconia mediante analisi agli elementi finiti". Supervisor: Prof. Santo Catapano.

- Laura Attorresi (2009), Facoltà di Medicina e Chirurgia, Scuola di Specializzazione in Ortognatodonzia, Tesi di Specializzazione in Ortognatodonzia. **“Distribuzione dello stress sulla superficie radicolare in seguito all’applicazione di forze sul lato vestibolare e linguale”**. Supervisor: Prof. Giuseppe Siciliani.

From this collaboration a paper was published and others are in progress:

“Optimal Palatal Configuration for Miniscrew Applications”. Lombardo L, Gracco A, Zampini F, Stefanoni F, Mollica F. Angle Orthodontist. 2010;80(1):145-152.

I also made some research activity in collaboration with Vortex Hydra S.r.l. on mathematical modelling of plants for concrete roof tiles:

Francesco Mollica, Filippo Stefanoni (2009), Relazione tecnica finale. **“Sviluppo di un modello matematico del processo di estrusione utilizzato da Vortex Hydra per realizzare manufatti in malta cementizia”**.

But I decide to write my thesis only on the main topic I studied, i.e. Tissue Engineering and in particular cell migration. This research was made in collaboration with CRIB (Interdisciplinary Research Centre on Biomaterials, University of Naples “Federico II”) and in particular with Dr. Maurizio Ventre. I do not know why this happened and how cell migration came to me and I also think that it is very strange and new for an Engineer to study such a subject, but this is the so called “interdisciplinary” of Tissue Engineering and in this research field you have to be prepared to everything as my supervisor learn me.

Thus I structured my thesis following my personal path into this new subject. The first chapter is introductory to the general concepts of Tissue Engineering. It is very general, because the field is very broad but it is necessary to outline the rationale behind the subsequent studies. The second chapter is about the physical

phenomenon I dealt with, i.e. cell migration. Here I put notions I studied from papers and books useful for me as a base and to develop new ideas. Then, the last three chapters are on my original work. Also if they are different in methods, they have in common the phenomenon of Durotaxis that is the real subject of this thesis. As better explained inside, this particular condition of cell migration is studied from a mathematical and an experimental point of view in chapters 3 and 4 and a possible applications of the phenomenon was developed in chapter 5.

Some of the material contained here was used for oral presentations and scientific talks in scientific congresses and Universities:

- **“Un Modello Numerico per la Durotassi”**. F Stefanoni, M Ventre, F Mollica, PA Netti. Congresso Nazionale Biomateriali SIB, Follonica (GR),17-19 Settembre 2008.
- **“Durotaxis: Modeling and Experimental Validation”**. F Stefanoni, M Ventre, M Diez, VA Schulte, MC Lensen, F Mollica, PA Netti. 22nd European Conference on Biomaterials, European Society for Biomaterials. Lausanne (CH), 7-11 Settembre 2009.
- **“A Numerical Model for Durotaxis”**. Stefanoni F, Ventre M, Diez M, Schulte VA, Lensen MC , Mollica F, Netti PA. XIX Congresso AIMETA. Ancona, 14-17 Settembre 2009.
- **“Cellular behavior on micro- and nanopatterned hydrogels”**. Diez M, Chen J, Mela P, Schulte VA, Cesa CM, Stefanoni F, Ventre M, Mollica F, Netti PA, Möller M, Lensen MC. ESF-EMBO Symposium: Biological Surfaces and Interfaces. Sant Feliu de Guixols (ESP),27 June-2 July 2009.
- **“Guiding cell migration: a key for tissue engineering”**. Ventre M, Netti PA, Mollica F, Stefanoni F. Scientific Talk at DWI-RWTH, Aachen (D), 24 October 2008.
- **“Studio dei modelli numerici per la determinazione delle proprietà dei tessuti in crescita”**. F Stefanoni, M Ventre. Scientific Talk at CRIB (VIV), Napoli 15 Giugno 2007.

I do not know what will happen to me in the next years and I do not know if I will continue to study these subjects. Anyway, this is the work I have done.

AKNOWLEDGMENTS

First of all I want to thank my supervisor Francesco Mollica. I know I have been his first PhD student so this was a new experience also for him. He was very careful with me and always ready to help me and to discuss concepts and ideas. We have had good and bad experiences working together and I hope that both have learned something from them. Surely I did.

Then thanks to Maurizio Ventre. He introduced me in the world of migrating cells and he was the first “Biological Engineer” I met. He also introduced me in Naples and in the fantastic world of the “Scamorza Affumicata”: I never forgot this experience! I want also to thank him and his mother, for giving me hospitality every time I went to Naples.

I also want to thank Dr. Marga C. Lensen for giving me the possibility to pass a two month period (9 February-7 April 2009) at the DWI-RWTH in Aachen (Germany) to study substrata for my experiments and all the people I met there.

Some words also for people I met at CRIB and during scientific congresses, schools and lectures: Ilaria De Santo, Maria Iannone, Silvia Orsi, Vincenzo Guarino, Edmondo Battista, Maria Grazia Raucci, Antonio Gloria, Ciccio Urciuolo, Tiziana Punzi, Tiziano Serra and Giampiero Pampolini. I really enjoyed those times!

I cannot forget people from the University of Ferrara daily with me: Mirko Morini, Alberto Minotti, Cristian Ferrari, Anna Vaccari, Michele Pinelli and all the people here around.

In the end, I want to thank my friends Carla, Giuseppe and Nicola, my parents Daniele and Cristina, my brother Simone, my grandmothers Ilde and Bruna, Ilaria, Nicola, Ester and Ruben, my aunt Laura, Paolo and Andrea. Every one of them is important for me and for my well-being, so they also contribute to this thesis!

TABLE OF CONTENTS

| | |
|--|----|
| PREFACE | 5 |
| ACKNOWLEDGMENTS..... | 9 |
| TABLE OF CONTENTS..... | 10 |
| ABSTRACT..... | 13 |
| SOMMARIO..... | 3 |
| | |
| CHAPTER 1 – Tissue Engineering | |
| 1. Introduction..... | 18 |
| 2. Methods..... | 21 |
| 3. Cell Culture..... | 23 |
| 4. Scaffolds..... | 29 |
| 5. Bioreactors..... | 33 |
| 6. Applications..... | 34 |
| 7. References..... | 36 |
| | |
| CHAPTER 2 – Cell Migration, Durotaxis and Collagen Deposition | |
| 1. Introduction..... | 39 |
| 2. Cell and Cell Functions..... | 39 |
| 3. Cell Cytoskeleton and Movement..... | 44 |
| 4. The Process of Cell Movement..... | 49 |
| 5. Influencing Factors of Cell Motion..... | 52 |
| 6. Durotaxis..... | 54 |
| 7. Cell Migration and Collagen Deposition..... | 56 |
| 8. References..... | 58 |
| | |
| CHAPTER 3 – A Computational Model for Durotaxis | |
| 1. Introduction..... | 62 |
| 2. The Langevin Equation in the Modelling of Cell Migration..... | 63 |
| 3. A Discrete Model for Durotaxis..... | 66 |
| 4. Two Particular Cases for Preliminary Validation..... | 70 |
| 5. Discussion..... | 75 |

| | |
|--------------------|----|
| 6. References..... | 77 |
|--------------------|----|

CHAPTER 4 – Experimental Validation of the Model

| | |
|--|----|
| 1. Introduction..... | 81 |
| 2. Preparation of the Samples..... | 81 |
| 3. Cell Migration Experiments over Biphasic Substrata..... | 84 |
| 4. Experimental Results..... | 85 |
| 5. Comparison with the Model..... | 87 |
| 6. Results and Conclusions..... | 89 |
| 7. References..... | 89 |

CHAPTER 5 - Study and Design of a Durotaxis-based Substratum

| | |
|---|-----|
| 1. Introduction..... | 92 |
| 2. Polyethylene glycol (PEG)..... | 92 |
| 3. Preparation of the Materials..... | 93 |
| 4. Cell Migration Experiments..... | 95 |
| 5. Results and Remarks..... | 96 |
| 6. The “Pattern of Elasticity” Substrata..... | 102 |
| 7. Preliminary Cell Adhesion Experiments..... | 107 |
| 8. Conclusions..... | 109 |
| 9. References..... | 109 |

| | |
|--------------------------------|-----|
| APPENDIX (Matlab scripts)..... | 112 |
|--------------------------------|-----|

ABSTRACT

Tissue Engineering is a very promising research field for the development of natural biological substitutes that restore damaged tissue functions. Cells play a crucial role in tissue regeneration and repair due to their characteristics of proliferation and differentiation, cell-to-cell interaction, biomolecular production and extracellular matrix formation. In particular cell migration is a phenomenon that is involved in different physiological processes such as morphogenesis, wound healing and new tissue deposition. In the absence of external guiding factors it is essentially a phenomenon that shares quite a few analogies with Brownian motion. The presence of biochemical or biophysical cues, on the other hand, can influence cell migration in terms of speed, direction and persistence, transforming it in a biased random movement. Recent studies have shown that cells, in particular fibroblasts, are able to recognize the mechanical properties of a substratum over which they move and that these properties direct the motion through a phenomenon called durotaxis. The aim of this thesis is to study this phenomenon for a better understanding of cell behaviour in durotaxis conditions and for Tissue Engineering applications. In order to do that, in the first part of the work a mathematical model for the description of durotaxis is presented. The model is based on a stochastic differential equation for the cell velocity which is derived from the Langevin equation: cell movement is affected by two forces, namely a deterministic one representing the dissipative effects of the system, and a stochastic one which is due to all the probabilistic processes that might affect cell motility (random fluctuations in motile sensing, response mechanisms, etc.). The original contribution of this work concerns the stochastic force, which has been modified to account for the directions of highest perceived local stiffness through a finite element scheme that reminds the cellular probing mechanism. Numerical simulations of the model provide individual cell tracks that can be qualitatively compared with experimental observations. The present model is solved for two important cases that are reported in literature and a comparison with experimental data obtained on PDMS substrata is presented. The degree of agreement is satisfactory thus the model could be utilized to quantify relevant parameters of cell migration as a function of substratum mechanical properties.

The second part of the work is concerned on the study and development of a durotaxis-based substratum, able to guide cells in their migration and in particular, able to guide cells along straight path. It was proved, in fact, that a relation exist between the alignment of collagen produced by fibroblasts or others tissue cells and their migration. Thus, the idea is to obtain an aligned tissue made of new collagen, giving to the cells the conditions to move along straight-lines through the mechanical properties of the substratum. To realize this substratum Polyethylenglycole (PEG) was used. First, smooth PEG was synthesized and cell migration experiments was performed over it to better understand its response. Then a specific technique was developed to produce durotaxis-based PEG substrata, and preliminary experiments of cell adhesion over it were performed showing aligned adhesion of cells over them.

SOMMARIO

L'Ingegneria dei Tessuti è un campo di ricerca molto promettente che si occupa dello sviluppo di sostituti biologici naturali che possono riparare tessuti danneggiati o non più in grado di svolgere le loro funzioni. Le cellule svolgono un ruolo cruciale in questo campo, per la loro capacità di proliferare e differenziare, per la loro interazione reciproca e per la loro capacità di produrre biomolecole e matrice extracellulare. In particolare, la migrazione delle cellule è un fenomeno importante in diversi processi fisiologici tra cui la morfogenesi, la cicatrizzazione e la deposizione di nuovo tessuto. In assenza di fattori esterni, si tratta di un fenomeno simile al moto Browniano di particelle. D'altro canto, la presenza di fattori biochimici o biofisici può avere un'influenza sul moto cellulare in termini di velocità, direzione e persistenza, rendendolo meno casuale. Studi recenti hanno dimostrato che le cellule e in particolare i fibroblasti, sono in grado di riconoscere le proprietà meccaniche di un substrato sopra il quale si muovono: queste sono quindi in grado di modificare il moto cellulare secondo un fenomeno chiamato durotassi.

Lo scopo di questa tesi è di studiare tale fenomeno, per meglio capire il comportamento delle cellule in queste condizioni e per possibili applicazioni in Ingegneria dei Tessuti. Per far ciò, nella prima parte del lavoro è stato sviluppato un modello matematico per la descrizione della durotassi. Il modello è basato su un'equazione differenziale stocastica per la velocità, derivante dall'equazione di Langevin: il movimento cellulare è influenzato da due forze, una deterministica che rappresenta gli effetti dissipativi del sistema, l'altra stocastica, dovuta a tutti i fattori probabilistici che possono avere un effetto sul moto (fluttuazioni casuali nel meccanismo di percezione dei segnali, nel meccanismo di risposta, etc.). Il contributo originale del lavoro riguarda il termine stocastico, che è stato modificato in modo da considerare la direzione di maggior rigidità percepita dalla cellula tramite un algoritmo agli elementi finiti. Le simulazioni numeriche del modello forniscono le singole traiettorie cellulari che possono quindi essere comparate direttamente con le osservazioni sperimentali. Il modello viene risolto in due casi noti da letteratura e viene riportato un confronto con dati sperimentali ottenuti su substrati di PDMS. Il grado di accordo risulta essere buono e quindi il modello può essere usato per

quantificare alcuni parametri del moto cellulare in base alla proprietà meccaniche del substrato.

La seconda parte del lavoro riguarda invece lo studio e lo sviluppo di un substrato che, grazie al fenomeno della durotassi, sia in grado di guidare le cellule lungo traiettorie rettilinee. E' stato infatti provato che esiste una relazione tra l'allineamento del collagene prodotto da fibroblasti e altre cellule del tessuto connettivo, e il loro moto. L'idea è quindi quella di ottenere, grazie ai substrati, nuovo tessuto collageneo allineato. Per realizzare ciò è stato utilizzato Polietilenglicole (PEG). Per prima cosa sono stati fatti esperimenti preliminari di migrazione su PEG liscio, per testarne la risposta. Dopodichè è stata sviluppata una nuova tecnica per produrre substrati di PEG in grado di guidare le cellule tramite durotassi. Esperimenti preliminari di adesione cellulare sono stati eseguiti mostrando un buon grado di allineamento delle cellule.

CHAPTER 1

Tissue Engineering

1. Introduction

One of the most famous definitions of Tissue Engineering (TE in the remainder) was given by Professor Robert Langer and Professor Joseph P. Vacanti in their article published on “Science” in 1993:

“Tissue Engineering is an interdisciplinary field that applies the principles of engineering and the life sciences toward the development of biological substitutes that restore, maintain, or improve tissue function.”

As an engineer-PhD student trying to study phenomena related to TE, I can say that the most important word in this statement is “interdisciplinary”. When you heard about this term just by someone else or during your lectures at University, you can not imagine its real meaning. But when you start your practical research in TE and when you keep contact with other researchers studying analogous phenomena, you feel the effect of this apparently abstract term in creating curiosity inside you, opening your mind to other points of view and expanding your knowledge. Nevertheless the other side of the coin is that you need time to understand concepts far from your background and you need to be psychologically prepared to study problems in which you can not deeply understand all the aspects.

So if you survive and if you are able to appreciate the positive aspects, TE is a very exciting research field that includes a great variety of phenomena that have as the main subject biological tissues.

TE represents the confluence of different lines of work from three quite different fields: clinical medicine, engineering and life science. The most obvious precursors to TE lie in the clinical domain. In fact, thinking of a surgeon, one of his frequent problems is about the removal of organs or of body structures. Sometimes this removal can be life-saving but the patient must cope with the functional effects of

tissue loss and in some cases, with the psychological impacts of disfigurements. And for those vital organs whose complete removal is incompatible with life he needs some way of replacing or reconstituting essential functions.

To solve these problems surgeons have adopted different strategies. They have sought to reconstruct anatomic structures using the patient's own tissues as raw material; they have pressed artificial materials into service as prostheses; and, most spectacularly, they have brought patients back from the brink of death by transplanting an ever-wider range of vital organs, primarily living organs, but in a few cases, with only very limited success to date, prototype artificial organs as well.

However, with experience, surgeons have come to understand in detail not only the benefits of such measures, but their limitations as well. Anatomic reconstruction using the patient's own tissue can cause substantial morbidity at the donor site; the improvised structures are usually functionally inferior to the natural organs they replace and less durable as well. Poor compatibility between artificial materials and mechanical systems and the internal environment and physiologic requirements of the human body can lead to dysfunctional interactions and new failure modes. Transplantation of living organs brings with it profound immunologic complications and the number of patient who can be treated in this way will always be severely constrained by the limited supply of organ suitable for use.

For a surgeon, then, the development of engineered tissues is a logical next step in the ongoing effort to improve the match between its various reparative and reconstructive contrivances and the requirements of human anatomy and physiology. So the clinical perspective on TE is strongly applications-oriented but viewed the other way around, in terms of enabling knowledge and technologies, TE is remarkable for the breadth of its footprint in fundamental and applied biomedical research.

In Table 1 is possible to see some fields and subfields involved in TE, just to have an idea of its interdisciplinary body and of the range, depth and character of the inputs to the field.

Cell and Developmental Biology

Cell differentiation, morphogenesis and tissue assembly

Cell-cell and cell-matrix interactions

Growth factors

| |
|--|
| Cell isolation and selection |
| Cell culture |
| Angiogenesis |
| Stem cells |
| Basic Medical and Veterinary Sciences |
| Anatomy |
| Cytology |
| Physiology and patho-physiology |
| Transplantation Science |
| Applied immunology, immunosuppression immunomodulation and immunoisolation |
| Organ preservation |
| Biomaterials |
| Natural and synthetic, biodegradable and non-biodegradable polymers |
| Polymer chemistry |
| Ceramics |
| Cell interactions with biomaterials |
| Controlled release of bioactive molecules |
| Microencapsulation |
| Microfabrication techniques |
| 3D fabrication techniques |
| Surface chemistry |
| Biophysics and Biomechanics |
| Molecular and cell transport |
| Micro- and macrocirculatory dynamics |
| Cells and tissue mechanics |
| Biomedical Engineering |
| Bioreactors |
| Membranes and filtration |
| Musculoskeletal joint engineering |
| Biomedical sensors |
| Biomedical signal processing, feedback and control |
| Electrical and mechanical engineering of biohybrid systems |
| Engineering design and system analysis |
| Quantitative tissue characterization |
| Biosensors and bioelectronics |

Table 1: Research field and subfields that have contributed to TE (National Science Foundation, 2003)

It is unclear who first used the term “Tissue Engineering” to mean what it does today. Realistically it was invented several times independently before it became of usage, but its origin can be clearly traced to a specific individual. In 1985, Y.C. Fung, a pioneer in the field of biomechanics and of bioengineering more broadly, submitted a proposal to National Science Foundation, for an Engineering Research Centre to be entitled “Centre for the Engineering of Living Tissues”. Fung’s concept drew on the traditional definition of tissue as a fundamental level of analysis of living organism,

between cell and organs. The proposal was not accepted, but the concept was born, so in the following years it took its shape, reaching the definition reported above of Langer and Vacanti.

2. Methods

Tissue Engineering is a broad term describing a set of tools at the interface of the biomedical and engineering sciences that uses living cells or attract endogenous cells to aid tissue formation or regeneration, and thereby produce therapeutic or diagnostic benefit. More practically, the most frequent procedure lies in seeding cells on a retaining structure composed of synthetic polymers or natural materials; then a tissue is matured *in vitro* in a bioreactor and the construct is thus implanted in the appropriate anatomic location as a prosthesis.

The retaining structure on which cells are seeded is called “scaffold”, a generic term indicating an artificial structure made, for example, of a bioresorbable polymer in a porous configuration or, of natural material such as collagen or chemically treated tissue: a scaffold is a sort of house for cells before the implantation, that furnishes them all the necessary conditions for spreading, proliferating and then for the generation of new tissue. A bioreactor is a device or a system that supports a biologically active environment, in which cells can proliferate and elaborate extracellular matrix (ECM). After the *in vitro* growth, the construct is implanted in the appropriate anatomic location, where *in vivo* remodelling is intended to recapitulate the normal functional architecture of an organ or tissue (Fig. 1).

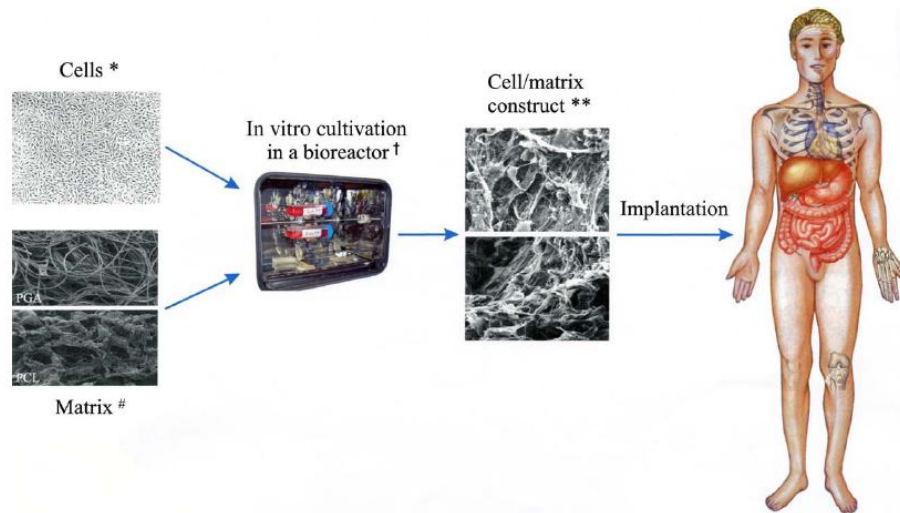


Fig. 1: Tissue engineering process: Cells, Matrix, Bioreactor and Cell/matrix construct (Shieh and Vacanti, 2005).

The key processes occurring during the in vitro and in vivo phases of tissue formation and maturation are:

- Cell proliferation, sorting and differentiation;
- Extracellular matrix production and organization;
- Degradation of the scaffold;
- Remodelling and potentially growth of the tissue.

The illustrated procedure is comprehensive of all the feasible operations, but sometimes incomplete procedures are adopted for example implanting directly the scaffold in the host without using of the bioreactor or using a scaffold that recruits endogenous cells directly inside the patient.

In any case, the three principal components of TE are cells, scaffold and bioreactor and all the parameters related to them have an impact upon the ultimate result. In Table 2 a series of these parameters are reported as factors that can be taken into account in a TE process.

| Cells | Biodegradable matrix/Scaffold |
|---------------|--|
| <i>Source</i> | <i>Architecture/Porosity/Chemistry</i> |
| | Composition/Charge |
| Allogenic | Homogeneity/Isotropy |
| Xenogenic | Stability/Resorption rate |
| Autologous | |

| | |
|---|-------------------------------|
| <i>Type/Phenotype</i> | Bioactive molecules/Ligands |
| Single versus multiple types | Soluble Factors |
| Differentiated cells from primary or other tissue | <i>Mechanical Properties</i> |
| Adult bone marrow stem cells | Strength |
| Pluripotent embryonic stem cells | Compliance |
| Density | Ease of manufacture |
| Viability | Bioreactor Conditions |
| Gene expression | <i>Nutrients/Oxygen</i> |
| Genetic manipulation | Growth Factors |
| | Perfusion and flow conditions |
| | <i>Mechanical Factors</i> |
| | Pulsatile |
| | Hemodynamic shear stresses |
| | Tension/Compression |

Table 2: Parameters involved in TE (Biomaterials Science, 2004)

3. Cell Culture

Cells play a crucial role to tissue regeneration and repair due to their characteristics of proliferation and differentiation, cell-to-cell interaction, biomolecular production, and extracellular matrix formation (details about cell functions are reported in chapter 2 of this thesis). As shown in Table 2, the sources of cells used in TE can be autologous, i.e. from the host, allogeneic, i.e. from another individual of the same species, or xenogeneic, i.e. from another individual of another species. Ideal donor cells for TE would be those that are easily accessible, that can easily expand without permanently altering the phenotype (i.e. all the observable properties of an organism, that are produced by the interaction of its genetic constitution, the genotype, and the environment) and function and without transmitting species-specific pathogens (agents producing a disease, e.g., virus or bacterium) that are multipotent to differentiate or transdifferentiate into a variety of tissue- or organ-specific cells with specialized function, and that have the least immunologic response.

Some cells, such as keratinocytes, fibroblasts, chondrocytes, endothelial cells, smooth muscle cells or skeletal muscle satellite cells, proliferate rapidly. They are good tissue-specific cell sources for TE. Two Food and Drug Administration (FDA)-approved living skin products engineered in the laboratory have been applied to a patient with diabetic or venous skin ulcers, and a FDA-approved autologous cell

product also has been used to repair an articular cartilage. However, other cells, such as hepatocytes or adult cardiomyocytes, proliferate slowly or not at all. Therefore, alternative sources of cells are needed.

Recent advances in stem cell biology have had a marked impact on the progress of TE. Stem cells, which are capable of self-renewal and differentiation into various cell lineages, hold great promise for treating affected tissue in which the source of cells for repair is limited or not readily accessible. Cells derived from human embryonic blastocysts (a structure formed in the early embryogenesis of mammals), after undifferentiated proliferation in vitro for 4-5 months, still maintain the developmental potential to form trophoblast (cells forming the outer layer of the blastocyst) and derivatives of all three embryonic germ layers including gut epithelium (endoderm), cartilage, bone, smooth muscle, and striated muscle (mesoderm), and neural epithelium, embryonic ganglia, and stratified squamous epithelium (ectoderm). Although these cell lines should be useful in human regenerative medicine, the ethical and legal issues are still under debate.

Adult bone marrow stem cells can replicate as undifferentiated cells that have the potential to differentiate into lineages of mesenchymal tissue, including bone, cartilage, fat, tendon, muscle and marrow stroma. They display a stable phenotype, remain as a monolayer in vitro, and could be induced to differentiate exclusively into adipocytic, chondrocytic, or osteocytic lineages. To date, the isolation of various autologous adult stem cells, including mesenchymal, hematopoietic, neural, muscle, and hepatic stem cells, are being investigated actively, because they are immunocompatible and have no ethical concerns. Nevertheless, there are a number of technical obstacles, such as how to isolate stem cell preparations without contamination by other cells, how to control the permanent differentiation to the desired cell types, and how to increase the production of the large number of cell needed to create tissue.

Other strategies aim at optimizing cells for TE and are focused on the host-immune response to allogenic or xenogenic cell. Starting from this point, researchers are trying to create “universal donor cells” by masking histocompatibility proteins on the cell surface to reduce the cell’s antigenicity (Shieh and Vacanti, 2005).]

The more recent research in this field is about nuclear transfer, or “therapeutic cloning”: it is a process wherein the nucleus of a somatic cell is injected into an

unfertilized enucleated oocyte. This transformation probably involves deletion of the existing epigenetic state (the actual expression of the genes of an organism) and expression. Through this nuclear manipulation any differentiated somatic cell can potentially be reprogrammed back to totipotency, which results in redifferentiation to the full repertoire of adult cells for any individual tissue repair. Although the goal of therapeutic cloning is to generate replacement cells and tissue that are genetically identical to those of the donor, non-self-mitochondria proteins derived from the recipient oocytes could render cloned tissue immunogenetic. All these findings bring closer the promise of therapeutic cloning and TE. The combination of nuclear transfer, gene therapy and cell transplantation as a possible applicable paradigm for genetic and phenotypic correction is a challenge to many active scientist worldwide. Regardless of the types of strategy, cells for TE practically come from cell culture. In fact, animal or plants cells, removed from tissues, will continue to grow if supplied with the appropriate nutrients and conditions and when carried out in laboratory, the process is called cell culture. This allows single cells to act as independent units, much like a microorganism such as a bacterium or fungus. Cells are capable of dividing, increase in size and, in a batch culture, they can continue to grow until limited by some culture variable such as nutrient depletion.

Cells can be isolated from tissue for *ex vivo* culture in several ways. They can be easily purified from blood, however only the white cells are capable of growth in culture. Mononuclear cells can be released from soft tissue by enzymatic digestion with enzymes such as collagenase, trypsin or pronase, which break down the ECM. Alternatively pieces of tissue can be placed in growth media and cells that grow out are available for culture.

Cultures normally contain cells of one type although mixed cultures, especially of bacteria, are common in food sciences and wastewater treatment studies. The cells in culture may be genetically identical (homogeneous population) or may show some genetic variations (heterogeneous population). A homogeneous population of cells derived from a single parental cell is called a "clone". Therefore all cells within a clonal population are genetically identical.

Cells that are cultured directly from a subject are known as primary cells. With the exception of some derived from tumours, most primary cell cultures have limited lifespan. After a certain number of population doublings cells undergo the process of

senescence and stop dividing, while generally retaining viability. After several sub-cultures onto fresh media, the cell line will either die out or transform to become a continuous cell line. Such cell lines show many alterations from the primary cultures including change in morphology, chromosomal variation and increase in capacity to give rise to tumours in host with weak immune systems. An established or immortalised cell line has acquired the ability to proliferate indefinitely either through random mutation or deliberate modification. There are numerous well-established cell lines representative of particular cell types and the major repositories are the American Type Culture Collection (ATCC) and the European Collection of Cell Cultures (ECACC). Some examples of immortalised lines are reported in Table 3. Cells are grown and maintained at an appropriate temperature and gas mixture, typically 37°C and 5% CO₂ for mammalian cells, in a cell incubator (Fig. 2).



Fig. 2: Cell incubator at CRIB (Interdisciplinary Research Centre on Biomaterials, University of Naples "Federico II")

Culture conditions vary widely for each cell type and variation of conditions for a particular cell type can result in different phenotypes being expressed. Aside from temperature and gas mixture, the most commonly varied factor in culture system is the growth medium. Recipes for growth media can vary in pH, glucose concentration, growth factors and the presence of other nutrients. The growth factors used to supplement media are often derived from animal blood such as calf serum.

Animal cell can be grown either in an unattached suspension culture or attached to a solid surface. Some cells naturally live in suspension, without being attached to a

surface, e.g. the cells of the bloodstream. There are also cell lines that have been modified to be able to survive in suspension cultures so that they can be grown to a higher density than adherent conditions would allow. Adherent cells require a surface such as tissue culture plastic, which may be coated with ECM components to increase adhesion properties and provide other signals needed for growth and differentiation. Most cells derived from solid tissue are adherent. Another type of adherent culture is organotypic culture which involves growing cells in a three dimensional environment as opposed to two dimensional culture dishes. This three dimensional culture system is biochemically and physiologically more similar to *in vivo* tissue, but is technically challenging to maintain because of many factors such as diffusion. As cells generally continue to divide in culture, they generally grow to fill the available area or volume. This can generate nutrient depletion in the growth media and accumulation of apoptotic or necrotic cells. Further cell-cell contact can stimulate cell life-cycle arrest, causing cell to stop dividing (contact inhibition or senescence) or cellular differentiation.

Among the common manipulations carried out on culture cells are media changes (directly by aspiration in adherent cultures), passaging cells (i.e. transferring a small number of cells into a new vessel to allow the culture for a longer time, using trypsin-ethylenediaminetetraacetic acid to detached the adherent cells) and transfecting cells (i.e. the introduction of foreign DNA by transfection). These are generally performed using tissue culture methods that rely on sterile technique. This technique aims to avoid contamination with bacteria, yeast or other cell lines. Manipulations are typically carried out in a biosafety hood or laminar flow cabinet to exclude contaminating micro organism (Fig. 3)



Fig. 3: Laminar flow cabinet at CRIB (Interdisciplinary Research Centre on Biomaterials, University of Naples “Federico II”)

There are a number of applications for animal cell cultures besides TE. They are utilized to investigate the normal physiology or biochemistry of cells (studies of cell metabolism), to test the effect of various chemical compounds or drugs on specific cell types (normal or cancerous cell type) or to synthesize valuable biologicals (specific proteins or viruses) from large scale cell cultures. The advantage of using cell culture for any of these applications is the consistency and reproducibility of results that can be obtained from using a batch of clonal cells. The main disadvantage is that, after a period of continuous growth, cell characteristics can change and may become quite different from those found in the starting population. Cells can also adapt to different culture environments (e.g. different nutrients, temperatures, salt concentrations, etc.) by varying the activities of their enzymes.

| Cell Line | Name Meaning | Species | Tissue | Morphology |
|-----------|--|---------|---------------------|------------------|
| 293-T | | Human | Embryonic Kidney | |
| NIH 3T3 | 3-Day Transfer, Inoculum-3 x 10 ⁵ cells | Mouse | Embryo | Fibroblasts |
| NIH L929 | | Mouse | | Fibroblasts |
| ALC | | Murine | Bone Marrow | Stroma cells |
| HCA2 | | Human | | Fibroblast |
| HEK-293 | Human Embryonic | Human | Embryonic Kidney | Epithelial Cells |

| | | | | |
|-----------------|--|----------------------------|------------------------------|--|
| HeLa | Kidney Henrietta Lacks | Human | Cervical Cancer | Epithelial Cells |
| HL-60 | Human Leukaemia | Human | Myeloblast | Blood Cells |
| HMEC | Human Mammary Epithelial Cells | Human | | Epithelial Cells |
| HUVEC | Human Umbilical Vein Endothelial Cells | Human | Umbilical Cord Vein | Endothelial Cells |
| MCF-7 | Michigan Cancer Foundation-7 | Human | Mammary Gland | Invasive Breast Ductal Carcinoma |
| MC3T3-E1 | | Mouse | | Osteoblast |
| MDCK II | Madin Darby Canine Kidney | Dog | Kidney | Epithelial Cells |
| MyEnd | Myocardial Endothelial | Mouse | | Endothelial Cells |
| RenCa | Renal Carcinoma | Mouse | | Renal Carcinoma Cells |
| T2 | | Human | | T Cell Leukaemia/B Cell Line Hybridoma |
| U373 | | Human | Glioblastoma- Astrocytoma | Epithelial Cells |
| Vero Cells | | African Green Monkey | Kidney | Epithelial Cells |
| WM39 | | Human | Skin | Primary Melanoma Cells |
| DU-145 | | Human | Prostate Cancer | Prostate Cancer Cells |
| A2780ADR | | Human | Ovary | Epithelial Cells |
| Hepa1c1c7 | Clone 7 of Clone 1 Hepatoma Line 1 | Mouse | Hepatoma | Epithelial Cells |
| NCI- H69/CPR | | Human | Lung | Lung Carcinoma Cells |

Table 3: Some examples of immortalised cell lines

4. Scaffolds

In the first phase of the production of an engineered tissue, the cultured, stem or cloned cells are seeded onto a scaffold. The rationale behind the use of such a system is based on empirical observations: dissociated cells tend to reform their original structures when given the appropriate environmental conditions in cell

culture. For example, capillary endothelial cells form tubular structures and mammary epithelial cells form acini that secrete milk on the proper substrata *in vitro* (Folkman and Haudenschild, 1980). Although isolated cells have the capacity to reform their respective tissue structure, they do so only to a limited degree since they have no intrinsic tissue organization and are hindered by the lack of template to guide restructuring. Then, most organ cell types are anchorage-dependent and require the presence of a suitable substratum in order to survive and retain their ability to proliferate, migrate and differentiate. Moreover, tissue cannot be transplanted in large volumes because diffusion limitations restrict the interaction with the host environment for nutrients, gas exchange, and elimination of waste products. Therefore, the implanted cells will survive poorly more than a few hundred μm from the nearest capillary or other source of nourishment. From these observations comes the approach to regenerate tissue by attaching isolated cells to biomaterials that serve as a guiding structure for initial tissue development.

Cell morphology on scaffold correlates with cellular activities and functions: strong cell adhesion and spreading often favours proliferation while rounded cell shape is required for cell-specific function. For example it has been demonstrated that the use of substrata with patterned surfaces morphologies or varied ECM surface coatings can modulate cell shape and function (Chen *et al.*, 1998; Mooney *et al.*, 1992, Singhvi *et al.*, 1994). Also gene expression in cells is regulated differently by bi-dimensional versus three-dimensional scaffolds (Aulthouse *et al.*, 1989).

Early works in TE demonstrated that bovine chondrocytes seeded onto a synthetic biodegradable scaffolding could produce neo-cartilage after transplantation into athymic mice. Cartilage can be created in predetermined shapes and dimensions by using cell transplantation on appropriate polymer templates even in a complex three dimensional architecture like a human ear (Shieh *et al.*, 2004). The delicate three dimensional polymer scaffolds of high porosity and surface are crucial to structural TE such as bone and cartilage (Shieh and Vacanti, 2005).

Thus scaffolds are designed to guide cell organization and growth allowing diffusion of nutrients to them. In general, the ideal scaffold should be three dimensional, highly porous with an interconnected pore network, biocompatible and bioresorbable with a controlled degradation rate; it should have an appropriate surface for cell adhesion, proliferation and differentiation and it should maintain proper mechanical properties.

It can be produced from natural material (collagen, fibrin, alginate, hydroxyapatite) or synthetic polymers (see Table 4). Natural materials may closely mimic the native cellular environment, whereas synthetic polymers have the advantages of being able to better control material properties. Synthetic bioresorbable polymers that are fully degradable into the body's natural metabolites by simple hydrolysis under physiological conditions are the most attractive scaffold materials. These synthetic polymers must possess unique properties specific to the tissue of interest as well as satisfy some basic requirements in order to serve as an appropriate scaffold.

Development of biomaterials poses significant challenge for TE scaffolds. The goal of early or first-generation biomedical materials, during the 1960s and 1970s, was to attain suitable physical properties to match the replaced tissue with a common feature of biological inertness. Second generation biomaterials were designed to produce bioactive responses that could elicit a controlled reaction in the physiologic environment. Such bioactive (ceramic, hydroxyapatite) or resorbable (polyglycolide, polyactide) materials have been applied in the medical needs of many fields successfully. Third-generation biomaterials are combining these two properties and are being designed to stimulate specific cellular responses at the molecular level. In fact several synthetic bioresorbable polymers are activated by either cells or genes and are designed to improve the complicated biological event of tissue repair. Incorporation of a signal peptide such as RGD (a small sequence of amino-acids, Arg-Gly-Asp) into the biomaterial has attempted to mimic the ECM, modulate cell adhesion and induce cell migration. An intermediate density of adhesive ligands is crucial for optimal cell migration. With recent advances in nanotechnology, nanoscale clustering of RGD peptides at surfaces using comb polymer is more effective for inducing cell adhesion and migration.

| Materials | Applications |
|---|---|
| Poly(α -hydroxy esters) | |
| Poly(L-lactic acid), PLLA | Bone, cartilage, nerve |
| Poly(glycolic acid), PGA | Cartilage, tendon, urothelium, intestine, liver, bone |
| Poly(D,L-lactic-co-glycolic acid), PLGA | Bone, cartilage, urothelium, nerve, RPE |
| PLLA-bonded PLGA fibres | Smooth muscle |
| PLLA coated with collagen or poly(vinyl alcohol), PVA | Liver |

| | |
|---|--------------------------------|
| PLLA and poly(ethylene glycol), PEG, block copolymer | Bone |
| PLGA and PEG blends | Soft tissue and tubular tissue |
| Poly(L-lactic acid-co- ϵ -caprolactone), PLLACL | Meniscal tissue, nerve |
| Poly(D,L-lactic acid-co- ϵ -caprolactone), PDLLACL | Vascular graft |
| Polyurethane/poly(L-lactic acid) | Small-calibre arteries |
| Poly(lysine-co-lactic acid) | Bone, cartilage, nerve |
| Poly(propylene fumarate), PPF | Bone |
| Poly(propylene fumarate-co-ethylene glycol), P(PF-co-EG) | Cardiovascular, bone |
| PPF/ β -tricalcium phosphate (PPF/ β -TCP) | Bone |
| Poly(ϵ -caprolactone) | Drug delivery |
| Polyhydroxyalkalonnate (PHA) | Cardiovascular |
| Polydioxanone | Bone |
| Polyphosphates and polyphosphazenes | Skeletal tissue, nerve |
| Pseudo-poly(amino-acids) | Bone |
| Tyrosine-derived polyiminocarbonates | |
| Tyrosine-derived polycarbonate | |
| Tyrosine-derived polyacrilates | |

Table 4: Scaffold materials and their applications (Biomaterials Science, 2004)

The techniques used to manufacture synthetic bioresorbable polymers into suitable scaffold depends on the properties of the polymer and its intended application as it is possible to see in Table 5. Scaffold processing usually involves heating the polymers above their glass transition or melting temperature, dissolving them in organic solvents and incorporating and leaching of porogens (gelatine microsphere, salt crystal, etc.) in water. The processes usually result in a decrease in molecular weight and have profound effects on biocompatibility, mechanical properties and other characteristics of the formed scaffold. Incorporation of large bioactive molecules such as proteins into the scaffolds and retention of their activity have been a major challenge.

| Processing technique | Examples |
|--|---------------------------------------|
| Fibre bonding | PGA fibres, PLA-reinforced PGA fibres |
| Solvent casting and particulate leaching | PLA, PLGA, PPF foams |
| Superstructure engineering | PLA, PLGA membranes |
| Compression molding | PLA, PLGA foams |
| Extrusion | PLA, PLGA conduits |
| Freeze-drying | PLGA foams |
| Phase separation | PLA foams |
| High-pressure gas foaming | PLGA, P(PF-co-EG) scaffolds |

Table 5: Examples of Scaffolds Processed by Various Techniques (Biomaterials Science)

In any case, the design requirements of a tissue engineering scaffold are specific to the structure and function of the tissue to be regenerated.

5. Bioreactors

The third component of TE is the bioreactor. The *in vitro* cultivation of 3D-constructs in the bioreactor that supports efficient nutrition of cells, possibly combined with the application of mechanical stimulation to direct cellular activity, differentiation and function, is an important step towards the development of functional grafts. Furthermore, the bioreactor provides a more well-defined culture condition than *in vivo* tissue regeneration, thus it is useful for systematic, controlled studies of cellular differentiation and tissue development in response to biochemical and mechanical cues. Today, a wide variety of bioreactor types, such as spinner flasks, perfusion systems, rotating wall vessel (RWV) or pulsatile flow reactor (Chen and Hu, 2006), have been developed for TE of tissues such vocal fold (Titze *et al.*, 2005), retina (Dutt *et al.*, 2003) and several others that include skin, muscle, ligament, tendon, bone, cartilage and liver.

Ideally, a TE bioreactor should enable robust control of environmental factors (e.g. pH, O₂, temperature, nutrient transfer and waste removal) at defined levels and also allow for aseptic operation (e.g. sampling and feeding) and automated processing steps. These attributes are pivotal not only for controlled, reproducible investigations but also for routine manufacturing of tissues for clinical applications.

Among these parameters, diffusion limitations of mass transport have severely curtailed efforts to engineer tissues that normally have high vascularity and cellularity. In particular, the O₂ level is critical in the production of ECM components in the context of cartilage engineering despite controversy concerning whether high or low oxygen concentration is more beneficial. It is well-established that mechanical forces improve or accelerate tissue regeneration *in vitro*. Fluid dynamics originated stress, induced by the fluid flowing across the construct surface and into the porous space, is believed to be the most important mechanical stimulus in activating the

mechanotransduction signalling. Consequently, fluid flow-induced shear stress is frequently used as a mechanical stimulus. Additionally, specific criteria for different tissues must be met. For example, pulsatile radial stress of tubular scaffolds seeded with smooth muscle cells improves structural organization of the engineered blood vessels, and enables the vessels to remain open for four weeks following in vivo grafting (Niklason *et al.*, 1999). The engineered artificial arteries require cyclic stretching/distension of constructs which enhances the proliferation and matrix organization by human heart cells. The cyclic stretch also increases tissue organization and expression of elastin by smooth muscle cells and improves the mechanical properties of tissues generated by skeletal muscle cells (Powell *et al.* 2002). Dynamic deformational loading or shear of chondrocytes embedded in a three-dimensional environment stimulates glycosaminoglycan (GAG) synthesis and enhances the mechanical properties of the resultant engineered cartilage. Translational and rotational strain of mesenchymal progenitor cells embedded in a collagen gel induces cell alignment, formation of orientated collagen fibres, and upregulation of ligament specific genes. Mechanical compression and cyclic hydrostatic fluid pressure are important regulators of cell physiology (e.g. alters gene expression and ECM synthesis) and can facilitate tissue formation, particularly in the context of musculoskeletal TE. Thus, specific mechanical loading conferred by the bioreactor might not only enhance the development of an engineered tissue but also direct the differentiation of multi-potent cells along specific lineages.

6. Applications

The technology of TE has been shown to be feasible; some products are already on the market and there is potential for the development of new products with significant clinical implant. Translation of research from the laboratory to the clinic requires animal studies and many questions remain about the suitable animal models for human conditions. Long-term rather than short-term investment money, business plans geared to realistic cost/benefit trade-offs, less hype, more sophisticated personnel skilled at product development and manufacturing scale-up are needed to

move the field toward the clinic. Along with these, continued progress on the fundamental side is needed to provide support for the translational advancements.

In the last two decades over 30 tissues of the body, with many showing sophisticated structure and function have been studied in animal replacement models. Five engineered tissues have been approved by FDA; several academic institutes as well as companies are making efforts to develop new products for regenerative medicine. One skin product, composed of human neonatal dermal fibroblasts grown on biodegradable scaffold and cryopreserved, has been used to treat diabetes related foot ulcers. Another product contains multi-layered skin, including both dermal and epidermal components. Several types of cartilage replacement therapy, as well as replacement therapies for corneas, blood vessels and bone, have been successfully used in clinical trials. Injection of autologous chondrocytes to correct vesicoureteral reflux in children and patients with urinary incontinence appears to be effective and safe.

Earlier work in TE of the musculoskeletal system addressing muscle, cartilage and bone was focused on using cell in conjunction with synthetic biocompatible scaffolds. Autologous fetal myoblast TE can be a viable alternative for diaphragmatic replacement in a lamb model. The engineered cartilage in the shape of a human ear was first reported. Further in vitro and in vivo studies in auricular TE bordered on actual clinical application. The significant accumulation of knowledge of optimal conditions for cartilage TE allows for the ability to engineer other types of cartilage tissue, such as those for nasoseptum, temporo-mandibular joint disc, composite tracheal tissue, meniscus and joint resurfacing.

For an osteochondral joint defect, in vitro generation of osteochondral tissue composites based on biodegradable polymer scaffolds with chondrogenic and osteogenic cells may provide better osteochondral repair with the development of a well-defined tissue-to-tissue interface. The formation of small phalanges and whole joints from bovine-cell source transplanted onto biodegradable polymer matrices in athymic mice was further described. Moreover the successful replacement of an avulsed phalanx with tissue-engineered bone suggests that the use of tissue-engineered bone may be an effective approach to the treatment of bone loss to trauma or disease.

In cardiovascular TE, the goal is to develop artificial blood vessels and heart valves. For blood vessel, the large diameter (major to 5 mm) grafts were commercialized by using Dacron and expanded polytetrafluoroethylene (Gore Tex ®). These materials lack growth potential; however they have a limited use in pediatric cardiovascular surgery. "Living" vascular graft engineered from autologous cells and biodegradable polymers functioned well in the pulmonary circulations as demonstrated in lambs. This work has evolved into the clinical applications of transplantation of a tissue-engineered pulmonary artery in a child with a complex congenital heart disease and pulmonary atresia. But, the TE of small-calibre blood vessel has been difficult and further investigation is ongoing.

For TE of heart valves, it has been demonstrated that a tissue-engineered valve leaflet constructed from its cellular components can function in the pulmonary valve position in lambs. A whole tri-leaflet tissue-engineered heart valve was then developed and implanted in the pulmonary position with appropriate function for 120 days in a lamb model.

For nerve TE, researchers have created a tubular nerve guidance conduit with a biodegradable scaffold and cultured Schwann cells, which possess the macro-architecture of a poly-fascicular peripheral nerve; works on this model have demonstrated the feasibility of in vivo regeneration through the conduit. Furthermore a biodegradable nerve guidance conduit loaded with growth factors was developed by using materials originally designed for drug delivery applications. Different designs of conduits seeded with Schwann cells are under investigation to promote guided peripheral nerve regeneration.

7. References

- [1] Aulthouse AL, Beck M, Griffey E, Sanford J, Arden K, Machado MA, Horton WA. Expression of the human chondrocyte phenotype in vitro. *In Vitro Cellular & Developmental Biology*. 1989;25(7):659-668.
- [2] Chaudry A. Cell Culture. The Science Creative Quarterly. 2004. (<http://www.scq.ubc.ca/>).
- [3] Chen CS, Mrksich M, Huang S, Whitesides GM, Ingber DE. Micropatterned surfaces for control of cell shape, position, and function. *Biotechnology Progress*. 1998;14(3):356-363.

- [4] Chen HC; Hu YC. Bioreactors for tissue engineering. *Biotechnology Letters*. 2006;28:1415-1423.
- [5] Dutt K, Harris-Hooker S, Ellerson D, Layne D, Kumar R, Hunt R. Generation of 3D retina-like structures from a human retinal cell line in a NASA bioreactor. *Cell Transplantation*. 2003;12(7):717-731.
- [6] Folkman J, Haudenschild C. Angiogenesis by capillary endothelial cells in culture. *Transactions of the Ophthalmological Societies of the United Kingdom*. 1980;100:346-353.
- [7] Folkman J; Haudenschild C. Angiogenesis in vitro. *Nature*. 1980;288(5791):551-556.
- [8] Hench LL; Polak JM. Third-generation biomedical materials. *Science*. 2002;295(5557):1014-1017.
- [9] Langer R, Vacanti JP. Tissue Engineering. *Science*. 1993;260(5110):920-926.
- [10] Masters JR. HeLa cells 50 years on: the good, the bad and the ugly. *Nature Reviews Cancer*. 2002;2:315-319.
- [11] Mooney D; Hansen L; Vacanti J; Langer R; Farmer S; Ingber D. Switching from differentiation to growth in hepatocytes control by extracellular matrix. *Journal of Cellular Physiology*. 1992;151(3):497-505.
- [12] National Science Foundation (U.S.A.). The Emergence of Tissue Engineering as a Research Field. 2004. (<http://www.nsf.gov/pubs/2004/nsf0450/start.htm>).
- [13] Niklason LE, Gao J, Abbott WM, Hirschi KK, Houser S, Marini R, Langer R. Functional arteries grown in vitro. *Science*. 1999;284(5413):489-493.
- [14] Powell CA, Smiley BL, Mills J, Vandeburgh HH. Mechanical stimulation improves tissue-engineered human skeletal muscle. *American Journal of Physiology-Cell Physiology*. 2002;283(5):C1557-C1565.
- [15] Ratner BD, Hoffman AS, Schoen FJ, Lemons JE. *Biomaterials Science, Second Edition: An Introduction to Materials in Medicine* (pp. 709-749). Elsevier Academic Press, 2004.
- [16] Shieh SJ; Terada S; Vacanti JP. Tissue engineering auricular reconstruction: in vitro and in vivo studies. *Biomaterials*. 2004;25(9):1545-1557.
- [17] Shieh SJ; Vacanti JP. State-of-the-art tissue engineering: From tissue engineering to organ building. *Surgery*. 2005;137(1):1-7.
- [18] Singhvi R, Kumar A, Lopez GP, Stephanopoulos GN, Wang DIC, Whitesides GM, Ingber DE. Engineering cell-shape and function. *Science*. 1994;264(5159):696-698.
- [19] Tabata Y. Tissue regeneration based on tissue engineering technology. *Congenital Anomalies*. 2004;44(3):111-124.
- [20] Titze IR, Broadhead K, Tresco P, Gray S. Strain distribution in an elastic substrate vibrated in a bioreactor for vocal fold tissue engineering. *Journal of Biomechanics*. 2005;38(12):2406-2414.

CHAPTER 2

Cell Migration, Durotaxis and Collagen Deposition

1. Introduction

As seen in chapter 1, cells and their functions play an important role in TE applications. Understanding functions and mechanisms of cells is strictly related to scaffold design and materials selection for this kind of applications.

In this chapter information about cell structure and normal cell function are exposed, giving particular attention to the process of cell movement. This process is explained and external influencing factors are introduced. In particular cell movement in conditions of durotaxis is described from the physical point of view as it is the main topic of this thesis. Finally a recent finding on the relation between cell movement and collagen deposition of fibroblasts are presented.

2. Cell and Cell Functions

The Latin term “cellula”, meaning small room, is due to Robert Hooke, one of the first users of the microscope, who in 1665 was able to obtain thin slice of cork and observing them with his ancient instrument he noted a lot of small cells in the structure, like a hive (Fig. 1). Obviously Hooke was not observing cells, but their walls, nevertheless he opened the way to the study of these unknown structures of living matter.

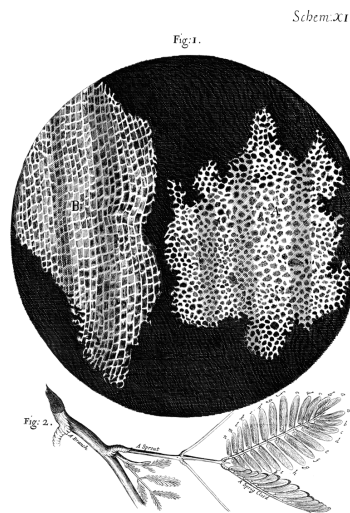


Fig. 1: Cork cell structure as seen by Robert Hooke (Encyclopedia Britannica)

After this discovery it took almost two centuries before the microscope was able to put its lights inside the cellular spaces, and before Mathias Schleiden, for vegetables, and Theodor Schwann, for animals, described the characteristics of the various cell types and tissues, and recognized the common structure of all cells. Then with the refining of microscope techniques and chemical analysis and with the help of electronic microscopy, the image of the cell becomes clearer and clearer and it confirmed its structural uniformity.

Composed of nucleic acids, proteins, and other large and small molecules, cells constitute the basic structural building blocks of all living matter. They are held together by cell-to-cell junctions to form tissues comprising four general types: epithelium, connective tissue, muscle, and nerve. Organs are assembled from these basic tissues, glued together by a largely proteinaceous extracellular matrix (ECM) synthesized by the individual cells. The organs, in turn, perform the various functions required by the intact living organism, including circulation, respiration, digestion, excretion, movement, and reproduction.

Conceptually, cells may be viewed as independent collections of self-replicating enzymes and structural proteins that carry out certain general functions. The most essential cell attributes are:

- Self-replication
- Protection from the environment

- Acquisition of nutrients
- Movement
- Communication
- Catabolism of extrinsic molecules
- Production of chemicals (especially proteins)
- Degradation and renewal of senescent intrinsic molecules
- Energy generation

Intracellular constituents exist in an environment made of water, ions, sugars, and small-molecular-weight molecules called the cytosol or cytoplasm. Within the cytosol there is also a source of energy, typically adenosine triphosphate (ATP). Although long conceptualized as a randomly diffusing bag of soluble molecules, the cell is, in fact, a structurally highly ordered and functionally integrated assembly of organelles, cytoskeletal elements, and enzymes.

The cytosol is delimited and protected from the environment by a phospholipids bilayer, the plasma membrane, which permits the cell to maintain cytosolic constituents at concentrations different from those in the surrounding environment. Because of its hydrophobic inner core, the plasma membrane is impermeable to charged and large polar molecules; however, it permits specific passage to incoming or outgoing material (ions, amino acids, etc.) by channel or transport proteins inserted through it. Most nutrient acquisition is thereby accomplished by the movement of substances either through pores or by energy-driven transport. Cells also have the capacity to internalize material from the outside environment by capturing bits of the extracellular environment in invaginated folds of the plasma membrane called vesicles. Depending on the volume and size of the ingested material, the process may be called phagocytosis ("cell eating") or pinocytosis ("cell drinking"). Transcytosis is the movement of vesicles from one side of a cell to another, and it may play an important role in mediating the increased vascular permeability that occurs around tumours or at sites of inflammation. The plasma membrane may also express a variety of specific surface molecules that facilitate interactions with other cells, soluble ligands (e.g., insulin), and with the extracellular matrix.

Many of a cell's normal housekeeping functions are compartmentalized within membrane-bounded intracellular organelles (Fig. 2) thus permitting adjacent regions of the cell to have vastly different chemistries. By isolating certain cellular functions within distinct compartments, potentially injurious degradative enzymes or toxic metabolites can be kept at usefully high concentrations locally without causing damage to more delicate intracellular constituents. Moreover, compartmentalization also allows the creation of unique intracellular environments (e.g., low pH, high calcium, or high concentration of a potent enzyme) that permit more efficient functioning of certain chemical processes, enzymes, or metabolic pathways.

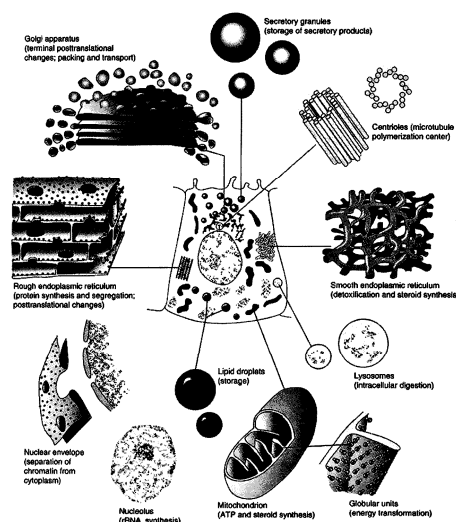


Fig. 2: General Schematic of a typical mammalian cell, demonstrating the general organization and major organelles (Biomaterials Science, 2004)

The enzymes and structural proteins of the cell are constantly being renewed by ongoing synthesis tightly balanced with intracellular degradation. Oversight for the new synthesis of macromolecules, including deoxyribonucleic acid (DNA) and ribonucleic acid (RNA), is provided by the nucleus. New proteins destined for the plasma membrane or for secretion into the extracellular environment are synthesized and packaged in the rough endoplasmic reticulum (RER) and Golgi apparatus; proteins intended for remaining in the cytosol are synthesized on free ribosomes. Smooth endoplasmic reticulum (SER) may be abundant in certain cell types where it is used for steroid hormone and lipoprotein synthesis, as well as for the modification of hydrophobic compounds into water-soluble molecules for export. Degradation of internalized molecules or senescent self-molecules into their constituent amino acids,

sugars, and lipids (catabolism) is the primary responsibility of the lysosomes and proteasomes. Peroxisomes play a specialized role in the breakdown of fatty acids, generating hydrogen peroxide in the process. Intracellular vesicles busily shuttle internalized material to appropriate intracellular sites for catabolism or direct newly synthesized materials to the plasma membrane or relevant target organelle. The architecture of the cell is maintained by a scaffolding of intracellular proteins collectively called the cytoskeleton, analogous in some ways to the support provided by bones of our bodies.

Cell movement, including both movement of organelles and proteins within the cell, as well as movement of the cell in its environment, is accomplished through rearrangement of the cytoskeleton. These structural proteins also provide basic cellular shape and intracellular organization, which are necessary for the maintenance of cell polarity (differences in cell structure and function at the top of a cell versus its side or base). For example, in many cell types, and particularly in epithelial tissues, it is critical for cells to distinguish, and keep separated, the top (apical) versus the bottom and side (basolateral) surfaces. The major energy source for macromolecular synthesis, metabolite degradation, and intracellular transport is the mitochondrion, using oxidative phosphorylation to generate adenosine triphosphate (ATP) from adenosine diphosphate (ADP). Finally, all of these organelles must be replicated (organellar biogenesis) and correctly apportioned in daughter cells following mitosis.

Every living organism possesses many cell types depending on the functions cells should accomplish. The specific functions of a given cell are reflected by the relative amount and types of organelles it contains. The relative predominance of specific types of organelles can be inferred by examination of tissue sections prepared by standard histological techniques and can be confirmed by transmission electron microscopy. For example, cells with high energy requirements can be expected to have a significantly greater capacity to generate that energy. Thus, kidney tubular epithelial cells (which reabsorb sodium and chloride against concentration gradients), and cardiac myocytes (which rhythmically contract 50-100 times per minute) have a generous complement of mitochondria. Conversely, cells specifically adapted to synthesize and export selected proteins (e.g., insulin in a pancreatic islet cell, or

antibody produced by a plasma cell) have a well-developed rough endoplasmic reticulum.

3. Cell Cytoskeleton and Movement

Movement is one of the normal functions of a cell. It is a highly dynamic phenomenon that is essential to a variety of biological processes such as the development of an organism, i.e. morphogenesis, wound healing, cancer metastasis and immune response. For example, during morphogenesis there is a targeted movement of dividing cells to specific sites to form tissue and organs. For wound healing to occur, cells such as neutrophils (white blood cells) and macrophages (cells that ingest bacteria) move to the wound site to kill the microorganism that cause infection, and fibroblasts (connective tissue cells) move there to remodel damaged structure. In all these examples, cells reach their target by crawling. In general, there are also other kinds of motility, such as the swimming of most sperm cells and the movement of some bacteria by the rotation of flagellar motors. Cell crawling however, is the most common mechanism employed by most motile eukaryotic animal cells.

Although cell movement was observed as early as 1675 when van Leeuwenhoek saw cells crawl across his microscope slide, the molecular mechanisms behind cell movement have become a scientific focus only in the past few decades. As a cell moves on a substratum (the ECM if the cell moves inside an organism or a cover slide if it moves outside an organism), it experiences external forces, which include the viscous force or resistance from the surrounding medium and cell-substratum interaction forces, and internal forces that are generated by the cytoskeleton. In most animal cells, the cytoskeleton is the essential component in creating these motility-driving forces, and in coordinating the entire process of movement. The cytoskeleton is a polymeric network, composed of three distinct biopolymer types: actin, microtubules and intermediate filaments. These biopolymers are differentiated principally by their stiffness, which can be described by the persistence length L_p . The persistence length is defined as the distance over which the filament is bent by thermal forces, and increase with increasing stiffness (Morse, 1998).

Actin filaments (AFs) are semi-flexible polymers with L_p of about 17 μm . They are about 7 nm in diameter, are built from dimer pairs of globular actin monomers, and are functionally polar in nature. This means that they have two distinct ends: a fast and a slow growing end (called the plus end and minus end respectively). The minus end has a critical actin monomer concentration that is about 6 times higher than that at the plus end. When the end of an AF is exposed to a concentration of monomeric actin that is above its critical concentration, the filament end binds monomers and grows by polymerization. Conversely, when the concentration is below the critical one, monomers detached from the filament end, and the filament shrinks by depolymerization. Simply by having these two different critical actin concentrations at the opposing ends of the filament, AFs can grow asymmetrically, and when the actin monomer concentration lies between the two values, only the plus end grows while the minus end shrinks. This process, where the length of the filament stays roughly constant and the polymerized monomers within the AF transfer momentum forward due to asymmetric plus end polymerization, is known as treadmilling: it is a critical aspect of how polymerizing AFs can generate forces. Microtubules (MTs) are the stiffest of the biopolymers constituting the cytoskeleton, with L_p ranging from 100 to 5000 μm depending on the filament length. MTs are rod-like polymers, with an outer diameter of about 25 nm. Tubulin protein subunits assemble into proto-filaments, and typically 13 of these proto-filaments then align to form a hollow tube, imbuing MTs with their incredible stiffness. MTs exhibit similar dynamics to those of actin: they are functionally polar, treadmill, and can impart a force through polymerization. Intermediate filaments (IFs) are much more flexible than AFs and MTs (L_p in the range 0.3-1.0 μm). They range in diameter from 8 to 12 nm, between that of AFs and MTs. There are different classes of IFs such as vimentin, desmin, keratin, lamin and neurofilaments, with different cell types having different IFs. Unlike AFs or MTs, IFs are not polarized, do not treadmill, do not generally depolymerize under physiological conditions once polymerized, and are therefore considered to be more static in nature than AFs and MTs.

These three kinds of biopolymers build the cytoskeleton, which is an organised and coherent structure formed by connecting these filaments via entanglements, and also crosslinking, bundling, binding, myosin and other proteins. These cytoskeletal assemblies then work together as a composite, dynamic material in cell functions

such as structural integrity, shape division, and organelle transport and cell motility. With respect to motility, although the other polymer assemblies in the cell also aid in coordinating movement and powering translocation, the actin cytoskeleton is regarded as the essential engine that drives cell protrusion, the first step of movement (Hofman *et al.*, 1999, Betz *et al.*, 2006). It is also integral to achieving the two other steps of movement: adhesion of the leading edge and de-adhesion at the cell body and rear, and translocation of the bulk of the cell. The actin cytoskeleton is highly dynamic and the actin structures in the cell can be readily reorganized by the cell to adapt their behaviour for movement according to the surrounding environment. The constant restructuring of the actin cytoskeleton and the transition from one actin structure to another is vital in enabling the cell to change its elastic properties quickly, and this dynamic response is fundamental for movement.

AFs *in vivo* can assemble into different structure such as networks and bundles. Mesh-like actin network consisting of short crosslinked AFs are primarily found at the leading edge of cells (Kaverina *et al.*, 2002). The growth of these meshworks i.e. the continuous creation of new actin network at the leading edge is considered to be essential for pushing the cell forward (Fig. 3).

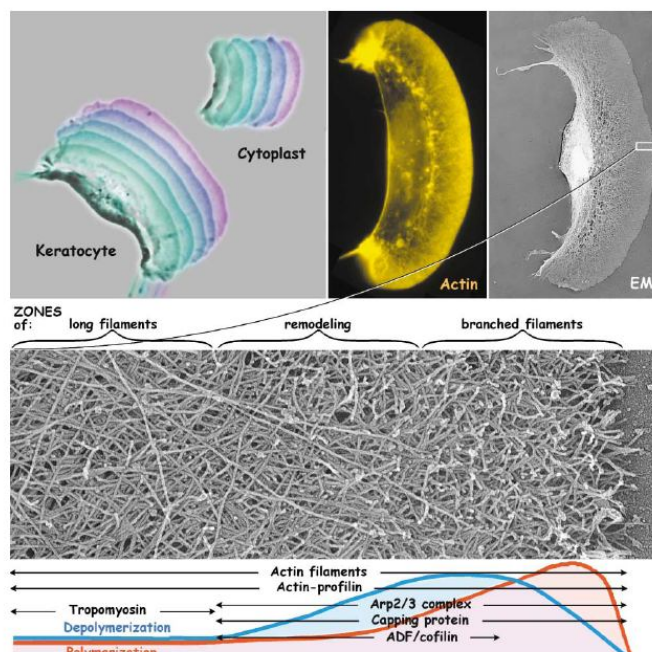


Fig. 3: Light and electron micrographs of motile keratocytes (fibroblastic stromal cells of the cornea, Top left) Overlays of two series of phase contrast micrographs taken at intervals of 15 seconds showing the motility of a keratocyte and a keratocyte cytoplast, i.e. the inner part of the cell without cell wall and plasma membrane. (Top middle) Fluorescence micrograph of a keratocyte stained with

rhodamine phalloidin to label the actin filaments. (Top right) Transmission electron micrograph of a keratocyte. Detail of region shown below with the three zones of actin filament organization labeled. The schematic diagram indicates the locations of key proteins. The curves (actin subunits per unit time) indicate actin filament assembly (red) and disassembly (blue). Areas under curves were made equal to denote steady state (Pollard *et al.*, 2003)

This network formation is carried out with the help of numerous accessory proteins. Activating proteins enable nucleator proteins (e.g. Arp2/3 complex) to initiate the polymerization and assembly of new actin filaments. Actin depolymerization promoting proteins can also aid network growth. Cofilin, also known as Actin Depolymerising Factor (ADF) removes actin filaments and creates new plus ends for the growth of new actin filaments. Actin binding proteins maintain a steady actin monomer pool for polymerization, while crosslinking and bundling proteins help form connected actin networks. Capping proteins control filament length by attaching to actin filament ends and stopping further polymerization, while severing and fragmenting proteins cut actin filaments and networks. All these proteins work together to coordinate actin network formation and bring about leading edge motility in several steps (Pollard *et al.*, 2003). This complex process is schematized in Fig. 4.

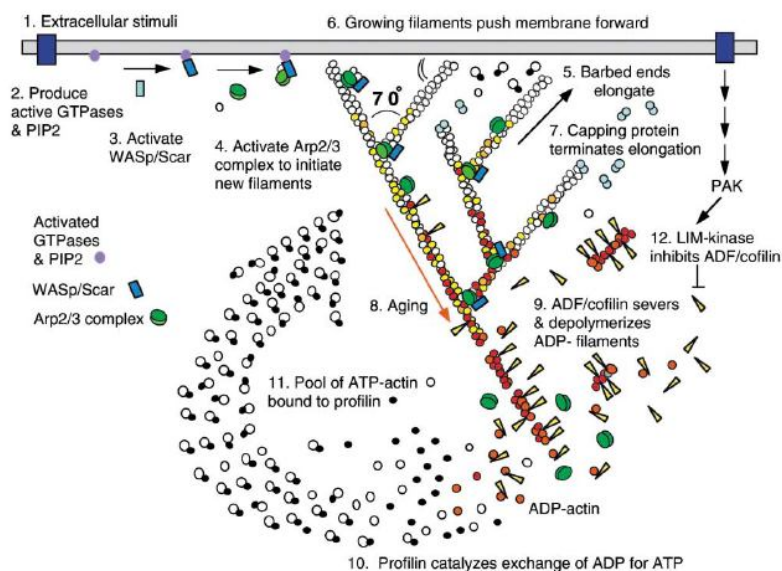


Fig. 4: Dendritic nucleation/array treadmilling model for protrusion of the leading edge. (1) Extracellular signals activate receptors. (2) The associated signal transduction pathways produce active Rho-family GTPases and PIP2 that (3) activate WASp/Scar proteins. (4) WASp/Scar proteins bring together Arp2/3 complex and an actin monomer on the side of a preexisting filament to form a branch. (5) Rapid growth at the barbed end of the new branch (6) pushes the membrane forward. (7) Capping protein terminates growth within a second or two. (8) Filaments age by hydrolysis of ATP bound to each actin subunit (white subunits turn yellow) followed by dissociation of the phosphate (subunits turn red). (9) ADF/cofilin promotes phosphate dissociation, severs ADP-actin filaments and promotes dissociation of ADP-actin from filament ends. (10) Profilin catalyzes the exchange of ADP for ATP

(turning the subunits white), returning subunits to (11) the pool of ATP-actin bound to profilin, ready to elongate barbed ends as they become available. (12) Rho-family GTPases also activate PAK and LIM kinase, which phosphorylates ADF/cofilin. This tends to slow down the turnover of the filaments (Pollard *et al.*, 2003).

Actin bundles are composed of parallel arrays of individual AFs that are closely packed and crosslinked by proteins such as fascin, fimbrin and scruin, and fulfil structural and sensory roles that are keys to cell movement. Often, these actin bundles connect distal point of adhesion, allowing tension to be propagated across the cell, and enabling the cell to apply forces on the substratum and move. They are approximately known as stress fibres, distributing forces and positively reinforcing adhesion sites. In some cells, actin bundles known as filopodia may extend out beyond the lamellar edge, and function as chemical and mechanical sensors, and aid the cell in the migrating through tissue.

AFs also generate motility forces through interactions with myosin motors. Myosin motors consist of a head, neck and tail region; while some myosin motors have one head and neck, others have two. The head/neck region is responsible for attachment and force production, while the tail region is principally believed to be used for connecting to cargo, such as other myosin, vesicles or filaments. Myosin motors work on actin filaments through a general three-step process of binding, power stroke and unbinding. This process is continuously repeated and leads to the generation of a contractile force (acto-myosin contractile force) thought to be essential in pulling the bulk of the cell forward during movement.

In most cell types the microtubules predominantly extend radially from the centrosome to the actin network at the cell periphery, with their plus ends towards the cell edge, and thus display a hub and spoke arrangement. These microtubules aid in determining the direction of cell movement (Euteneuer *et al.*, 1986).

Intermediate filaments create a fibrous network that spans the cell interior and connects the nucleus to the cell membrane, providing structural integrity to cells. Due to their more static properties, it has long been held that IFs are of little importance for cell movement since cell movement requires the cytoskeleton to be dynamic and to reorganize rapidly.

4. The Process of Cell Movement

The adhesion of a cell to a substratum is a necessary requirement for it to spread and crawl. It is known that this phase is mediated by complex molecular assemblies that link the extracellular matrix, via transmembrane matrix receptors (integrins) to the actin cytoskeleton. Different types of adhesion complexes are reported in Fig. 5.

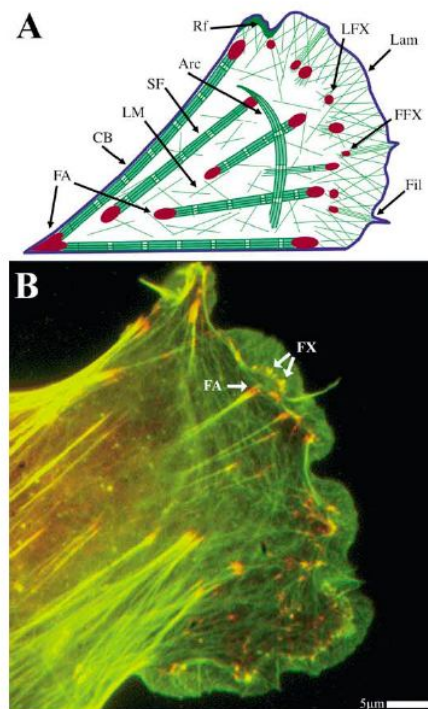


Fig. 5: Subcompartments in the actin cytoskeleton and substratum adhesion complexes. (A) Schematic representation of subcompartments in the actin cytoskeleton (green) and adhesion complexes (red). Lam: lamellipodium; Fil: filopodium (microspike); Rf: ruffle; SF: stress fibres; Arc: dorsal arc; CB: concave bundle; LM: loose meshwork; FA: focal adhesions; FFX: filopodia-based focal complexes; LFX: lamellipodia-based focal complexes. (B) Fluorescence image of a mouse Swiss 3T3 fibroblast that was fixed and then immuno-labelled for vinculin (red) and counterstained for F-actin with phalloidin (green). FA: focal adhesion; FX: focal complexes. (Kaverina *et al.*, 2002).

The adhesion site genesis is correlated to actin cytoskeleton subcompartments of a spreading and moving cell at which they are attached. These subcompartments are schematically represented in Fig. 5. The first compartment is the lamellipodium and its ramifications at the advancing cell front, which include membrane ruffles. The lamellipodium is made up of a laminar meshwork of actin filaments, up to about 5 μm in width and around 0.2 μm or less thick. It is often punctuated by radially oriented bundles of actin filaments, ranging from 0.1 to 0.25 μm in diameter, termed

microspikes or filopodia. The filaments of these bundles merge into the meshwork of the lamellipodium, from which they clearly arise and they can extend as finger-like projections beyond the lamellipodium tip. Lamellipodia and filopodia are composed of filaments polarised with their fast growing ends directed to the cell front, consistent with a protrusive function. As protrusive organelles they are both engaged in cell motility. Adhesion sites in lamellipodia are commonly of a punctate or oblong nature and may be elongated beneath microspikes or filopodia that are adherent. They are called “focal complexes”. Actin filaments behind the lamellipodium are organised either into bundled arrays, or into more loose networks. At least five types of bundled arrays can be distinguished, three of which are evident in Fig. 5: linear bundles, or stress fibres that traverse the cytoplasm; concave bundles at the cell edge, either alone or at the base of lamellipodia; convex, circumferential bundles at the cell edge (characteristic of epithelial cells); polygonal networks; and dorsal arcs. In contrast to lamellipodia and filopodia, these bundles feature anti-parallel arrays of actin that contain myosin and are therefore contractile. Dorsal arcs and polygonal arrays are not directly associated with the substratum and since they are inconsistent features of motile cells. Stress fibres and concave bundles are anchored to the substratum at their ends to well defined, mainly elongated adhesion sites, corresponding to the focal adhesions.

An adherent cell begins to crawl in response to an external signal in its surrounding environment. This can be a physical, chemical, diffusible or non-diffusible signal that is detected by receptor proteins located on the cell membrane, and transmitted by them via signaling cascades to the cell interior. A cell, such as a white blood cell, yeast cell or slime mold cell, is believed to sense the signal direction by spatially recognizing external gradients (receptor proteins become more concentrated on the side of the cell where the signal is present; Parent and Devreotes, 1999). Once cell movement begins, the process, which involves the constant restructuring of the actin cytoskeleton, can be schematized into three stages in most cells (Fig. 6). First, a cell propels the membrane forward by orienting and reorganizing the actin network at its leading edge. Second, it adheres to the substratum at the leading edge and de-adheres at the cell body and rear of the cell. Finally, contractile forces, generated largely by the action of the acto-myosin network, pull the cell forward.

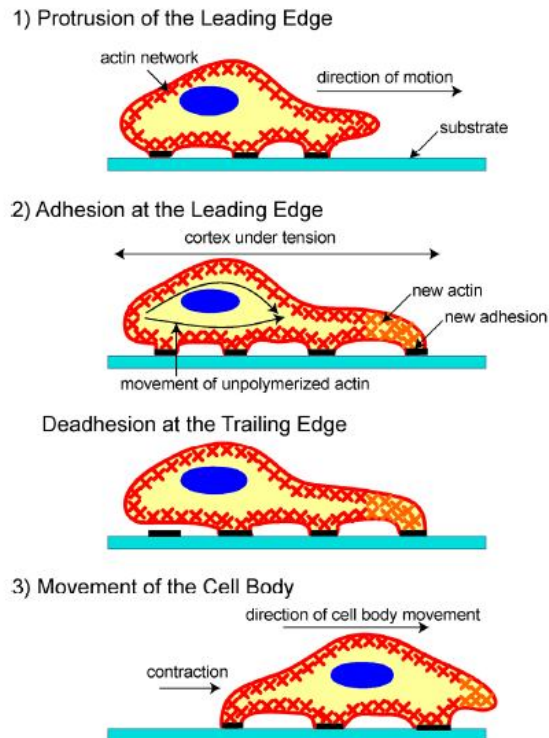


Fig. 6: A schematic of the three stages of cell movement: after determining its direction of motion, the cell extends a protrusion in this direction by actin polymerization at the leading edge. It then adheres its leading edge to the surface on which it is moving and de-adheres at the cell body and rear. Finally, it pulls the whole cell body forward by contractile forces generated at the cell body and rear of the cell. (Ananthakrishnan and Ehrlicher, 2007)

After sensing the signal, the cell starts moving in response to it by polymerizing actin. If the signal is a chemo-attractant, for example, actin polymerizes in the region of the cell closest to the signal, whereas if the signal is a chemo-repellent, the cell moves away by polymerizing actin in the opposite side. As the extending edge moves forward, the cell constantly monitors the signal directions and tailors its direction of motion accordingly.

Soon after the leading edge begins to protrude, adhesion molecules (integrins but also selectins, vinculin, talin) gathered in the extending region help attach the leading edge to the substratum forming adhesion complexes (Fig. 7).

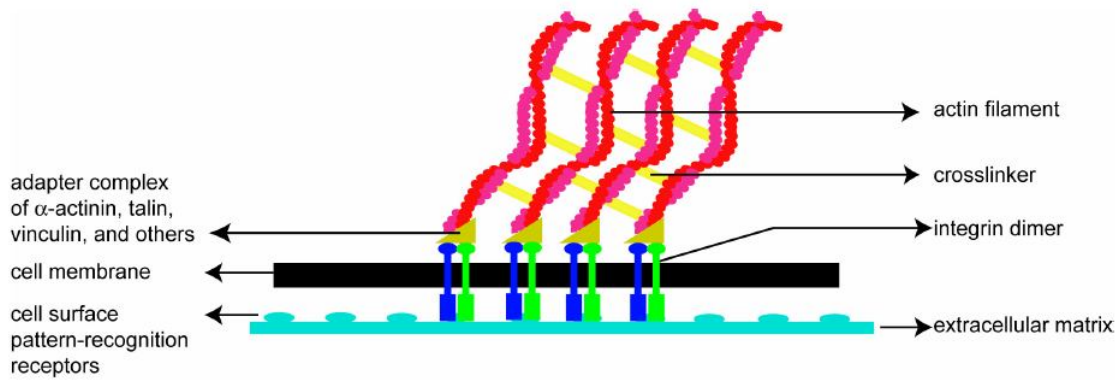


Fig. 7: A scheme showing how the cell adheres to the substratum. Cell-substratum attachments are formed when actin bundles connect to the substratum at certain sites via adhesion molecules such as vinculin, talin and integrin. (Ananthakrishnan and Ehrlicher, 2007)

These attachments prevent the protruding leading edge from retracting. As the cell continues to adhere at the leading edge, it de-adheres at the cell body and rear of the cell, possibly by the disassembly or contraction of its attachments (actin bundles). Finally the rest of the cell is pulled forward, mainly by contractile forces that are produced by myosin motors sliding on actin filaments, which are in the cell body and at the rear.

All the stages or processes described above are continuously running as the cell moves on the substratum, with the actin cytoskeleton transitioning between a solid-like elastic material and a solution-like viscous material. These transitions are crucial for cell movement. They are likely caused by the constant net actin polymerization and network assembly at the leading edge and depolymerization and disassembly at the rear of the cell. These processes lead to local changes in the elasticity of the cell as it moves.

5. Influencing Factors of Cell Motion

In the absence of external signals, the stages described in the process of cell migration occur randomly and the whole process is called random motility: a single cell moving over a homogeneous and isotropic substratum will follow a quasi-straight path over short time intervals while over longer time intervals such a motion exhibits

a Brownian-like structure, i.e. it has the characteristics of a persistent random walk (Lauffenburger and Linderman, 1993).

On the other hand, it is well known that cells are able to feel a certain number of external signals that are capable of influencing their movement. These are, for example, the presence of a soluble chemical agent, or of a gradient thereof, the presence of an electric field, or of a particular distribution of adhesion molecules on the substratum. When guided by these external factors, cell migration takes different names depending upon the particular influencing factor, so one talks about chemotaxis, galvanotaxis and haptotaxis, respectively (Ionides *et al.*, 2004).

Chemotaxis is the most investigated and apparent reason for cell movement. The phenomenon is the result of the cell's response to a spatial chemical gradient in the surrounding environment. Experiments clearly show an almost instant migratory response to a change in the chemistry of a substratum. This response is observed as a movement towards or away from the source of chemical variation. This is considered the leading factor for orchestrating cell movement. Galvanotaxis is the ability to control cell-motility by the application of a potential gradient. Both *in vivo* and *in vitro* experiments have shown an ability to either encourage or impede the surroundings cells infiltration of a wound site, or to change the traction force of a cell by applying different potential gradients (Erickson and Nuccitelli, 1984; Brown and Loew, 1994). Haptotaxis is the different behaviour caused by a variation in surface-attached chemicals gradient in an underlying substratum (Harris, 1973). Other guiding mechanism such as phototaxis, i.e. cell response to gradients of light intensity (Saranak and Foster, 1997) and geotaxis, i.e. the response to gravitational potential (Lowe, 1997) have been studied in the last years.

Recently it was discovered that also mechanical properties of a substratum influence cell motion. Following the previous nomenclature, this phenomenon was called "durotaxis". This mechanism is a little bit different from the previous ones and will be explained next.

6. Durotaxis

As introduced before, cells receive mechanical feedback from the substratum to which they adhere even in the absence of external applied forces. This phenomenon was firstly showed in the work of Lo and coworkers (2000). To test the effect of mechanical properties on cell migration, authors made experiments of cell migration over biphasic substrata. These substrata were made with a stiffness gradient, i.e. they were composed of two different regions of collagen coated polyacrylamide mixtures with different stiffness. Putting NIH 3T3 cells on these substrata, cells were in the conditions that they could only detect the stiffness gradient by a process of active tactile exploration. After seeding for 15 hours the cells, their migration was followed by time-lapse microscopy. The results they obtained are synthesized in Fig. 8. In Fig. 8a, a cell approaching the boundary region between the two materials from the soft side, moves in favour of the stiff side. In contrast (Fig. 8b), when a cell approached the boundary from the stiff side, it changed shape and orientation and reorient itself to move parallel to or away from the boundary; eventually it turned back to the stiff side. Always in this paper, authors showed that also stretching and pulling the substratum with a micro-needle they can influence cell migration; in this way they demonstrated that mechanical input generated by substratum deformation also regulates the formation and retraction of protrusion. This is to be expected in an active sensing system, because the force/deformation caused by the external manipulation will be superimposed on the effects of the cellular probing forces. From this follows that stiffness-guided movement takes place only when there are no other cells in the vicinity. At high densities, cells from the soft or the stiff side can move freely across the rigidity gradient, most likely as a result of pulling or pushing forces from neighbour cells transmitted via direct contact or through the elastic substratum. Thus, in conclusion of this seminal work on the phenomenon, it was proved that cultured isolated cells can guide their movement by probing the substratum stiffness and they prefer to migrate over stiffest regions.

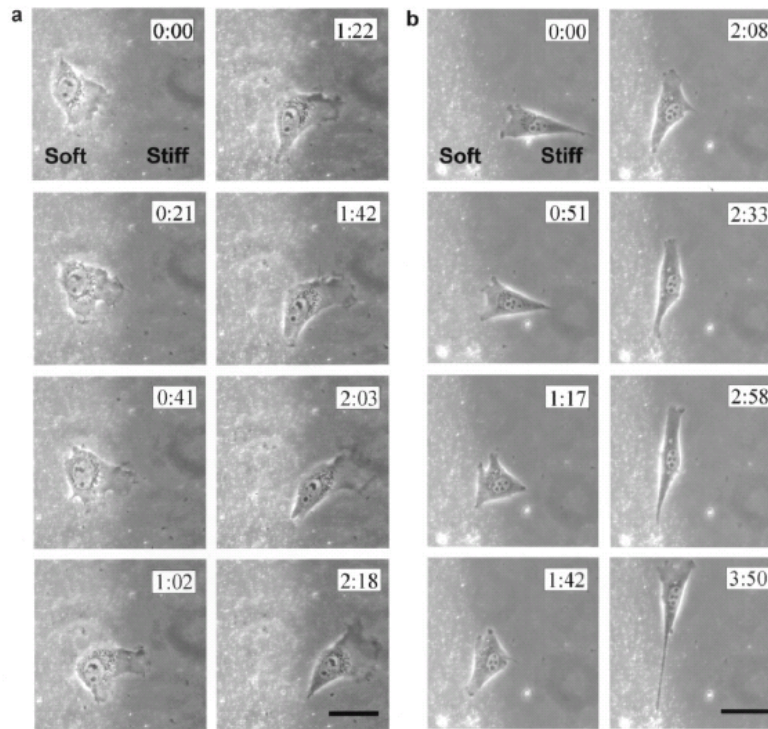


Fig. 8: Movements of NIH 3T3 cells on substrata with a rigidity gradient. Changes in substrata rigidity can be visualized as changes in the density of embedded fluorescent beads. (a) A cell moved from the soft side of the substratum toward the gradient. The cell turned by 90° and moved into the stiff side of the substratum. Note the increase in spreading area as the cell passed the boundary. (b) A cell moved from the stiff side of the substratum toward the gradient. The cell changed its direction as it entered the gradient and moved along the boundary. Bar, 40 μm . (Lo *et al.*, 2000)

The way in which mechanical stimuli are translated into intracellular signals is called “mechanotransduction”. When cells bind to the substratum, integrin begins to cluster, which leads to the recruitment of structural and signalling proteins to form the focal adhesion complexes at the site of integrin clustering. The formation and maturation of focal adhesions requires the application of mechanical forces to these adhesions. Cells can actively generate these forces themselves using actin-myosin complexes, which are part of their cytoskeleton. On a hard substratum, cells generate large forces which lead to the formation of mature focal adhesion and a highly organized cytoskeleton with abundant stress fibres. In contrast, a soft substratum cannot provide enough resistance to counterbalance large cell-generated forces. Therefore, on soft substrata cells do not develop abundant stress fibres and generate smaller forces, making adhesion sites on these region less stable. In this way, a cell moving on a region with a stiffness gradient moves towards the stiffest side.

Changes in cytoskeleton organization are important not only for movement. The cytoskeleton is involved in many signalling pathways that transfer mechanical

feedback into chemical response. Furthermore, the cytoskeleton also determines the shape of a cell, which in turn is intimately connected to cell behaviour (Breuls *et al.*, 2008) and differentiation of stem cells (McBeath *et al.*, 2004, Engler *et al.*, 2006).

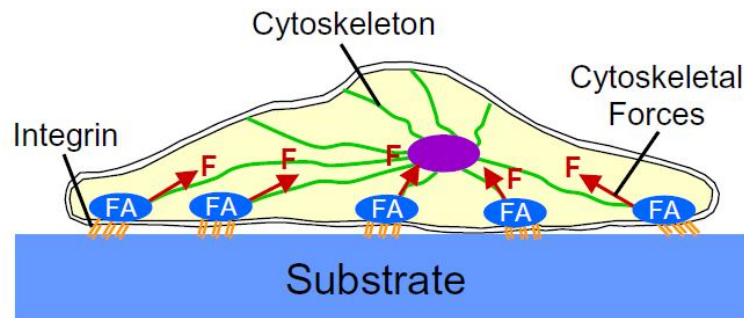


Fig. 9: Schematic representation of a cell which has attached to a substratum. Cells attach to a substratum with transmembrane molecules called integrins. When cells bind to a substratum, integrins begin to cluster which leads to the formation of focal adhesions (FA). The maturation of focal adhesions requires the application of mechanical forces (F) to these adhesions which can be generated by the cytoskeleton. (Breuls *et al.*, 2008)

Tissue Engineering applications and scaffolds, can take advantages from durotaxis. Scaffold materials and structure can be chosen and selected exploiting this phenomenon, to influence cell migration and behaviour. Some studies on the development of specific substrata have already been made (Cortese *et al.*, 2009; Fuard *et al.* 2007; Guo *et al.*, 2006; Ren *et al.*, 2008; Saez *et al.*, 2007) and they seem to be very promising.

7. Cell Migration and Collagen Deposition

All the mechanisms involved in cell migration described above can find applications in TE and in particular in the control of the mechanical properties of cell-produced collagenous matrix. In fact it was observed that cell migration determines the alignment of the collagenous matrix produced by some cell types such as fibroblasts or osteoblasts. Hence migration has an influence on the mechanical properties of the cell-produced tissue.

For example, ligaments and tendons are well-organized fibrous connective tissues. They are mainly composed of parallel collagen fibres interspersed with spindle-shaped fibroblasts aligned along the fibres in the longitudinal direction of the ligaments. After ligament injury cells in the healing site are found to have no specific orientation. The resulting collagen matrix is also less organized and this has been associated with the decrease in mechanical properties of the healing tissue.

One of the principal works on this phenomenon is the paper of Wang and coworkers (2003). In this paper, MC3T3-E1 cells, able to produce abundant collagenous matrix within a relatively short cultured period, were seeded on both silicone micro-grooved and smooth substrata. After four weeks in culture cells were oriented along the microgrooves in micro-grooved substrata as shown and randomly oriented in the smooth ones and they had produced matrices made principally of type I collagen (Fig. 10).

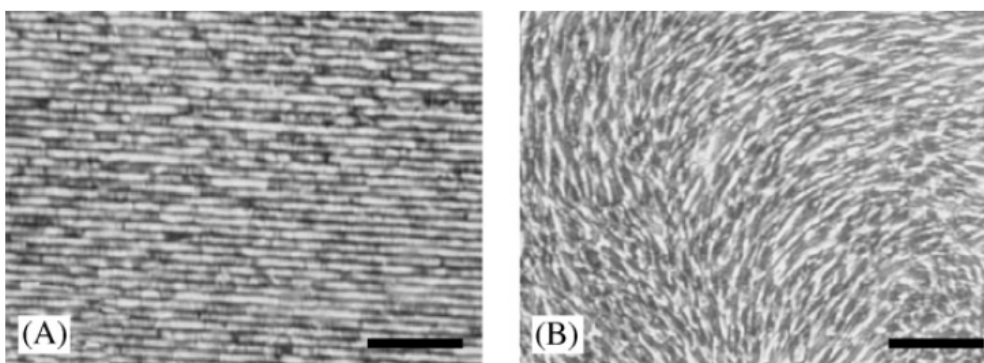


Fig. 10: Phase contrast microphotographs of MC3T3-E1 cells on the microgrooves (A) and smooth surfaces (B). The cells on the microgrooves were aligned along the direction of the microgrooves, that is, the horizontal direction, whereas the cells on the smooth surface were randomly oriented (Bar: 100 μ m; Wang *et al.*, 2003).

Checking the quality of new tissue produced with polarized light it emerges that cells oriented along the microgrooves produced highly aligned collagen fibres that were also aligned in the direction of the microgrooves; the matrix produced on the smooth substrata, conversely, is randomly oriented and disorganized (Fig. 11).

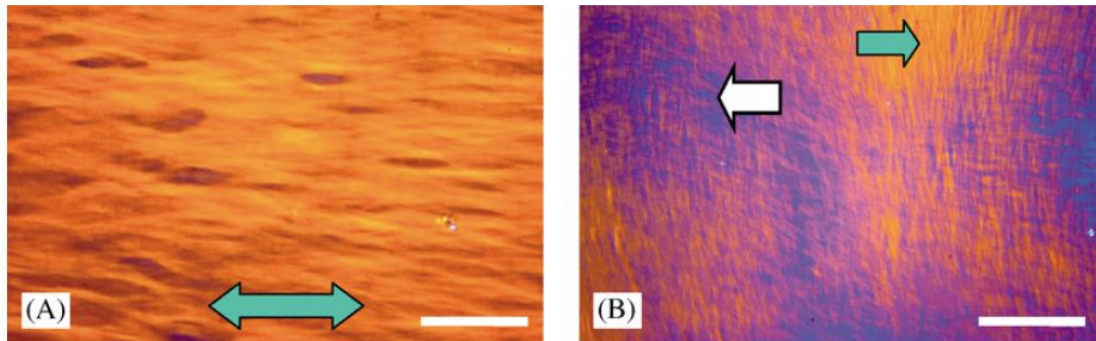


Fig. 11: The dense collagenous matrix produced by the cells in the microgrooves shows uniformly yellow under polarized microscope, indicating the collagenous fibres were aligned in the same direction as the microgrooves (green arrow, A). However, the collagen matrix produced by the cells in smooth surfaces shows multiple colours (B) and in this case, yellow (green arrow) and blue (white arrow). The multiple colours mean that the collagenous fibres had multiple orientations (Bar: 60 mm, Wang *et al.*, 2003).

The mechanisms for production of aligned collagen fibres by the aligned cell may be due to cell contractility and motility. The cells in culture aligned in the direction of microgrooves and were elongated in shape and cells with this morphology have been shown to apply contraction forces along the cell's long axes (Wang *et al.*, 2002). This directional contraction force may align collagen fibres in the same direction as that of cells (Guido and Tranquillo, 1993). This increased alignment leads to an increased tissue stiffness which should increase the contractile force from the cell. Having this in mind, different substrata based on durotaxis will be produced and tested as shown in the following chapter of this thesis.

8. References

- [1] Ananthakrishnan R, Ehrlicher A. The forces behind cell movement. *International Journal of Biological Sciences*. 2007;3(5):303-17.
- [2] Betz T, Lim D, and Kas JA. Neuronal growth: a bistable stochastic process. *Physical Review Letters*. 2006;96(9):098103/1-098103/4.
- [3] Brown MJ and Loew LM. Electric field-directed fibroblast locomotion involves cell surface molecular reorganization and is calcium independent. *The Journal of Cell Biology*. 1994;127:117-128.
- [4] Cortese B, Gigli G, Riehle M. Mechanical Gradient Cues for Guided Cell Motility and Control of Cell Behavior on Uniform Substrates. *Advanced Functional Materials*. 2009;19(18):2961-2968.
- [5] Cukierman E, Pankov R, Stevens DR, Yamada KM. Taking Cell-Matrix Adhesions to the Third Dimension. *Science*. 2001;294(5547):1708-12.

- [6] Chicurel M. Cell migration research is on the move. *Science*. 2002;295(5555):606-9.
- [7] Discher DE, Janmey P, Wang YL. Tissue cells feel and respond to the stiffness of their substrate. *Science*. 2005;310(5751):1139-43.
- [8] Engler AJ, Sen S, Sweeney HL, Discher DE. Matrix elasticity directs stem cell lineage specification. *Cell*. 2006;126(4):677-89.
- [9] Erickson CA and Nuccitelli R. Embryonic fibroblast motility and orientation can be influenced by physiological electric fields. *The Journal of Cell Biology*. 1984;98:296-307.
- [10] Euteneuer U, and Schliwa M. The Function of Microtubules in Directional Cell Movement. *Annals of the New York Academy of Sciences*. 1986;466(1):867-886.
- [11] Fuard D, Tzvetkova-Chevolleau T, Decossas S, Tracqui P, Schiavone P. Optimization of poly-di-methyl-siloxane (PDMS) substrates for studying cellular adhesion and motility. *Microelectronic Engineering*. 2008;85:1289-1293.
- [12] Guido S, Tranquillo RT. A methodology for the systematic and quantitative study of cell contact guidance in oriented collagen gels. Correlation of fibroblast orientation and gel birefringence. *Journal of Cell Science*. 1993;105 (Part 2):317-331.
- [13] Guo WH, Frey MT, Burnham NA, Wang YL. Substrate rigidity regulates the formation and maintenance of tissues. *Biophysical Journal*. 2006;90(6):2213-20.
- [14] Harris AK. Behavior of cultured cells on substrata of variable adhesiveness. *Experimental Cell Research*. 1973;77:285-297.
- [15] Hofman P, D'Andrea L, Guzman E, Selva E, Le Negrate G, Far DF, Lemichez E, Boquet P, Rossi B. Neutrophil F-actin and myosin but not microtubules functionally regulate transepithelial migration induced by interleukin 8 across a cultured intestinal epithelial monolayer. *European Cytokine Network*. 1999;10(2):227-36.
- [16] Ionides EL, Fang KS, Isseroff RR, Oster GF. Stochastic models for cell motion and taxis. *Journal of Mathematical Biology*. 2004;48(1):23-37.
- [17] Kaverina I, Krylyshkina O, Small JV. Regulation of substrate adhesion dynamics during cell motility. *The International Journal of Biochemistry & Cell Biology*. 2002;34(7):746-61.
- [18] Lauffenburger DA, Linderman JJ. Receptors: *Models for binding, trafficking, and signaling* (pp. 266 – 276). Oxford University Press, 1993.
- [19] Lo CM, Wang HB, Dembo M, Wang YL. Cell movement is guided by the rigidity of the substrate. *Biophysical Journal*. 2000;79(1):144-52.
- [20] Lowe B. The role of Ca²⁺ in deflection-induced excitation of motile, mechanoresponsive balancer cilia in the ctenophore statocyst. *The Journal of Experimental Biology*. 1997;200:1593-1606.
- [21] McBeath R, Pirone DM, Nelson CM, Bhadriraju K, Chen CS. Cell shape, cytoskeletal tension, and RhoA regulate stem cell lineage commitment. *Developmental Cell*. 2004;6(4):483-95.
- [22] Morse DC. Viscoelasticity of concentrated isotropic solutions of semiflexible polymers. 1. Model and stress tensor. *Macromolecules*. 1998;31(20):7030-7043.
- [23] Morse DC. Viscoelasticity of concentrated isotropic solutions of semiflexible polymers. 2. Linear response. *Macromolecules*. 1998;31(20):7044-7067.
- [24] Parent C and Devreotes P. A Cell's Sense of Direction. *Science*. 1999;284:765-770.
- [25] Pelham RJ Jr, Wang Y. Cell locomotion and focal adhesions are regulated by substrate flexibility. *Proceedings of the National Academy of Sciences of the United States of America*. 1997;94(25):13661-5.

- [26] Pollard TD, and Borisy G. Cellular motility driven by assembly and disassembly of actin filaments. *Cell*. 2003;112(4):453-465.
- [27] Ratner BD, Hoffman AS, Schoen FJ, Lemons JE. *Biomaterials Science, Second Edition: An Introduction to Materials in Medicine* (pp. 246-260). Elsevier AcademicPress, 2004.
- [28] Ren KF. Polyelectrolyte multilayer films of controlled stiffness modulate myoblast cell differentiation. *Advanced Functional Materials*. 2008;18(9).1378-1389.
- [29] Saranak J, and Foster KW. Rhodopsin guides fungal phototaxis. *Nature*. 1997;387:465- 466.
- [30] Saez A. Rigidity-driven growth and migration of epithelial cells on microstructured anisotropic substrates. *Proceedings of the National Academy of Sciences of the United States of America*. 2007;104(20):8281-8286.
- [31] Wang JHC, Jia FY, Gilbert TW, Woo SLY. Cell orientation determines the alignment of cell-produced collagenous matrix. *Journal of Biomechanics*. 2003;6(1):97-102.
- [32] Wang N, Tolic-Norrelykke IM, Chen J, Mijailovich SM, Butler JP, Fredberg JJ, Stamenovic D. Cell prestress. I. Stiffness and prestress are closely associated in adherent contractile cells. *American Journal of Physiology-Cell Physiology*. 2002;282(3):C606-C616.
- [33] Encyclopædia Britannica Online (<http://www.britannica.com/>)

CHAPTER 3

A Computational Model for Durotaxis

1. Introduction

The experimental findings regarding cell migration mechanisms can benefit from modelling work, as mathematical models are a tool for better interpreting such observations. Therefore, quite a few mathematical models have been developed and provide physical insight into cell migration. The two principal ways to model cell migration and correlated phenomena consist in a diffusive approach and a discrete approach. The discrete approach is often based on the mechanical equilibrium of a single cell considered as a point mass subjected to external forces; other approaches, on the other hand, are based on a weighted balance of vectors representing the factors influencing cell motion. In any case, with this approach it is possible to obtain the path of each simulated cell as a result and this can be interesting for the comparison with cell-tracking experiments in which individual cell paths are collected, and for checking the validity of specific hypotheses. Unfortunately, though, it is very difficult with this procedure to take into account cell-cell interactions, so it is generally used for low cell densities.

In the diffusive approach cells appear through their concentration, whose changes in time and space are used to describe cell migration. As a result, this approach allows to consider high cell densities easily, since cell-cell interactions need not be modelled explicitly, but it does not allow to solve for the single cells trajectories. From the mathematical point of view, cells are considered like the concentration of a certain diffusible substance, therefore the equations comprising the model are essentially derived from Fick's laws of diffusion. The first papers using this approach date back to the seminal works of Patlak (1953) and of Keller and Segel (1971). For instance, Barocas and Tranquillo (1997) used a diffusive model to study the interplay between cell migration and tissue reorganization. Anyway, for a recent review on other continuous models the reader is referred to the review by Painter (2009).

Concerning the discrete approach, different kinds of cell motion are modelled: Zaman and coauthors (2005) model random motility in three dimensional matrices, Dickinson and Tranquillo (1992) model both random motility and haptotaxis, Tranquillo and Lauffenburger (1987), Stokes and Lauffenburger (1991) and Jabbarzadeh and Abrams (2005) model chemotaxis in different conditions; in the works of Dallon and coauthors (1999) and of McDougall and coauthors (2006), a discrete model for cell migration and tissue reorganization is considered. Moreover, galvanotaxis is modelled using stochastic differential equations by Schienbein and Gruler (1993). Concerning durotaxis modelling, to author's knowledge, it has been studied only using the diffusive approach by Moreo and coworkers (2008).

In the present work a simple discrete model for durotaxis was developed, through which one can obtain simulated cell paths on different types of substrata. Such a model is based on a force balance considering the forces acting on the cell. The substratum stiffness is taken into account by using a procedure that is reminiscent of the probing mechanism that cells actually use during motion.

2. The Langevin Equation in the Modelling of Cell Migration

In a cell tracking experiment cell migration is conveniently studied by time lapse microscopy, i.e. by taking a regularly distributed series of microscope scans of a group of motile cells that are moving over a substratum. In this way the apparent trajectory obtained from each cell is a broken line that links together cell centroid locations evaluated at different time steps. In the absence of external guidance cues, such steps are taken randomly, so that the process of cell motility appears to be a probabilistic or stochastic process. These features inspired a similarity between the phenomenon of cell migration and Brownian motion of particles within a fluid at rest: although the fundamental mechanisms by which cells move are radically different from the thermally originated movement of particles, the observation of the motility of individual cells reveals comparable random walk-like behaviour, indicating a similar stochastic nature and suggesting that a related mathematical description might be appropriate (Dunn and Brown, 1987; Stokes *et al.*,1991; Schienbein and Gruler, 1993; Ionides *et al.*,2004; Selmeczi *et al.*, 2005).

A very common model that is used for Brownian motion is the Langevin equation, which is one of the easiest dynamical stochastic differential equations. Its solution is an Ornstein-Uhlenbeck process, that is the simplest type of continuous autocorrelated random motion process (Papoulis 1991; Stokes *et al.*,1991). Letting $\mathbf{x}(t)$ be the position of a cell on the substratum, as a function of time t , the formulation of the Langevin equation resembles Newton's second law of motion under the assumptions that the cell experiences two forces, namely:

- (i) a systematic (deterministic) force $-\zeta \frac{d\mathbf{x}}{dt}$ which is proportional to the velocity of the cell and represents the dissipative forces that tend to slow cell movement down;
- (ii) a fluctuating (stochastic) force $\mathbf{F}(t)$, often called the Langevin force, which is due to all the probabilistic processes that might affect cell motility.

The resulting equation then reads:

$$m \frac{d^2 \mathbf{x}}{dt^2} = -\zeta \frac{d\mathbf{x}}{dt} + \mathbf{F}(t) \quad (1)$$

where m is the mass of the cell. Following the work of Doob (1942) this equation can be rewritten in incremental form as follows:

$$d\mathbf{v}(t) = -\beta \mathbf{v}(t) dt + d\mathbf{B}(t) \quad (2)$$

in which the velocity $\mathbf{v}(t)$, i.e. the time derivative of $\mathbf{x}(t)$, has been employed and the coefficient β is such that $\zeta/m = \beta$. In writing the stochastic term in the incremental form, it becomes a stochastic differential process per unit mass, namely $d\mathbf{B}(t)$.

In order to solve the Langevin equation some assumptions need to be made about the stochastic nature of $d\mathbf{B}(t)$. In particular, $\mathbf{B}(t)$ is usually considered a Wiener process, thus $d\mathbf{B}(t)$ is a Gaussian distributed stochastic process with average zero and standard deviation equal to αdt , where α is a constant and dt is the incremental time interval (Coffey *et al.*, 1996). In the case of Brownian motion, if one assumes that the stochastic process is independent of the position $\mathbf{x}(t)$ and uses the

equipartition theorem of energy, the Langevin equation can be solved for the average value of $\mathbf{x}(t)$ (Coffey *et al.*, 1996). Indicating with E the expected-value operator it is possible to obtain a function $\langle D^2 \rangle(t) = E\{\left[\mathbf{x}(t) - \mathbf{x}(0)\right]^2\}$ (i.e. the mean square displacement, or MSD), that depends on the time considered in the integration, as reported in Stokes *et al.* (1991).

Numerical solutions for the Langevin equation are also possible using a random number generator and a stochastic numerical method. In a stochastic numerical method the solution is sought in a stepwise fashion, for example in the case of the stochastic Euler method (Wright, 1974), the stochastic differential equation must be discretised regularly in time using time increments Δt

$$\mathbf{v}(t + \Delta t) - \mathbf{v}(t) = -\beta\mathbf{v}(t)\Delta t + \mathbf{B}(t + \Delta t) - \mathbf{B}(t) \quad (3)$$

and the solution in terms of velocity is then stepwise constructed knowing the initial velocity. The trajectory, i.e. the cell position as a function of time $\mathbf{x}(t)$, can then be constructed by integration with respect to time t , knowing the initial position of the particle.

If the Langevin equation is used to model cell migration, one can reproduce the most important aspects of cell motion, including the basic elements of randomness as well as persistence or inertia, i.e. the tendency of a cell to continue moving in the same direction (Lauffenburger and Lindermann, 1991). This equation has in fact been successfully used to model cell migration in the case of random motility and also in the case of chemotaxis the Langevin equation can be slightly modified by adding a drift term that depends on the position and strength of the chemoattractant and yields significant results comparable with experimental observations (Stokes *et al.*, 1991). The case of durotaxis, though, is more complex and can hardly be reproduced by using a simple drift term. In this case it can be inspiring to recall the actual cell behaviour.

3. A Discrete Model for Durotaxis

The cell movement over a substratum (e.g. a cell culture plastic dish) occurs typically in a discontinuous manner, i.e. as a sequence of steps separated by a quiescence time, as seen in chapter 2. By carefully observing a migrating cell at the microscope it can be seen that, before each step is taken, the cell sends local protrusions (lamellipodia), mainly composed of actin, around its body in a few directions and exerts through them contractile forces on the substratum. The objective of this procedure seems to be to probe the substratum local stiffness: cell-extracellular matrix (ECM) linkage through focal adhesions is more stable on stiff substrata; in contrast, focal adhesion of cells on soft substrata are more dynamic (Pelham and Wang, 1997). Since this mechanism takes place at every cell step, it inevitably generates a bias that guides the cell away from soft regions and towards stiffer regions. However, migration would still remain a fundamentally stochastic phenomenon. For instance, the cell does not probe each and every direction, random fluctuations can occur in the dynamics of focal complexes that regulate adhesion or in the intracellular signal trafficking that governs the motile sensing and response mechanism. (Friedrichs *et al.*, 2007). A model for durotaxis should take this cellular behaviour into account, a possible way for doing this is described next.

First, let consider the standard Langevin equation, and for simplicity let restrict to the 2-dimensional case. Both scalar components of the stochastic term in (2), $d\mathbf{B}(t)$, have a normal distribution (i.e. a Gaussian distribution with zero mean) in a Cartesian coordinate system, by definition. Representing it in polar coordinates, then the radial and angular components do not follow a normal distribution anymore, but a Rayleigh distribution and a uniform distribution between 0 and 2π , respectively (Papoulis, 1991). The uniform distribution for the angular component in case of an isotropic and homogeneous substratum is very reasonable: basically it states that every direction is equiprobable.

In durotaxis conditions this is no longer true, thus the uniform probability distribution of the angular component must be substituted with one that makes the directions of higher stiffness more probable. One example of this is migration occurring over an anisotropic substratum. Moreover, if the substratum is inhomogeneous, such a distribution must be also position dependent, in contrast with the simple Eq. (2).

A way for constructing such a probability distribution can be inspired by the probing mechanism described before. This, in fact, can be schematized as a mechanical problem: the cell applies a known distribution of forces around its perimeter in order to check the local deformation of the substratum. Here, for simplicity, it will be assumed that the cell is a circle of diameter d and that the forces will be radial and oriented towards the cell centre (Fig. 1).

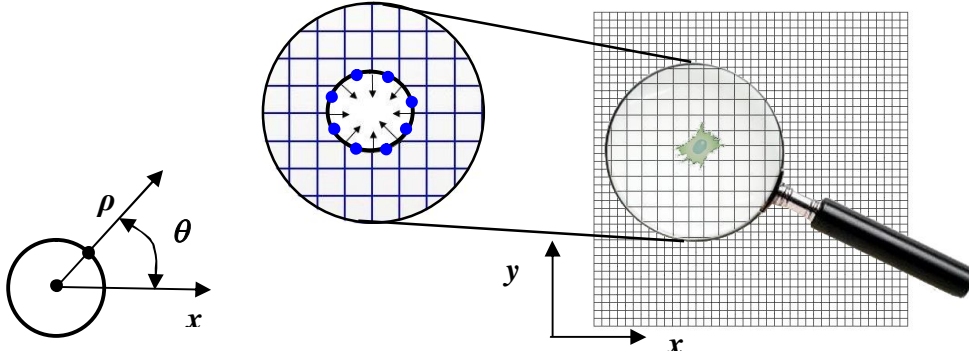


Fig. 1: Schematization utilized in the model, of the substratum probing done by a single cell and direction of the stiffness $k(\vartheta)$ measured through the computational algorithm.

As a result local stiffer directions will yield smaller displacements. A suitable measure of the local stiffness as a function of the direction ϑ can then be chosen as

$$k_{\bullet_x}(\vartheta) = \frac{1}{\lambda} \quad \lambda = \max \{ \mathbf{u}(\vartheta) \cdot \boldsymbol{\rho}, \lambda_0 \} \quad \vartheta \in [0, 2\pi] \quad (4)$$

where $\mathbf{u}(\vartheta)$ is the displacement field along the cell border, $\boldsymbol{\rho}$ is the unit vector directed from the point on the cell border to the cell centre, and $\lambda_0 = 10^{-3}d$ is assumed to be the minimum displacement that the cell is able to sense. Basically Eq. (4) states that a suitable measure for the local stiffness as a function of direction is the reciprocal of the radial displacement component. Notice that the subscript \bullet_x has been used on k to mean that the stiffness measure implied by (4) is local, as in general it will depend on the geometry (i.e. shape, constraints) and the mechanical properties of the substratum but also on the position of the cell.

Once k_{\bullet_x} is known, a suitable probability density function P_k can be constructed as follows:

$$P_k(\vartheta) = \frac{k_x(\vartheta)}{\int_0^{2\pi} k_x(\xi) d\xi} \quad \vartheta \in [0, 2\pi], \quad (5)$$

which indeed has the property of having higher values along directions where the local stiffness, measured through k_x , is higher.

Concerning the radial component of the stochastic term $d\mathbf{B}$ it will simply maintain the Rayleigh probability distribution, i.e. the distribution it would have if cell migration occurred as in the standard Langevin equation. Thus the new model takes the form

$$d\mathbf{v}(t) = -\beta\mathbf{v}(t)dt + d\tilde{\mathbf{B}}(t, k_x(\theta)), \quad (6)$$

where the new stochastic term $d\tilde{\mathbf{B}}$ that depends on the local stiffness has been employed.

The determination of k_x must be performed at every cell step at the position occupied by the cell at current time t . This is akin to a standard problem of solid mechanics: despite its analytical solution might be too difficult to obtain, except in very simple cases, its numerical solution is quite straight forward and therefore it can be conveniently implemented, for example, through the Finite Element Method (FEM) once the cell position, the geometry of the substratum and its mechanical properties are known. The details of this implementation are given below.

The model was solved using a dimensionless method. To do that the following non dimensional variables were used:

$$\mathbf{V} = \frac{\mathbf{v}}{\sqrt{\alpha/\beta}} \quad (7)$$

$$\mathbf{X} = \frac{\mathbf{x}}{\sqrt{\alpha/\beta^3}} \quad (8)$$

$$\tau = t\beta \quad (9)$$

Substituting these definitions into equations (2)

$$d\mathbf{V}(\tau) = -\mathbf{V}(\tau)d\tau + d\hat{\mathbf{B}}(\tau, k_x(\mathcal{G})) \quad (10)$$

and for the position

$$\mathbf{X}(t) = \mathbf{X}_0 + \int_0^t \mathbf{V}(\tau')d\tau' \quad (11)$$

in which $d\hat{\mathbf{B}}$ is the dimensionless stochastic term.

In order to simulate the cell paths equations (2) and the subsequently evaluation of the position have been solved numerically using the stochastic Euler method combined with the random number generator of MATLAB. In particular, velocity and position at the i -th time step, \mathbf{V}_i and \mathbf{X}_i , are given by:

$$\mathbf{V}_i = \mathbf{V}_{i-1}(1 - \Delta t) + \Delta\hat{\mathbf{B}}_i \quad (12)$$

and

$$\mathbf{X}_i = \mathbf{X}_{i-1} + \mathbf{V}_i\Delta\tau \quad (13)$$

Notice that in this scheme the cell velocity is calculated using an explicit method while position is calculated with an implicit method. Such a procedure yields better results in the case of random motility, i.e. in the case where the standard Langevin equation case has to be recovered.

In order to obtain the angular probability distribution for the stochastic term $\Delta\hat{\mathbf{B}}_i$, the stiffness k_x must be evaluated at every cell step. This can be done by solving a linear elasticity problem numerically using the FEM. The domain is discretised using four nodes square elements with two degrees of freedom per node. For the case of random motility 10000 elements were used while for the biphasic domain case a total of 6400 elements were used¹. Once the position of the cell is known, a radial forces distribution is applied at 12 equally spaced points along a circumference whose

¹ the computational algorithm for the biphasic domain is more complex so less elements are used to avoid computational problems

centre is the cell position and radius equals $25\ \mu\text{m}$ (see Fig. 1). The force intensity is assumed to be equal to 1nN , in agreement with the work of Oliver and coworkers (1994). The points where the forces are applied are points of singularity where the displacement cannot be evaluated, therefore the measure of the displacement is done on a different set of points, i.e. the ones denoted with a blue dot in Fig. 1; these points are in fact shifted by 15° along the same circumference. Once the displacements are known at these points, the displacement of all the points of the circumference can be evaluated by interpolation, so that the stiffness k_x can be evaluated and finally the local probability distribution can be obtained. This procedure must be repeated for every cell and at every cell step. The MATLAB scripts of the model is reported in the Appendix of this thesis.

The model presented has been solved for two particular cases, namely migration over a homogeneous and isotropic substratum and migration over a biphasic substratum, i.e. a substratum composed of two adjacent isotropic regions possessing markedly different mechanical properties. The first case is important to check that the standard Langevin equation is recovered as a particular case in conditions of random motility. The second case is the one studied by Lo and coworkers (2000) and it is important since in that paper was durotaxis first introduced and discussed from an experimental point of view.

4. Two Particular Cases for Preliminary Validation

In order to compare the predictions of the model to the experimental results that can be found in the literature, first it is necessary to introduce a certain number of measurable quantities that can be used to describe and quantify the phenomenon of cell migration in an averaged sense. These quantities should also allow to compare the model predictions with the experimental findings.

One of the most widely used of such quantities is the MSD, already introduced in section 2 of this chapter. The MSD gives information about the average distance travelled by a cell during migration as a function of time. Clearly the MSD does not contain any information regarding directionality in the cell movement, therefore, in order to complete the characterisation of cell migration it is worthy to introduce two

angular quantities, namely the angles between adjacent segments of the cell paths, indicated with γ_i , and the angles of every path segment with respect to a fixed direction (e.g. the x direction), denoted with δ_i . Angles similar to these, have also been used in the in the works of Gail and Boone (1970) and of House and coworkers (2009) and in the review by Beltman and coauthors. (2009). Indicating with \mathbf{r}_i the i -th cell path step, γ_i and δ_i have the following expressions:

$$\gamma_i = \arccos\left(\frac{\mathbf{r}_i \cdot \mathbf{r}_{i+1}}{\|\mathbf{r}_i\| \|\mathbf{r}_{i+1}\|}\right) \quad (7)$$

$$\delta_i = \arccos\left(\frac{\mathbf{r}_i \cdot \mathbf{e}_x}{\|\mathbf{r}_i\|}\right)$$

For the sake of clarity these two quantities are pictured in Fig. 2 for a generic cell path. By definition γ_i is related to the tendency of the cell of moving in a rectilinear fashion, while δ_i represents the direction chosen by the cell at every step. It immediately follows from (7) that both γ_i and δ_i belong to the interval $[0, \pi]$.

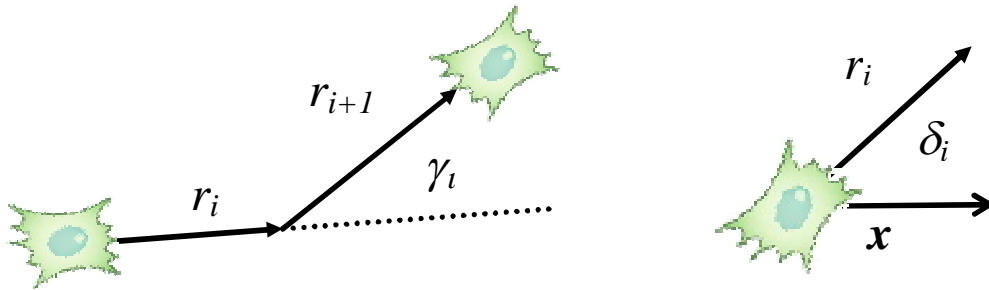


Fig. 2: The definition of the angles used to describe cell migration. In particular, γ_i is the angle between adjacent segments in a path and δ_i is the angle between a path segment and a fixed direction.

Let us consider first the case of cell migration over a homogeneous and isotropic substratum. As there is nothing that guides cell motion, random motility should be observed, thus this case will be used to compare the results of the model with the results of the standard Langevin equation. In particular, the MSD of the cells calculated on the basis of the simulation will be checked against the analytic expression of the MSD obtained by Doob (1942):

$$\langle D^2 \rangle(\Delta t) = 2 \frac{\alpha}{\beta^3} (\beta \Delta t - 1 + e^{-\beta \Delta t}). \quad (8)$$

In particular, in keeping with the experimental work of Stokes and coworkers (1991) for endothelial cells, the migration parameters can be assumed to be $\alpha = 23.2 \mu\text{m}^2/\text{h}^3$ and $\beta = 0.15 \text{ h}^{-1}$. Concerning the model prediction, the paths of 50 cells followed for 24 hours were simulated, over a $800 \times 800 \mu\text{m}$ square region, having assumed as the starting point for each cell the centre of the square region. For simplicity, the substratum is assumed to be linearly elastic and isotropic with a Young's modulus of 100 MPa and a Poisson's ratio of 0.2 (Table 1).

| Random Motility Parameter | |
|---------------------------|-----------|
| E [MPa] | 100 |
| Poisson ratio | 0.2 |
| Applied force [N] | 10^{-9} |
| Number of cells | 50 |
| Length of simulation [h] | 24 |

TABLE 1: Parameters utilized in the case of random motility.

| Biphasic Domain Parameters | |
|----------------------------|-----------|
| E_1 [MPa] | 1 |
| E_2 [MPa] | 1000 |
| Poisson ratio | 0.2 |
| Applied force [N] | 10^{-9} |
| Number of cells | 50 |
| Length of simulation [h] | 12 |

TABLE 2: Parameters for the solution of the biphasic domain configuration.

The paths of the cells are reported in Fig. 3, while the comparison of the MSDs is shown in Fig. 4. Using these paths also the angles γ_i and δ_i have been evaluated and are reported in the histograms of Fig. 5 and 6.

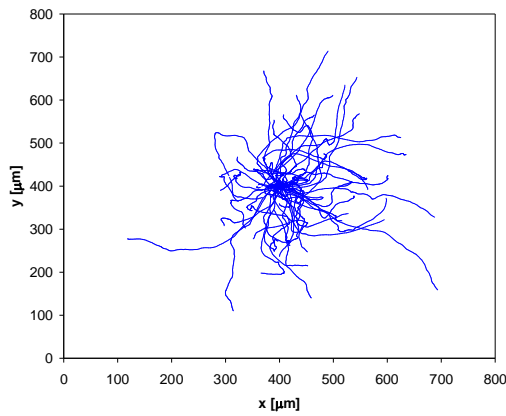


Fig. 3: Graphical windrose representation of 50 cells trajectories starting from the centre, over an isotropic square domain of 800 x 800 μm for 24 hours. The trajecotires are random and there is not preferred direction of migration, so one can speak of random motility.

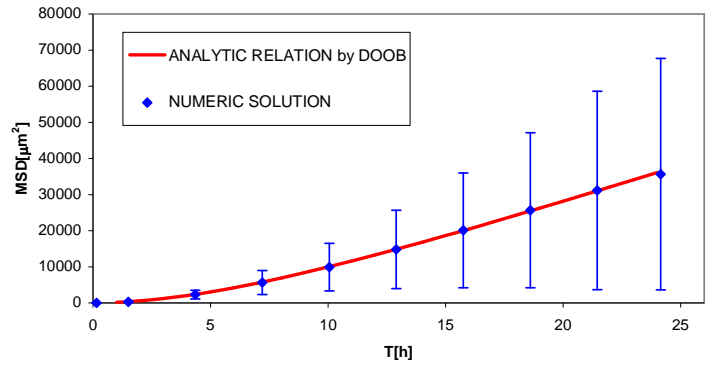


Fig. 4: Comparison between the analytic expression of $\langle D^2 \rangle(\Delta t)$ obtained by Doob, and the numerical evaluation of the same quantity from the model in the case of random motility (50 cell paths, 24 hours over a region of 800x800 μm , with a time step of 9 minutes) and with $\alpha = 23.2 \mu\text{m}^2/\text{h}^3$ and $\beta = 0.15 \text{ h}^{-1}$.

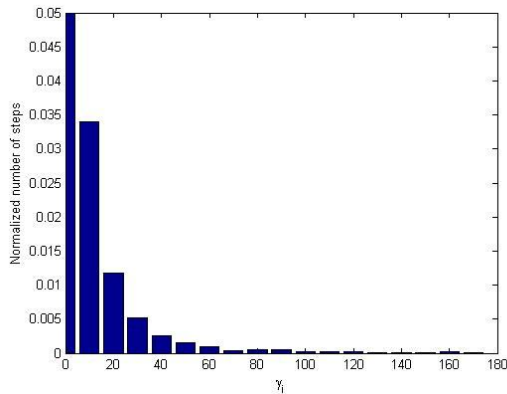


Fig. 5: Graphical representation of the distribution of angles between adjacent segments of the cell paths of 50 cells on an isotropic substratum (i.e. in the case of random motility). Most of the angles have the same value, that means the walk is persistent.

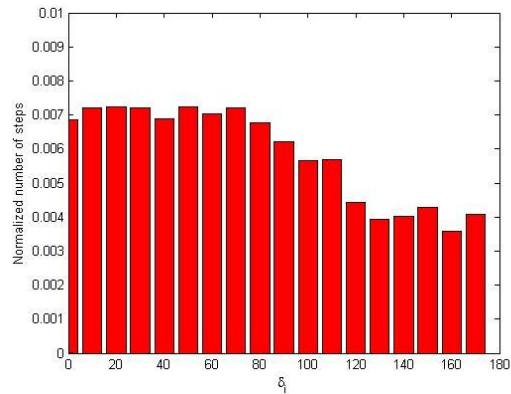


Fig. 6: Graphical representation of the distribution of the angles of the paths' segments respect to a fixed (horizontal) direction, evaluated for 50 cells on a isotropic substratum (i.e. in the case of random motility). It is possible to note that there are not preferred direction and the angle approximately assume all the possible values.

In the second case of interest, i.e. the biphasic domain, durotaxis can be fully appreciated (Lo *et al.*, 2000), thus a square domain has been considered, measuring 500x500 μm , composed of two regions, both linearly elastic, but with different mechanical properties (Table 2). As in the previous analysis, 50 cells starting from

the centre of the substratum have been considered and their trajectories simulated (Fig. 7).

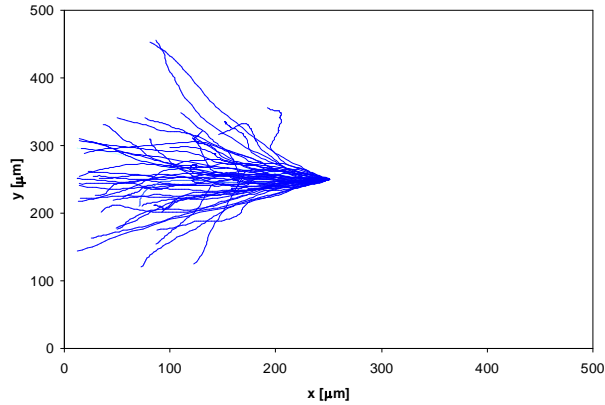


Fig. 7: Trajectories of 50 cells spreading from the centre, over a biphasic square domain of 500x500 μm for 12 hours. All the cells move from the centre to the stiff region of the domain, as expected from the experimental studies of Lo and coworkers (2000).

The evaluations of γ_i and δ_i for this case are reported in Fig. 8 and Fig. 9.

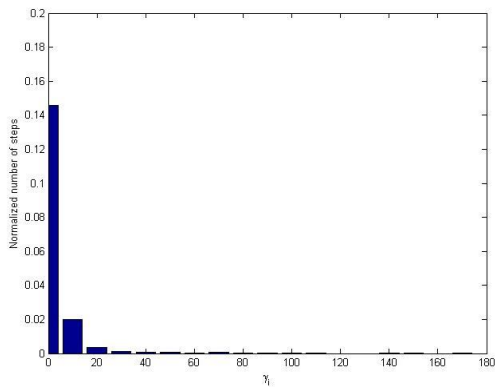


Fig. 8: Graphical representation of the distribution of angles between adjacent segments of the cell paths of 50 cells on a biphasic substratum. Also in this case the walk is persistent, as one can see from the peak of the figure.

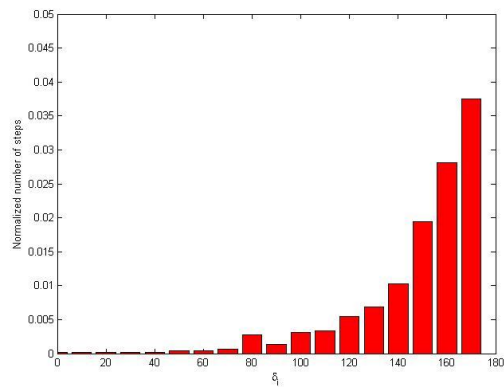


Fig. 9: Graphical representation of the distribution of the angles of the paths' segments respect to a fixed (horizontal) direction, evaluated for 50 cells on a biphasic substratum. As cells migrate preferentially on the stiff region, i.e. on the left part of the substratum, most of the angles are between 90° and 180° .

In Fig. 10 the trajectory of two cells starting from the stiffer region and of two cell starting from the softer region are reported, to make a direct comparison with the experiment of Lo and coworkers (2000).

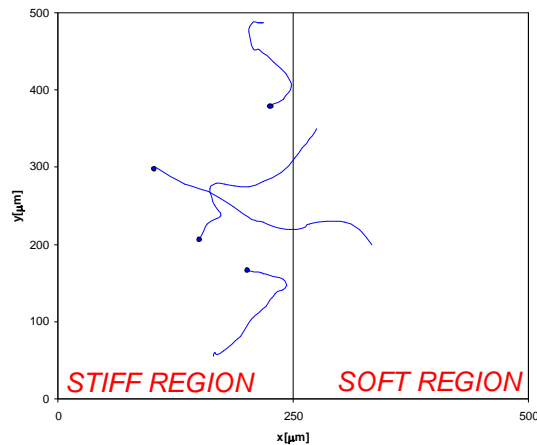


Fig. 10: Simulated result for the experimental evidence of Lo and coworkers (2000). Cells moving from the stiffer region does not move to the softer; cells moving from the softer region moves toward the stiffer one. (The ending point is evidenced)

5. Discussion

Considering the random motility case, from Fig. 3 it is clear that the cells move in every direction, as expected. In addition, comparing the curve obtained from the numerical evaluation of the MSD with Eq. (8), the agreement is very good (Fig. 4). From Fig. 5 it appears that most of the angles between adjacent segments (i.e. the γ_i angles) are very small, say, less than 10° : this means that this is a case of a persistent random walk, while from Fig. 6 showing the histogram of the δ_i angles, it is clear that the path segments are oriented along a quasi uniform distribution, as in the standard Langevin equation. Therefore it is possible to say that when cell migration occurs over an homogeneous and isotropic substratum, the model recovers the standard Langevin equation as a particular case and this is a preliminary validation for the present model.

Considering the results for the biphasic domain; it is clear to see from Fig. 7 that all the cells that were simulated starting from the centre of the domain migrate towards the stiff region, in agreement with the experimental findings of Lo and coworkers (2000). Also in this case the cells follow a persistent walk, since the distribution of angles between adjacent path segments has a peak near the zero direction as depicted in Fig. 8. From Fig. 9 all the δ_i angles are distributed predominantly in the 90° - 180° interval and this suggests that cells move towards the stiffer region. There

are no quantitative data known to the author regarding cell migration on biphasic substrata, therefore an experimental campaign to provide quantitative validation to the model will be presented in the next chapter.

After observing that the model gives results that are at least in qualitative agreement with experimental data from the literature, some considerations about the hypotheses that were formulated can be made. Although the model that was formulated does not require using a linearly elastic constitutive law for the substratum, such a law is assumed for both the substrata simulated. Despite a more general viscoelastic perhaps even nonlinear law would have been more adequate, it must be considered that during the probing phase the cell applies forces on the substratum within a characteristic time scale that is in the range of 100 ms up to 1s (Kress *et al.*, 2007). If such characteristic times are much smaller than the average relaxation times of the substratum, then it appears to the cell as if it were substantially elastic. Moreover, it is also assumed that due to the very small forces applied by the cells (Oliver *et al.*, 1994; Kress *et al.*, 2007), deformations of the substratum are also very small and this leads to the hypothesis of linearity in the elastic response. Needless to say, these assumptions permit to simplify the FEM setting of the problem, and thus to reduce the computational time requested for the numerical solution.

The major limitation of the present model is that it can be compared only with experiments using low cell densities. This limitation is common to all the discrete models published so far (Flaherty *et al.*, 2007). In fact, if many cells are considered, the stiffness perceived by a single cell is altered by the contractile forces exerted by the other ones in its neighbourhood (Lo *et al.*, 2000). In addition, cell-cell contacts may occur and these are known to influence the migratory behaviour (Nakao *et al.*, 2008). Since the multiple and simultaneous events that take place during cell-cell contact are largely unknown, it is very difficult to quantify and model such interactions.

This notwithstanding, a large body of experimental data on cell migration are indeed based on low cell density assays and this model does represent this situation (Walmod *et al.*, 2001). Moreover, the model is simple and versatile so one can easily implement it for different substrata. In this analysis it has been specialised to two relatively simple cases, but it can be easily adapted also to cases with more complex geometries and materials. Even though it does not describe all the mechanisms that

take part at the cell cytoskeleton (e.g. Di Milla *et al.*,1991), it is able to relate the mechanical properties of the substratum to the path followed by a cell migrating over it, yielding the influence of the substratum stiffness on the cell migration.

Further, the model can be a useful tool to study tissue regeneration and reorganization due to cell migration in tissue engineering applications. In fact, it is known that fibroblasts migration along straight lines leads to the alignment of the newly produced extracellular matrix, mainly collagen, on a scaffold (Wang *et al.*, 2003). Thus the model can be used as a starting point to design a scaffold that guides cell migration through its mechanical properties (see chapter 5) and this leads to the production of an engineered tissue with a predetermined collagen alignment.

6. References

- [1] Barocas VH and Tranquillo RT. An anisotropic biphasic theory of tissue-equivalent mechanics: the interplay among cell traction, fibril network deformation, and contact guidance. *Journal of Biomechanical Engineering*. 1997;119(2):135-147.
- [2] Barocas VH and Tranquillo RT. A finite element solution for the anisotropic biphasic theory of tissue-equivalent mechanics: the effect of contact guidance on isometric cell traction measurement. *Journal of Biomechanical Engineering*. 1997;119(3):261-269.
- [3] Beltman JB, Marée AF, de Boer RJ. Analysing immune cell migration. *Nature Reviews Immunology*. 2009;9(11):789-98.
- [4] Carletti M. Numerical solution of stochastic differential problems in the biosciences. *Journal of computational and applied mathematics*. 2006;185(2):422-440.
- [5] Coffey WT, Kalmykov YP, Waldron JT. *The Langevin Equation: With Applications in Physics, Chemistry, and Electrical Engineering* (pp. 1-143). World Scientific, 1996.
- [6] Dallon JC, Sherratt JA, Maini PK. Mathematical Modelling of Extracellular Matrix Dynamics using Discrete Cells: Fiber Orientation and Tissue Regeneration. *Journal of Theoretical Biology*.1999;199:449-471.
- [7] Dickinson RB, Tranquillo RT. A stochastic model for adhesion-mediated cell random motility and haptotaxis. *Journal of Mathematical Biology*. 1993;31(6):563-600.
- [8] DiMilla PA, Barbee K, Lauffenburger DA. Mathematical model for the effects of adhesion and mechanics on cell migration speed. *Biophysical Journal*. 1991;60(1):15-37. Erratum in: *Biophysical Journal*. 1991;60(4):983.
- [9] Doob JL. The Brownian Movement and Stochastic Equations. *Annals of Mathematics*.1942;43:351-369.
- [10] Dunn GA, Brown AF. A unified approach to analysing cell motility. *Journal of Cell Science-Supplement*. 1987;8:81-102.
- [11] Flaherty B, McGarry JP, McHugh PE. Mathematical models of cell motility. *Cell Biochemistry and Biophysics*. 2007;49(1):14-28.

- [12] Friedrichs J, Taubenberger A, Franz CM, Muller DJ. Cellular remodelling of individual collagen fibrils visualized by time-lapse AFM. *Journal of Molecular Biology*. 2007;372(3):594-607.
- [13] Gail MH, Boone CW. Locomotion of Mouse Fibroblasts in Tissue Culture. *Biophysical Journal*. 1970;10(10):980-993.
- [14] Ghosh K, Ingber DE. Micromechanical control of cell and tissue development: implications for tissue engineering. *Advanced Drug Delivery Reviews*. 2007. 10;59(13):1306-18.
- [15] Gracheva ME, Othmer HG. A continuum model of motility in ameboid cells. *Bulletin of Mathematical Biology*. 2004;66(1):167-93.
- [16] House DM, Walker M, Wu Z, Wong J, Betke M. Tracking of Cell Populations to Understand their Spatio-Temporal Behavior in Response to Physical Stimuli. In *IEEE Conference on Computer Vision and Pattern Recognition Workshop on Mathematical Modeling in Biomedical Image Analysis (MMBIA 2009)*. 2009:186-193.
- [17] Ionides EL, Fang KS, Isseroff RR, Oster GF. Stochastic models for cell motion and taxis. *Journal of Mathematical Biology*. 2004;48(1):23-37.
- [18] Jabbarzadeh E, Abrams CF. Chemotaxis and random motility in unsteady chemoattractant fields: a computational study. *Journal of Theoretical Biology*. 2005;235(2):221-32.
- [19] Keller EF, Segel LA. Model for Chemotaxis. *Journal of Theoretical Biology*. 1971;30(2):225-234.
- [20] Kress H, Stelzer EH, Holzer D, Buss F, Griffiths G, Rohrbach A. Filopodia act as phagocytic tentacles and pull with discrete steps and a load-dependent velocity. *Proceedings of the National Academy of Sciences of the United States of America*. 2007;104(28):11633-8.
- [21] Lo CM, Wang HB, Dembo M, Wang YL. Cell movement is guided by the rigidity of the substrate. *Biophysical Journal*. 2000;79(1):144-52.
- [22] Martens L, Monsieur G, Ampe C, Gevaert K, Vandekerckhove J. Cell_motility: a cross-platform, open source application for the study of cell motion paths. *BMC Bioinformatics*. 2006;7:289.
- [23] McDougall S, Dallon JC, Sherratt JA, Maini PK. Fibroblast migration and collagen deposition during dermal wound healing: mathematical modelling and clinical implications. *Philosophical Transactions of Royal Society Series A*. 2006;364:1385-1405.
- [24] Moreo P, García-Aznar JM, Doblaré M. Modeling mechanosensing and its effect on the migration and proliferation of adherent cells. *Acta Biomaterialia*. 2008;4(3):613-21.
- [25] Nakao S, Platek A, Hirano S, Takeichi M. Contact-dependent promotion of cell migration by the OL-protocadherin-Nap1 interaction. *Journal of Cell Biology*. 2008;182(2):395-410.
- [26] Oliver T, Lee J, Jacobson K. Forces exerted by locomoting cells. *Seminars in Cell Biology*. 1994;5(3):139-147.
- [27] Painter KJ. Continuous Models for Cell Migration in Tissues and Applications to Cell Sorting via Differential Chemotaxis. *Bulletin of Mathematical Biology*. 2009;71(5):1117-1147.
- [28] Papoulis A. *Probability, Random Variables and Stochastic Processes. Third Edition* (pp. 124-150). McGraw-Hill, 1991.
- [29] Patlak C. Random walk with persistence and external bias. *Bulletin of Mathematical Biology*. 1953;15(3):311-338.

- [30] Reddy JN. *An Introduction to the Finite Element Method. Second Edition.* Mc Graw-Hill, 1993.
- [31] Ridley AJ, Schwartz MA, Burridge K, Firtel RA, Ginsberg MH, Borisy G, Parsons JT, Horwitz AR. Cell migration: integrating signals from front to back. *Science.* 2003;302(5651):1704-9.
- [32] Schienbein M, Gruler H. Langevin equation, Fokker-Planck equation and cell migration. *Bulletin of Mathematical Biology.* 1993;55(3):585-608.
- [33] Selmecki D, Mosler S, Hagedorn PH, Larsen NB, Flyvbjerg H. Cell motility as persistent random motion: theories from experiments. *Biophysical Journal.* 2005;89(2):912-31.
- [34] Stokes CL, Lauffenburger DA. Analysis of the roles of microvessel endothelial cell random motility and chemotaxis in angiogenesis. *Journal of Theoretical Biology.* 1991;152(3):377-403.
- [35] Stokes CL, Lauffenburger DA, Williams SK. Migration of individual microvessel endothelial cells: stochastic model and parameter measurement. *Journal of Cell Science.* 1991;99:419-30.
- [36] Tranquillo RT, Lauffenburger DA. Stochastic model of leukocyte chemosensory movement. *Journal of Mathematical Biology.* 1987;25(3):229-62.
- [37] Walmod PS, Hartmann-Petersen R, Berezin A, Prag S, Kiselyov VV, Berezin V, Bock E. Evaluation of individual-cell motility. *Methods in Molecular Biology.* 2001;161:59-83.
- [38] Wang JHC, Jia FY, Gilbert TW, Woo SLY. Cell orientation determines the alignment of cell-produced collagenous matrix. *Journal of Biomechanics.* 2003;6(1),97-102.
- [39] Wright D. The digital simulation of stochastic differential equations. *IEEE Transactions Automatic Control.* 1974;19(1):75-76.
- [40] Zaman MH, Kamm RD, Matsudaira P, Lauffenburger DA. Computational model for cell migration in three-dimensional matrices. *Biophysical Journal.* 2005;89(2):1389-97.

CHAPTER 4

Experimental Validation of the Model

1. Introduction

In parallel to the theoretical study of durotaxis, an experimental campaign of cell migration experiments were performed with the aim of obtaining an experimental validation of the model presented in chapter 3

The idea was to reproduce substrata on which cells can move in condition of durotaxis and to perform cell migration experiments over them to obtain cell trajectories. Thus, these trajectories can be compared to their simulated counterparts to verify the results of the model.

The material used was polydimethylsiloxane (PDMS), commonly known as silicone. In particular, one of its elastomeric derivatives, Sylgard 184 (Dow Corning) was chosen thanks to its chemical and physical properties.

This part of the work was possible thanks to the collaboration with CRIB (Interdisciplinary Research Centre on Biomaterials, University of Naples “Federico II”), in the person of Dr. M. Ventre, where the materials used were produced and where the experiments were performed.

2. Preparation of the Samples

To obtain an experimental validation of the model similar substrata to those used by Lo et al. (2000) are produced. These substrata have been already described in chapter 2 and 3, and are called biphasic substrata. They are made of two regions of different mechanical properties and this structure generates the durotaxis conditions for cells at the interface. In the cited work the authors used a collagen coated polyacrylamide gel, because in this manner they were able to obtain a series of chemically identical substrata with a wide range of flexibility (Pelham and Wang

1997). Here, PDMS Sylgard 184 (Dow Corning Corp. Midland, MI, USA) was used, inspired by the work of Chou et al. (2009)

PDMS or polydimethylsiloxane is an inorganic polymer of the silicones family. Its structure is reported in Fig.1.

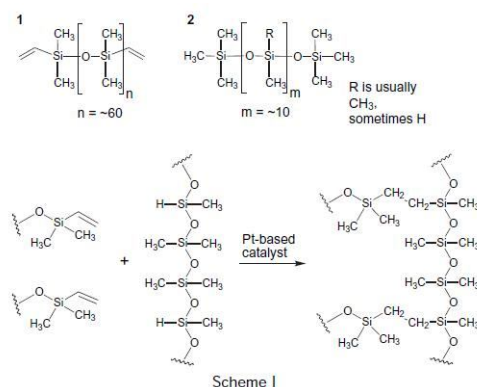


Fig. 1: PDMS Sylgard 184 chemical structure

This polymer is widely used for medical applications (e.g. contact lenses), because it is chemically inert, biocompatible, non flammable and non toxic. After polymerization and cross-linking, solid PDMS samples will present an external hydrophobic surface. This surface chemistry makes it difficult for polar solvents (such as water) to wet the PDMS surface, and may lead to adsorption of hydrophobic contaminants. Solid PDMS samples will not allow aqueous solvents to infiltrate and swell the material. Thus PDMS structures can be used in combination with water and alcohol solvents without material deformation.

The Sylgard 184 PDMS used, is marketed as a kit that contains a “base” and a “curing” agent. The chemistry that leads to the cross-linked polymer is summarized in Fig.1. Both components of the kit contain siloxane oligomers terminated with vinyl groups (1). The curing agent also includes cross-linking siloxane oligomers (2), which contain at least three silicon-hydride bonds. The base includes a platinum-based catalyst that cures the elastomer by an organometallic cross-linking reaction. When (1) ,(2) and the platinum-based catalyst are mixed together, the catalyst aids in the curing of the elastomer, i.e. the addition of the Si-H bonds of (2) across the double bonds of (1) forming Si-CH₂-CH₂-Si linkages (Scheme I); this process is referred to

as hydrosilation of the double bonds. The multiple reaction sites on (2) allow for three dimensional cross-linking (Campbell et al., 1999). One advantage of this type of addition reaction is that no waste products are generated. The cured elastomer obtained is transparent and colorless and changing the curing agent-to-base ratio alters its properties: as the ratio of curing agent-to-base increases, a stiffer elastomer results. Increased temperature will accelerate the cross-linking reaction.

Thus, a 5:1 of base-to-curing ratio of Sylgard 184 was used for the stiff region, and a 30:1 ratio for the soft region. The Young's modulus of the 5:1 PDMS was approximately 800 kPa, and the one of the 30:1 PDMS was approximately 200 kPa (Brown et al., 2005). A plastic sheet with circular holes was put on a glass slide and the holes were filled with the two prepared mixtures. Poly(lactic-co-glycolic acid) (PLGA) micro-spheres were embedded in the stiff region, to be able to recognize it from the soft one, once the samples are observed at the optical microscope. In fact both the mixtures were transparent and with the same refractive index, so they are not optically distinguishable. The samples were cured for 2 hours at 120°C. The procedure is schematized in Fig 2a and the resulting sample observed at the microscope was reported in Fig. 2b.

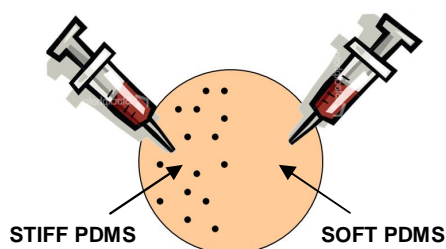


Fig. 2a: Scheme of the procedure used to produce the samples.

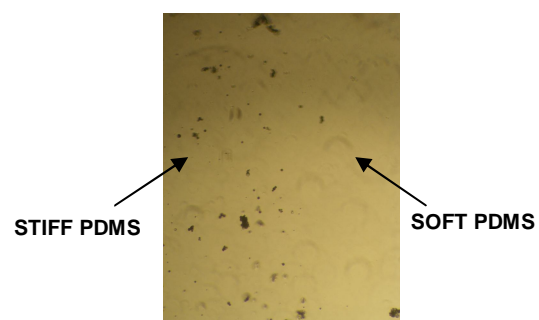


Fig. 2b: Optical microscope image of interface between the two regions in the samples obtained

In this way different biphasic samples were prepared and cell migration experiments were performed over them.

3. Cell Migration Experiments over Biphasic Substrata

To perform cell migration experiments, all the samples produced, were ethanol sterilized and pre-incubated in Dulbecco's modified Eagle Medium (DMEM) for one hour. Primary bovine fibroblast were dissociate from the tissue culture plate. Then the cells (5×10^3 cells/ml) were seeded over the substrata and cultured in an incubator at 37°C and $5\% \text{CO}_2$ in DMEM supplemented with 10% fetal bovine serum (FBS), 2mM L-glutamine, 1000U l^{-1} penicillin and 100mg l^{-1} streptomycin. Cell were pre-incubated for 24 hours to allow for them to attach and spread. Once fibroblast adhered on the samples the migration experiments started. To do this it, time-lapse microscopy technique was used. The instrument used (Fig. 3) is based on an inverted phase contrast optical microscope (IX50, Olympus) equipped with an incubation chamber kept at 37°C , humidified, with $5\% \text{CO}_2$ atmosphere, an x-y-z computer stage, PROSCAN (Prior, USA) and a CCD cool-snap camera (RS Photometrix, USA). The camera and the computerized stage were synchronized by a specific code to follow several cells in the same experiment.

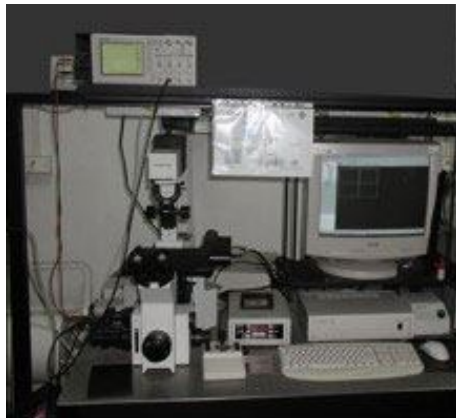


Fig. 3a: Time lapse workstation at CRIB.

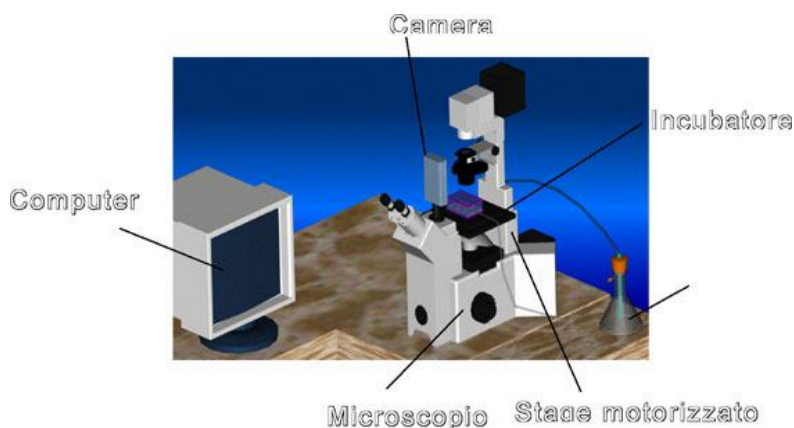


Fig. 3b: Scheme of the time lapse microscopy utilized for the experiments.

The choice of the region to monitor is very important for the attempt to observe durotaxis, because, as already explained, this phenomenon concerns single cells that do not interact with other migrating cells, in a region near the interface. So only single cells near the interface were individuated and monitored. The images were

captured every 10 minutes for 24 hours and analyzed by using the image analysis software Metamorph 5.0 (Fig.4).

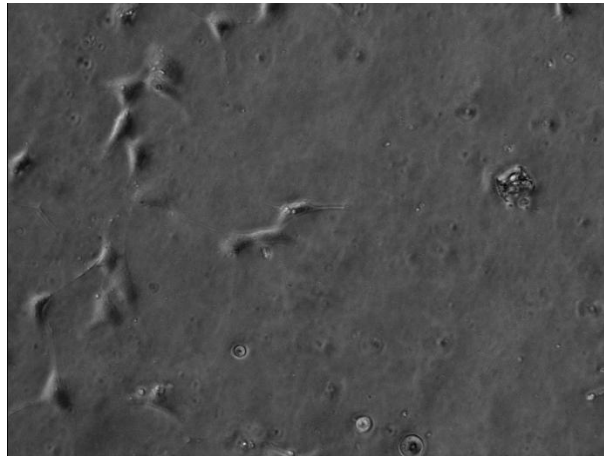


Fig. 4: Primary bovine fibroblasts adhering on a PDMS sample (Optical microscope, 10x Magnification).

Cell trajectories were reconstructed from the positions of the centroid of individual cells at each time point, using an automated image analysis algorithm. X and Y positions of individual cell centroid were stored in a text file.

4. Experimental Results

Following only isolated cells near the interface is a big limitation because not so many cells meet those requirements. In fact, of the tens of cells monitored, just sixteen were suitable for durotaxis analysis. As a consequence, only these trajectories were considered and elaborated with a specific script built using MATLAB (the script is reported in the Appendix). These trajectories are reported in Fig.5.

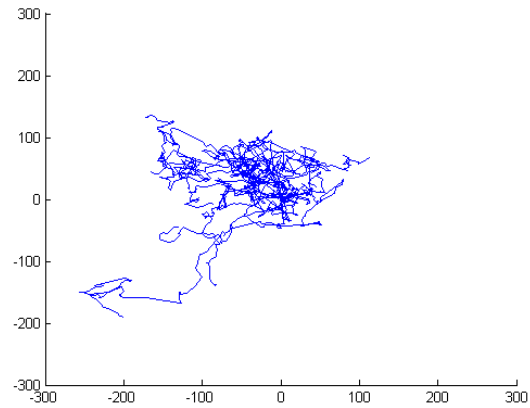
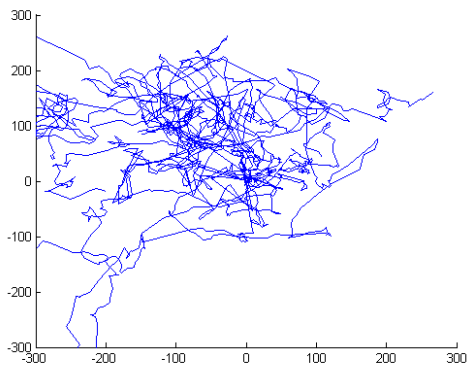


Fig. 5a :Cell trajectories obtained from the experiments.

Fig. 5b: Cell trajectories collapsed in a single point of the domain.

The analysis of the numeric trajectories presented in chapter 3 was based on two angles, namely γ_i and δ_i . In the experimental case evaluating these quantities has no meaning, because cells had different starting points, and this have a big influence on the migration and on all the parameters related to it.

Thus, a different kind of examination was necessary. The cells were split into two groups: the first starting from the stiff region (the left side in the sample monitored) and the second starting from the soft region (the right side) as reported in Fig. 6.

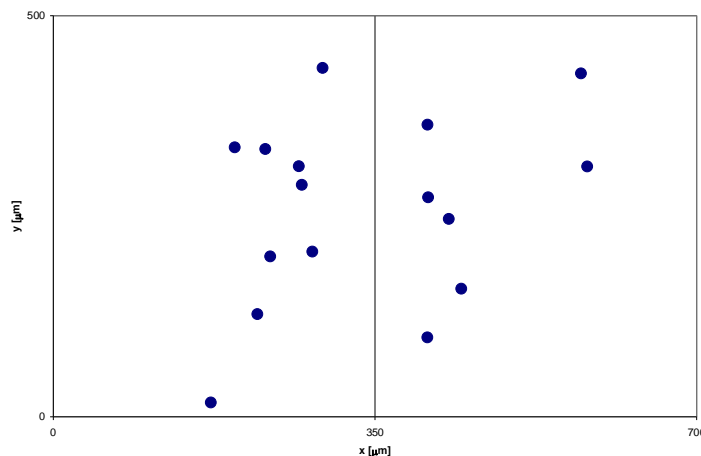


Fig. 6: Starting points of the two groups of cells.

To understand the net movement direction of the cells, the head-tail vectors of every trajectory was evaluated for both groups. Plotting all these vectors from the same point, we obtained the graphs in Fig 6.

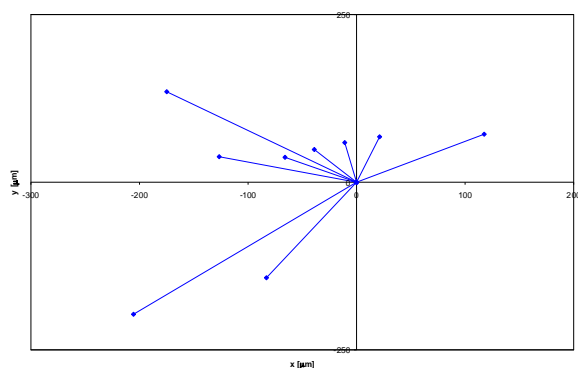


Fig. 6a: Head-tail vectors of cells starting from the stiff region.

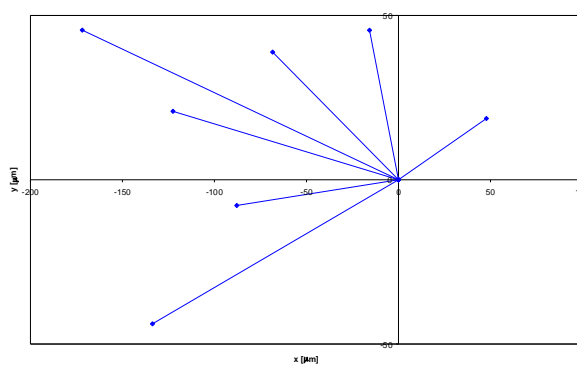


Fig. 6b: Head-tail vectors of cells starting from the soft region.

From these graphs it is clear that the cells starting from the stiff zone move towards the left or if they move to the right, they do not pass the interface; on the other side, almost all the cells starting from the soft region move towards the stiff one, except one.

In conclusion these experiments show a different behaviour of the two groups of cell due to durotaxis. These trajectories are used to make a comparison with the model.

5. Comparison with the Model

When the numerical model described in chapter 3 was developed, it was thought as a tool to aid the analysis of cell behaviour in relation to the mechanical properties of a substratum. In fact, the model gives the possibility to run numeric experiments in pre-determined condition and to obtain information on the behaviour of a population of cells moving on a specific substratum without making tests. Time-lapse imaging experiments are complicated to carry out, and the tracking of cell movement from the resulting outputs is a laborious and error-prone process (Beltman *et al.*, 2009). Such a tool thus can be very helpful, if reliable. To test its reliability the results presented in the previous paragraph were utilized.

The phenomenon of durotaxis is a tendency to move towards a specific region of a substratum, that cells show under specific conditions such as the movement over a biphasic substratum. In the case of chemotaxis, for example, cells tend to move towards a specific point and an index exist to quantify these tendency (the CI index,

see Tranquillo and Lauffenburger, 1987). In the durotaxis case, at author's knowledge, no indexes are defined and used to quantify it. This is mainly because durotaxis is a local effect and is influenced by multiple factors, such as the starting point of the cell, the distance to the interface or the presence of others cells. For these reasons only a qualitative comparison between the numeric and the experimental data is possible.

In order to do that, cells in the same conditions of those monitored in the time lapse-experiments should be simulated, i.e. cells moving on a substratum with the same structure and with the same mechanical properties of the ones described in paragraph 2. Further, also the starting point should be taken into account.

Considering the two groups of cells of Fig. 6, two average distances from the ideal interface (considered as a line) were calculated. Thinking that the vertical coordinate has no influence, all the starting points were collapsed into only two points (the red points of Fig.8) in the middle of the y-axis and at the average distances calculated.

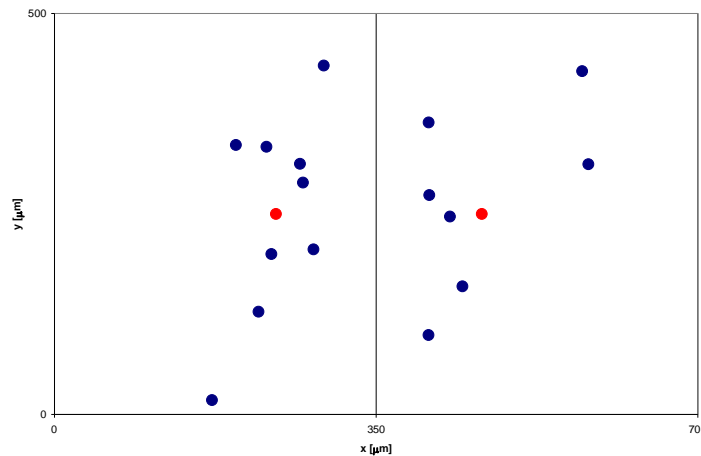


Fig. 8: Mean starting points for the two groups of cell (in red).

From this two points, two populations of 50 cells each were simulated for a 24 hours migration experiment, to observe if the different behaviour emerged from the experiments will be reproduced by the model. As cell parameters of the model (α and β) the same values used in chapter 3 were used (Stokes *at al.*, 1991), while Young's moduli of the PDMS mixtures was considered for the substratum.

6. Results and Conclusions

From the simulated trajectories it is possible to reconstruct the graph of Fig. 9, in which with the two mean starting points, all the final points of the two populations of numeric cells are reported.

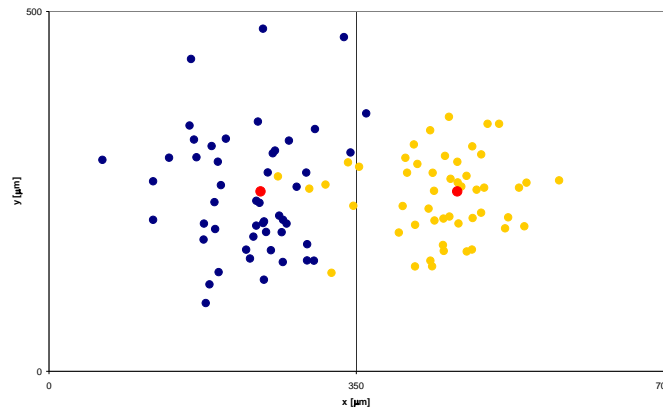


Fig. 9: End points of the two population of 50 cells each simulated for the comparison with experimental data. The blue dots are the end points of the stiffer PDMS starting group; the yellow dots of the softer PDMS starting group.

From the graph it emerges a different behaviour of the two populations and in particular it can be observed that cells starting from the left side tend to move towards the stiff region, as it happens in the experiments. The right side population does not show this tendency and the cells tend to spread inside the stiff region. Both this behaviour are in qualitative agreement with the experimental data.

To conclude, this kind of analysis, despite it being qualitative, allows to understand how the numerical results are related to the experiments and how much the model is reliable. Although many simplifying assumptions are made, for example the interface between the two region that was considered as a perfect line or the roughness of the substrata that was not considered at all, the model could be considered a good compromise between the problem complexity and computational complexity.

7. References

[1] Beltman JB, Marée AF, de Boer RJ. Analysing immune cell migration. *Nature Reviews Immunology*. 2009;9(11):789-98.

- [2] Campbell DJ, Beckman KJ, Calderon CE, Doolan PW, Ottosen RM, Ellis AB, Lisensky GC. Replication and compression of bulk and surface structures with polydimethylsiloxane elastomer. *Journal of Chemical Education*. 1999;76(4):537-541.
- [3] Chou SY; Cheng CM; Leduc PR. Composite polymer systems with control of local substrate elasticity and their effect on cytoskeletal and morphological characteristics of adherent cells. *Biomaterials*. 2009;30(18):3136-3142.
- [4] Guarneri D, De Capua A, Ventre M, Borzacchiello A, Pedone , Marasco D, Ruvo M, Netti PA. Covalently immobilized RGD gradient on PEG hydrogel scaffold influences cell migration parameters. *Acta Biomaterialia*. Article in press.
- [5] Lo CM, Wang HB, Dembo M, Wang YL. Cell movement is guided by the rigidity of the substrate. *Biophysical Journal*. 2000;79(1):144-52.
- [6] Stokes CL, Lauffenburger DA, Williams SK. Migration of individual microvessel endothelial cells: stochastic model and parameter measurement. *Journal of Cell Science*. 1991;99:419-30.
- [7] Tranquillo RT, Lauffenburger DA. Stochastic model of leukocyte chemosensory movement. *Journal of Mathematical Biology*. 1987;25(3):229-62.
- [8] Xin Q. Brown, Keiko Ookawa, Joyce Y. Wong. Evaluation of polydimethylsiloxane scaffolds with physiologically-relevant elastic moduli: interplay of substrate mechanics and surface chemistry effects on vascular smooth muscle cell response. *Biomaterials*. 2005;26(16):3123-3129.

CHAPTER 5

Study and Design of a Durotaxis-based Substratum

1. Introduction

This part of the work has the aim to study and develop a durotaxis-based substratum, able to guide cells in their migration and in particular, able to guide cells along straight path. Recalling what already explained in chapter 2, it exists a relation between the alignment of collagen produced by fibroblasts or others tissue cells and their migration (Wang et al., 2003). Thus, the idea is to obtain an aligned tissue made of new collagen, giving to the cells the conditions to move along straight-lines.

To realize this substratum Polyethylenglycole (PEG) was used. Its usage was possible thanks to the collaboration with the research group of Dr. Marga C. Lensen at the DWI an der RWTH (Aachen, Germany). This group, composed mainly of chemists, have already studied the material (Lensen et al. 2007, Lensen et al. 2008) so on the basis of their experiences PEG was used to produce the substrata that were the goal of this work.

First, smooth PEG was synthesized and cell migration experiments was performed over it to better understand its response. Then a specific technique was developed to produce durotaxis-based substrata, and preliminary experiments of cell adhesion over it were performed.

2. Polyethylene glycol (PEG)

PEG, also known as PEO (Polyethylenoxide) or POE (Polyoxyethylene), is a polyether and is a polymer of the ethylene oxide. It is an oligomer or a polymer of ethylene oxide (Fig.1). It is a liquid or a low-melting solid depending on its molecular weight.

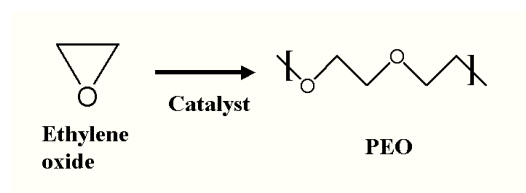


Fig. 1: PEG structure.

PEG materials are prepared by polymerization of ethylene oxide and are commercially available over a wide range of molecular weights (300-10.000.000 g/mol). Different forms of PEG are also available dependent on the initiator used for the polymerization process. The most common of which is a monofunctional methyl ether PEG (abbreviated in mPEG). PEGs are also available with different geometries. Branched PEGs have 3 to 10 PEG chains emanating from a central core group. Star PEGs have 10-100 PEG chains emanating from a central core group. Comb PEGs have multiple PEG chains normally grafted to a polymer backbone.

All these materials are hydrogels, i.e. polymeric networks which absorb and retain large amounts of water. In the network hydrophilic groups or domains are present which are hydrated in an aqueous environment creating the hydrogel structure. Crosslink have to be present to avoid the dissolution of the hydrophilic polymer chains; it also induces a visco-elastic and sometimes pure elastic mechanical behaviour. In general, hydrogels possess a good biocompatibility. Their hydrophilic surface has a low interfacial free energy in contact with body fluids, which results in a low tendency for proteins and cell to adhere to these surfaces (Hennik and van Nostrum, 2001).

At the DWI, Dr. Lensen and her group were working on star PEG, in particular on a star PEG with functional groups at the end of the chains. In particular they have developed a technique to imprint a grooved topography on the material (Lensen et al. 2007) and they were working on the influence of that topography on cell behaviour.

3. Preparation of the Material

To study the cellular response on the smooth material, PEG substrata were realized. The synthesis of the acrylate-functionalized star PEG was performed according to

the following procedure developed in Aachen (Lensen et al., 2008). Prior to the end-capping reaction, the hydroxyl-terminated star PEG (Dow Chemical) was precipitated in cold diethyl ether (-80°C) and dried thoroughly during 4 hours at 10^{-2} mbar at 80°C oil bath temperature. Under a nitrogen atmosphere, 0.4 g (1.3 equiv) of acrylic anhydride was slowly added to a mixture of 5.0 g of the star PEG pre-polymer and 0.3 ml (1.5 equiv) of water free pyridine in 15 ml toluene. The resulting mixture was stirred for 24 hours at room temperature. After removal of the solvent and pyridine, the crude product was dried at room temperature during 8 hours at 10^{-2} mbar. Unreacted acrylic anhydride was separated from the product by precipitation in diethyl ether at -80°C (stirring at maximum speed), leaving the product as a colorless oil. The purified product was dried at room temperature during 8 hours at 10^{-3} mbar. The purity of the product was verified by different tests (Matrix Assisted Laser Desorption, H-NMR, C-NMR and Gel Permeation Chromatography). The results confirmed that all six-end groups were acrylated (Fig. 2a).

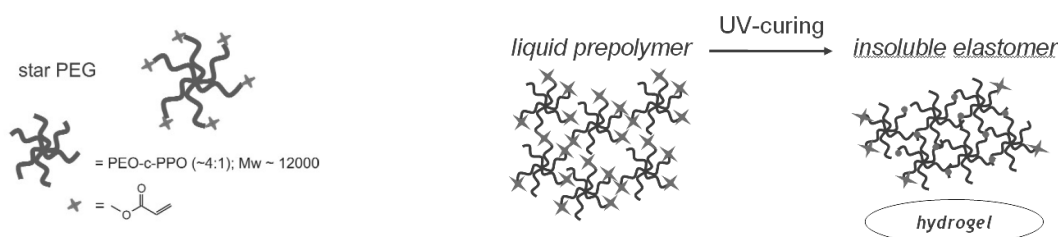


Fig. 2a: Functionalized star PEG produced. Fig 2b: Structure of the PEG hydrogel.

The network was then obtained by UV-curing (Fig 2b). Acetone was used as a solvent for the star PEG precursor. Typically, 200 μl of star PEG was mixed with an acetone solution of the photoinitiator benzoin methyl ether (1 wt %) and pentaerythritol triacrylate (PETA) as a cross-linking agent (5 wt %). For PEG material with variable elasticity and stiffness, various concentrations of photoinitiator (0.5-1.5 wt %) and crosslinker (0-15 wt %) were used. After thorough mixing and subsequent evaporation of the solvent, the photocurable mixture was drop-cast on a glass slide in a nitrogen-filled glovebox, where the UV-curing was carried out under a UV-lamp ($\lambda=366$ nm) positioned about 8 cm above the sample. After curing, the elastomeric replica was mechanically peeled-off with tweezers.

The different mechanical properties of the PEG obtained are reported in Table 1 with the relative Young's modulus evaluated through a rheometer shear test. Only on three of these mixtures we perform cell migration experiments: 0.5/5, 1/5 and 1/10.

| Mixture name | P.I. [wt %] | C.L. [wt %] | E [MPa] |
|--------------|-------------|-------------|---------|
| 0.5/0 | 0.5 | 0 | 0.22 |
| 1/0 | 1 | 0 | 0.56 |
| 0.5/5 | 0.5 | 5 | 0.18 |
| 1/5 | 1 | 5 | 0.75 |
| 2/5 | 2 | 5 | 1.1 |
| 1/10 | 1 | 10 | 2.7 |
| 1.5/10 | 1.5 | 10 | 9 |
| 1/15 | 1 | 15 | 15 |
| 1/30 | 1 | 30 | 30 |

Table 1: Produced PEG mixtures (P.I = photoinitiator, C.L. = crosslinker) and Young's modulus.

4. Cell Migration Experiments

All the experiments described below were performed at CRIB thanks to the collaboration of Dr. M. Ventre. The three mixtures chosen were useful to have an idea of the cellular response on these materials. The adopted procedure was as follows. Two discs of 0.5/5 gel, two discs of 1/5 gel and two discs of 1/10 gel were hydrated in distilled sterile water for 6 hours. All the samples were ethanol sterilized. Then they were pre-incubated with 40 $\mu\text{g}/\text{ml}$ fibronectin for 180 minutes; 1 ml of cell suspension (primary bovine dermal fibroblasts 5×10^3 cell/ml, trying to reduce cell-cell contacts) was put on each slice and the culturing plate was stored in an incubator for 120 minutes to allow for cell adhesion. After the incubation, the samples were transferred to new wells and approximately 2 ml of Eagle's minimal essential medium (EMEM) was added. After 24 hours incubation there was extensive adhesion and spreading of fibroblasts on them.

Time-lapse microscopy technique was used to follow the migration. The method was the same described in chapter 4 for the PDMS substrata. Different cell trajectories

were obtained and they were analysed calculating the MSD and the distribution of γ_i , with a purpose-made MATLAB script (see the Appendix). Both quantities have been introduced in chapter 3 (Gail and Boone,1970, House et al. 2009, Beltman *et al.*,2009).

5. Results and Remarks

On the 0.5/5 samples (soft PEG) cells displayed a flat and spread morphology with several cellular protrusions (Fig. 3) typical of migrating cells.

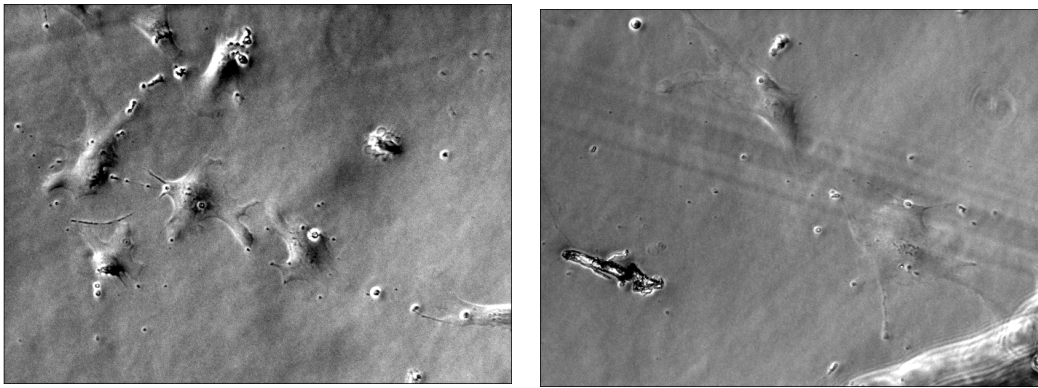


Fig. 3: Spreading cells on 0.5/5 substrata (Optical microscope, 10x Magnification).

As expected, cell trajectories are randomly distributed all over the plane, as it is shown in the following chart (Fig. 4).

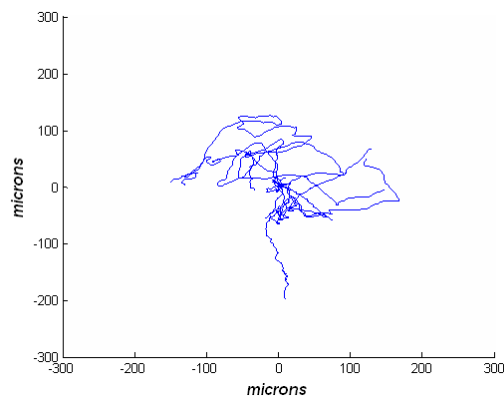


Fig. 4: Trajectories of cells migrating on the 0.5/5 mixture

To have a measure of the area covered by the cell during their migration, the plot of the MSD as a function of the time interval (log/log plot) for every cell tracked is reported in Fig. 5.

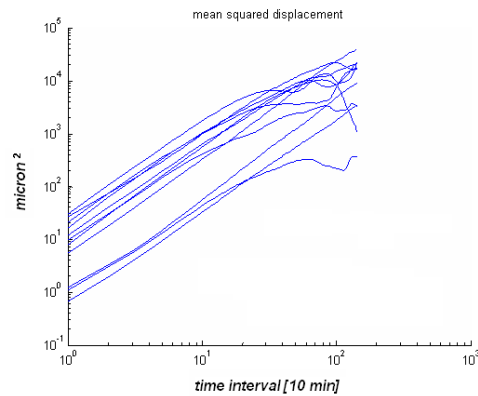


Fig. (5): Log/log plot of the MSD of the cells spreading over the 0.5/5 substrata.

In particular the average MSD after 1000 minutes (chosed as reference time to make a comparison between the three mixtures) is $9323.5 \mu\text{m}^2$. In order to characterize persistence, the distribution of the angles between two consecutive steps (γ_i) has been evaluated and reported in Fig. 6. Even though cell paths are randomly distributed the higher distribution around 0° indicates a sort of inertia of the cells to change direction abruptly.

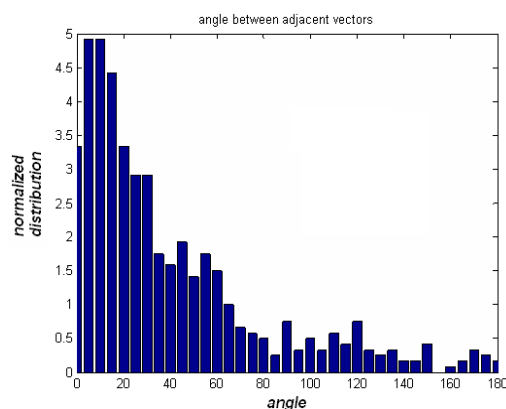


Fig. 6: Histogram of the angles between adjacents steps for the 0.5/5 migratin cells.

Also in the case of the 1/5 PEG (Medium PEG), cells adhered and displayed lamellipodia, however they seemed to assume a more spindled morphology with a less flat cell body (Fig. 7).

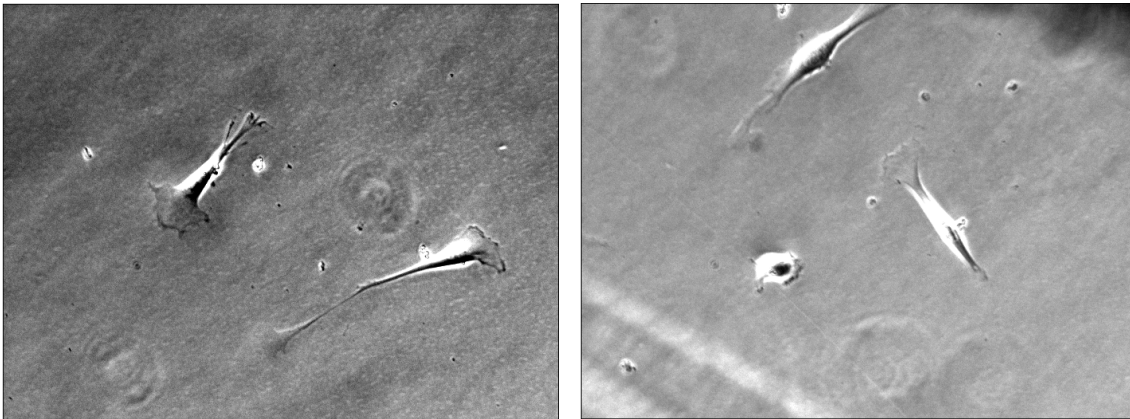


Fig. 7: Spreading cells on 1/5 substrata (Optical microscope, 10x Magnification).

Cell trajectories are randomly distributed on the surface as in the previous case. In this experiment, the trajectories seem to be more scattered, covering a larger area (Fig. 8).

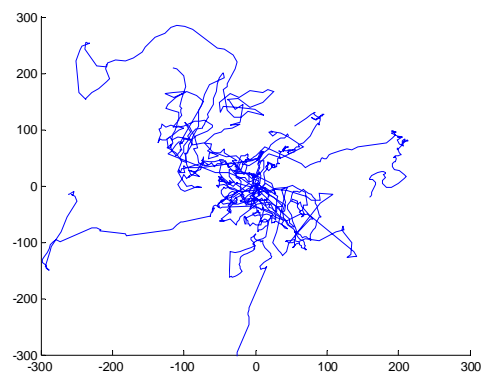


Fig. 8: Trajectories of cells migrating on the 1/5 mixture.

These features are confirmed by the angle distribution and the MSD as reported in Fig.9 and in Fig.10.

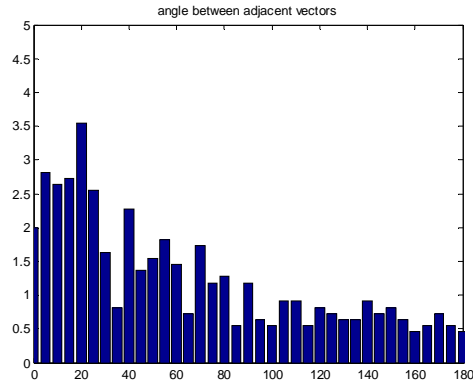


Fig. 9: Histogram of the angles between adjacents steps for the 1/5 migratin cells

The distribution of angles is shallower respect to the 0.5/5 samples, indicating more directional changes of the cells and the MSD at after 1000 minutes is $28178 \mu\text{m}^2$.

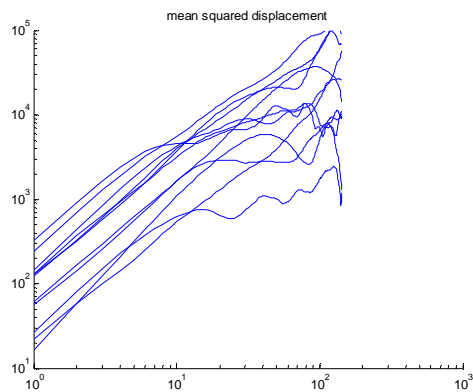


Fig. 10: Log/log plot of the MSD of the cells spreading over the 1/5 substrata.

On the 1/10 samples (Stiff PEG) cells adhere, but they assumed a more rounded shape. Also the principal axis of the cell body seems shorter with respect to the previous experiments (Fig. 11).

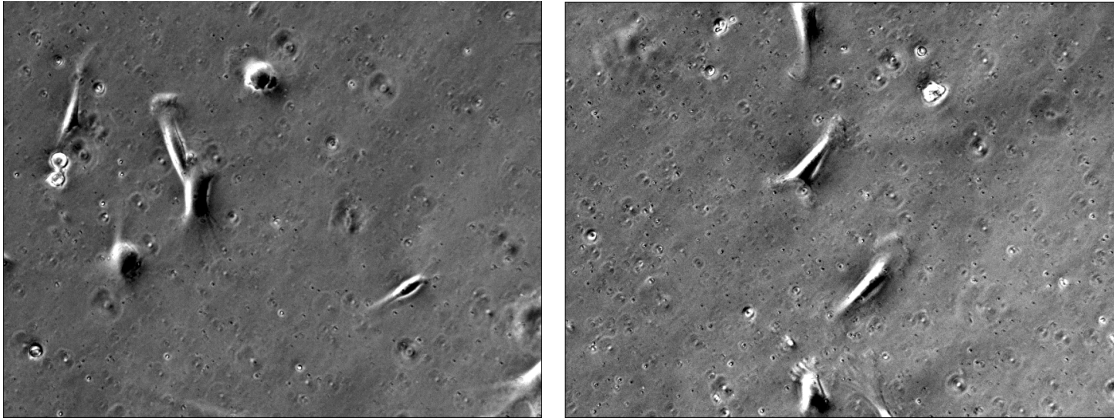


Fig. 11: Spreading cells on 1/10 substrata (Optical microscope, 10x Magnification).

Again, cell trajectories are randomly distributed on the surface (Fig.12) and the motion is persistent (Fig. 13).

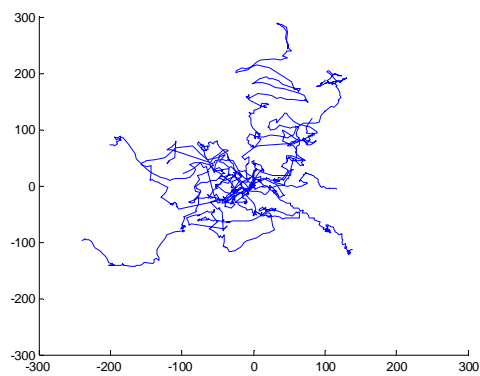


Fig. 12: Trajectories of cells migrating on the 1/10 mixture.

The MSD is comparable to the one observed in the case of 1/5 mixture, namely $17800 \mu\text{m}^2$ after 1000 minutes.

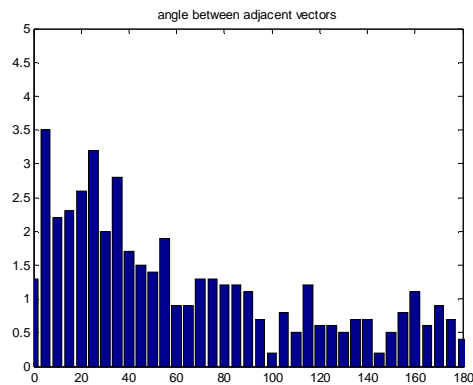


Fig .13: Histogram of the angles between adjacents steps for the 1/5 migratin cells

In conclusion of these experimental part of the work, it is possible to say that the processes observed on the soft PEG seem to stabilize cell motion in producing a more stable adhesion and a more persistent migration. On the other hand, primary cells do not adhere strongly on stiff and medium PEG and this probably causes the cells to travel faster, maybe de-adhering and re-adhering, but in a chaotic fashion. Taken together these results do not allow to draw out any definitive conclusion mainly for two reasons. First, primary fibroblasts are known to display a heterogeneous behaviour: some cells move fast, some other go very slowly and this of course causes large errors in evaluating cell population parameters. Larger statistical pool has to be taken into account in order to (partially) overcome such a limitation. Second, it is not possible to address changes in migration parameters exclusively on substratum stiffness. Since the substrata were treated with proteins (such as fibronectin) to improve cell adhesion, it is reasonable to hypothesize that different materials can adsorb proteins differently. Probably, cell behaviour on the stiffest substrata could be attributed at least partly to a reduced fibronectin and other proteins adsorption.

In order to have a better insight into the dynamics of cell migration on PEG mixtures, it could be useful to perform experiments incubating the materials with fluorescently labelled fibronectin and than evaluate protein adsorption and surface distribution via laser microscopy; assessing, in a quantitative way, the degree of cell adhesion by monitoring the evolution of cells migration parameters as a function of time. In any case the PEG mixtures produced and tested seem to be suitable for cell adhesion

and migration and they were used to develop a new procedure for building a durotaxis-based substratum.

6. The “Pattern of Elasticity” Substrata

The idea to build a durotaxis-based substratum is to use the mixtures of PEG analyzed before, combined together. This material has two main advantages in doing so: first, it is easily workable and second, it is available in different mixtures with different mechanical properties as shown above. Thus, the objective is to obtain a substratum with stripes of different PEG. In this manner cells like fibroblasts should recognize the different stiffness and should prefer to move on the stiffest stripes in a quasi-straight manner.

On this basis a technique to gain such a structure was developed. The procedure is as follows. A selected mixture of PEG called “PEG A” was drop-cast on a silicon master (Amo GmbH, Aachen) in a nitrogen-filled glovebox. The silicon master is patterned with grooves, in such a way that its negative reproduction was given to the “PEG A”. Then the UV-curing was carried out under a UV-lamp ($\lambda = 366 \text{ nm}$) positioned about 8 cm above the sample, as in the classic procedure described for smooth PEG (Fig.14a). After curing, the elastomer patterned replica was mechanically peeled off with tweezers and put over a glass slide, with the patterned surface in contact with the glass. Then a drop of a different mixture of PEG called “PEG B” was drop down near the replica and it fills its channels for capillarity. The structure made in this way was again UV-cured to permit “PEG B” to crosslink and to form stripes inside the channels of “PEG A”. The processes is schematized in Fig.14b.

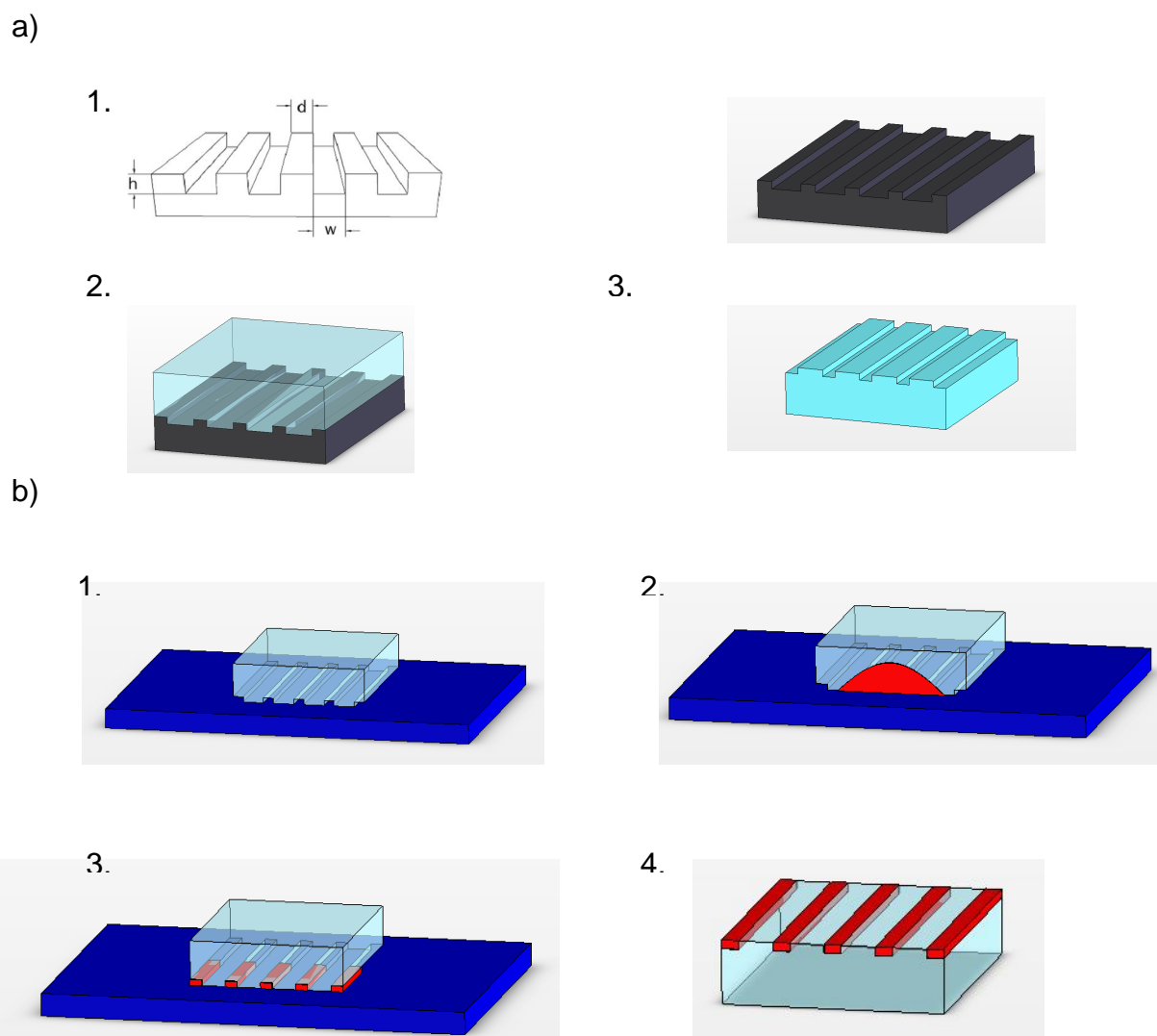


Fig. 14: Scheme of the technique developed for the “Pattern of Elasticity substrata”. a) Production of the PEG A: 1.Silicon master (named by its dimension d_w_h in the remainder); 2. Imprinting of PEG A on the silicon master; 3. PEG A replica. b) Filling of the PEG A: 1. The PEG A replica was put on a glass slide; 2. A drop of PEG B was put on the glass slide; 3. The drop fills the channel of the PEG A replica; 4. Final form of the samples, with a surface made of stripes of PEG A (blue) and PEG B (red).

Different silicon master to imprint the PEG A were used producing different dimensions of the stripes. All the dimensions produced are reported in Table 2.

| Sample Name (Silicon Master) | PEG A | | PEG B | |
|---------------------------------|---------|-----------------------------------|---------|-----------------------------------|
| | Mixture | Stripe Width [μm] | Mixture | Stripe Width [μm] |
| 10_20_5 | 0.5/5 | 20 | 1/10 | 10 |
| 20_10_5 | 1/10 | 10 | 0.5/5 | 20 |
| 50_10_5 | 0.5/5 | 10 | 1/10 | 50 |

10_50_5

1/10

50

0.5/5

10

Table 2: Composition of the “Pattern of Elasticity” samples produced. Samples are named by the silicon masters they were produced.

The samples were then checked with the optical microscope. The images obtained in this manner are reported in Fig. 15.

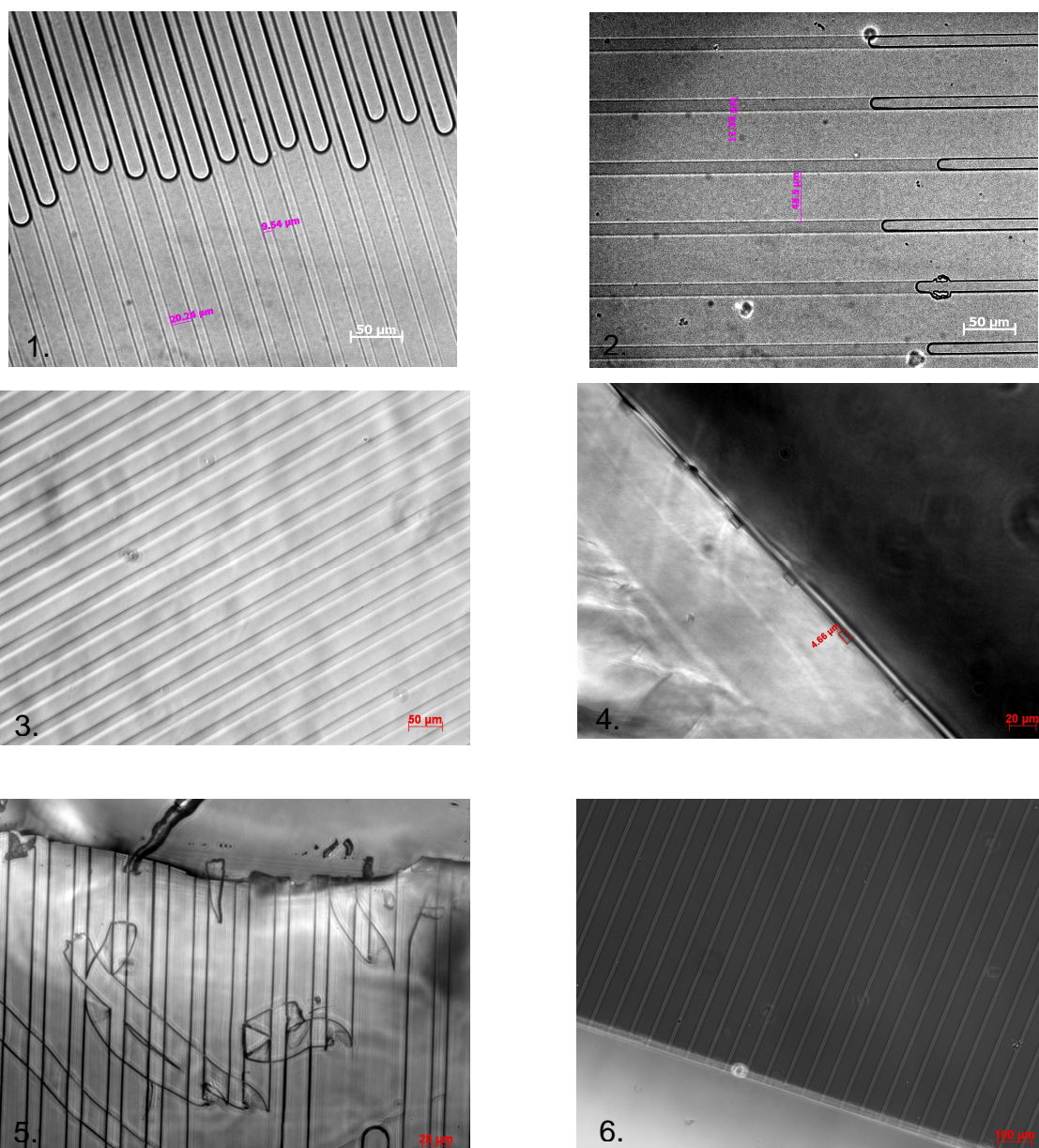


Fig. 15: Optical microscope images of the samples produced. 1. 10_20_5 sample with a filled and an unfilled region; 2. 50_10_5 sample with a filled and an unfilled region; 3. Filled region of a 20_10_5 samples; 4. Cross section of a 50_10_5 sample; 5. Detached PEG B stripes on a 10_20_5 sample; 6. Filled region of a 50_10_5 samples.

The samples were also observed with the Field Emission Scanning Electron Microscope (FESEM). Visualizing the mistakes (detached stripes or purpose made cuts) in the structure it was possible to check in more details the structure and to know that they were made as wanted. Images obtained with the FESEM are reported in Fig. 16.

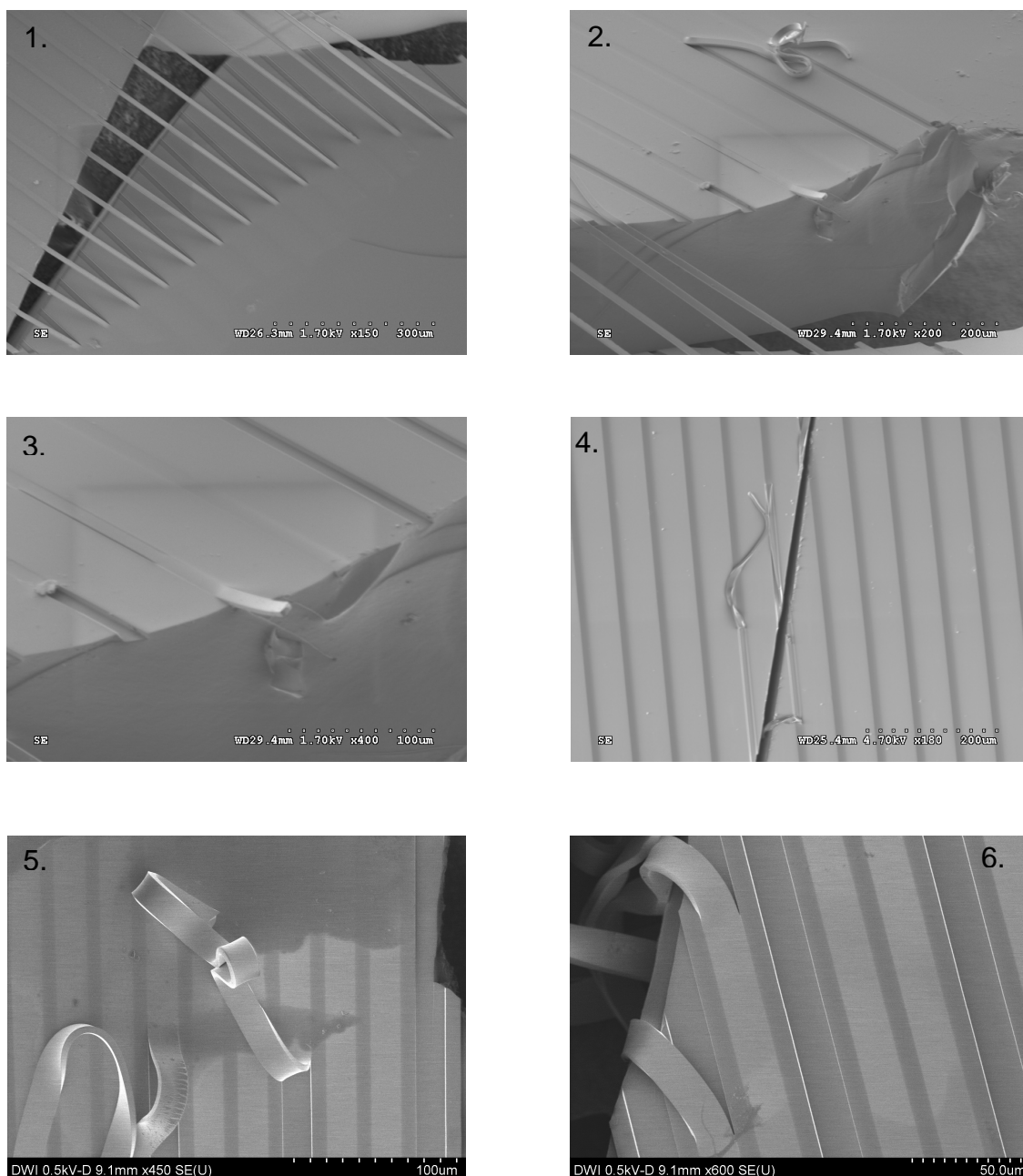


Fig. 16: FESEM images of the samples. 1. and 2. mistakes and free stripes in 50_10_5 samples; 3. Border of a 50_10_5 samples with a free stripe; 4. purpose made cut on a 50_10_5; 5. ruffled stripes on 10_20_5 samples; 6. stripes of a 10_20_5 sample.

Observing the sample at the FESEM it appears that sometimes the samples or some region of them are covered by a thin layer (Fig. 17)

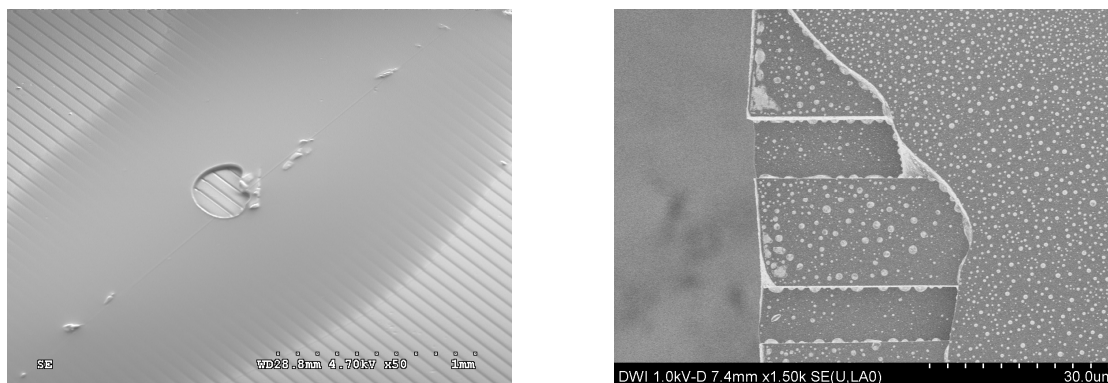


Fig. 17: Thin layer of PEG B over a 50_10_5 samples: the layer comes from a non perfect adhesion between PEG A and the glass slide.

The film is probably the PEG B used in the production of the samples that overcome the PEG A replica and cover all the samples once UV-cured. This problem can be due to a non perfect contact between PEG A and the glass slide and it is not clear whether this happened only on some parts of the edges or also on greater areas of the samples. So this should be taken into account to improve the method.

Another problem of these samples was about their capability of maintaining the structure in water. As already mentioned, PEG is a hydrogel and it absorbs a large amount of water. Different mixtures of PEG absorb different quantities of water and swell in a different way. In particular stiffer PEG swell less than softer PEG because they have an higher crosslinkage and so they absorb less water. So when the samples realized are immersed in water, as in the case of cell migration experiments, this differential swelling could cause the leak of the structure. For this reason, the samples were tested in water for 24 hours. It was observed that some stripes of “PEG B” detached and leave the samples. It was observed also that samples in which “PEG A” was the softest PEG (0.5/5 in these cases) had a better behaviour under water (Fig. 18)

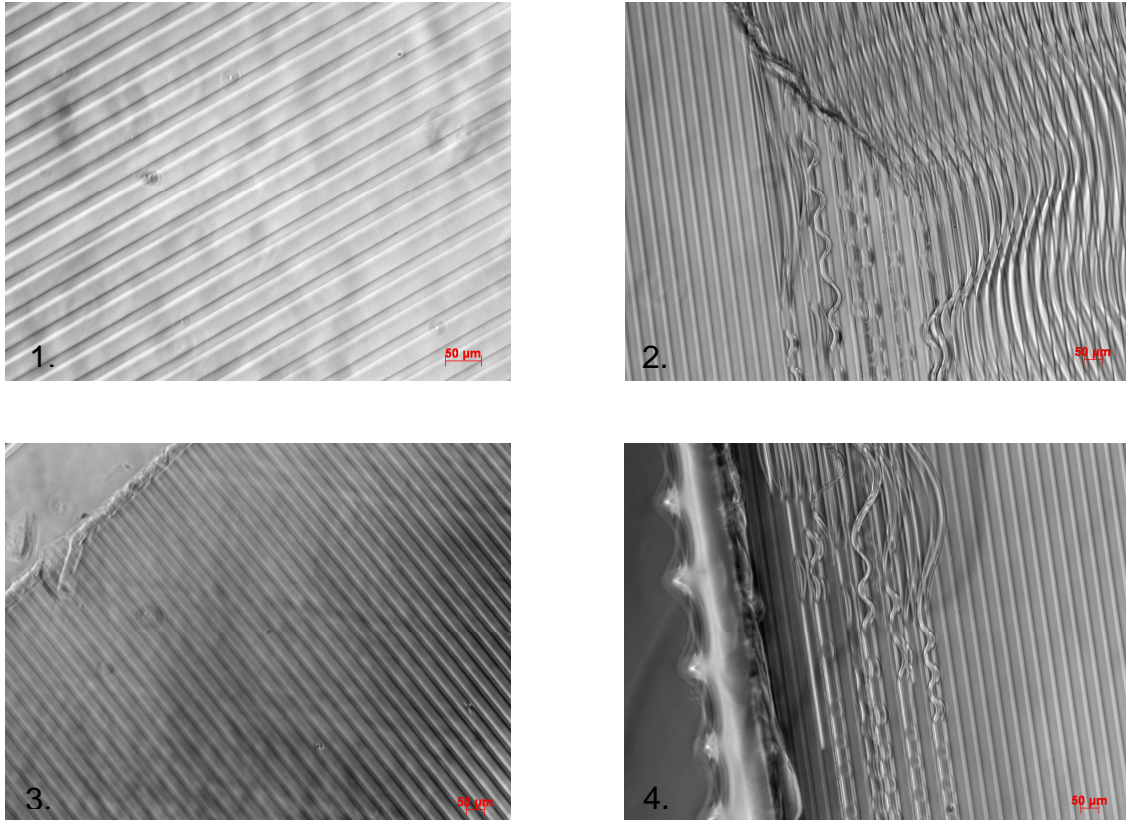


Fig. 18: Comparison between the water behaviour of a 20_10_5 samples with the softer mixture as PEG a (1. and 3.), and a 10_20_5 samples (2. and 4.) with the stiffer mixture as PEG A. The 10_20_5 maintain its structure also after 24 hours in water.

7. Preliminary Cell Adhesion Experiments

Once the samples were produced, they were tested for their cellular response. Cell adhesion experiments were performed as follows. The samples were cleaned by incubation in 70 % ethanol for 10 minutes and subsequent rinsed with sterile water and PBS. L929 fibroblasts were harvested with trypsin-EDTA and resuspended in fresh RPMI medium supplemented with 10% FBS and 1% penicillin and streptomycin. Then 1,5 ml of a 40.000 cell/ml suspension were seeded on the substrata and live images were taken after 3 h, 5h and 24 h. After 24 h cells were fixed with formalin. One part of the samples was immuno-stained with Phalloidin and DAPI and the second part was dried with an ethanol series and analyzed with FESEM. Some of the images obtained are reported in Fig. 18.

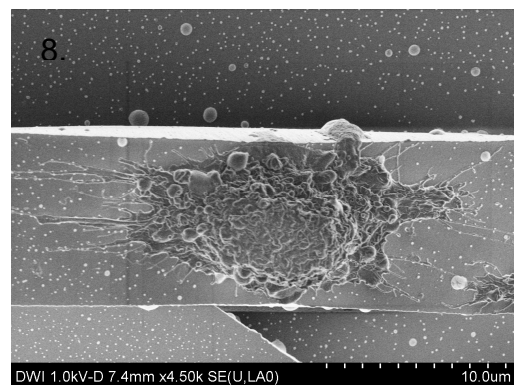
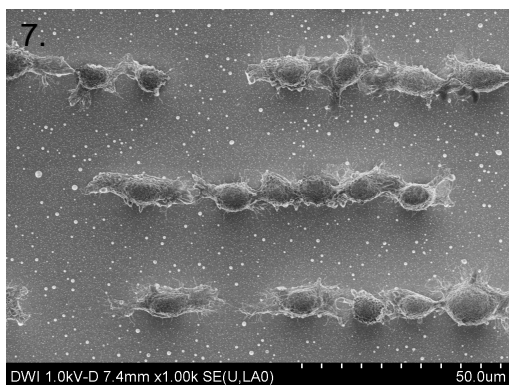
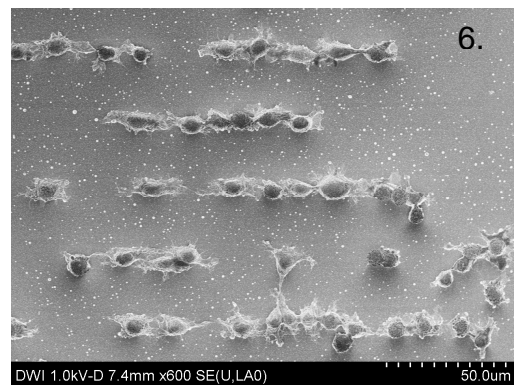
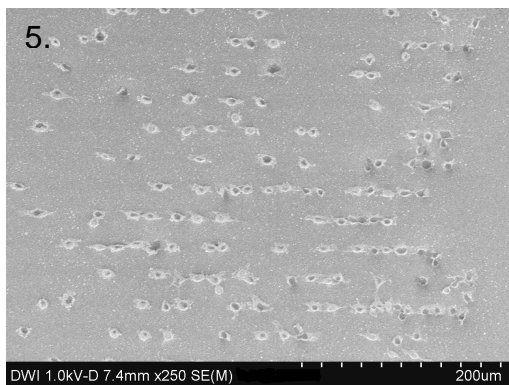
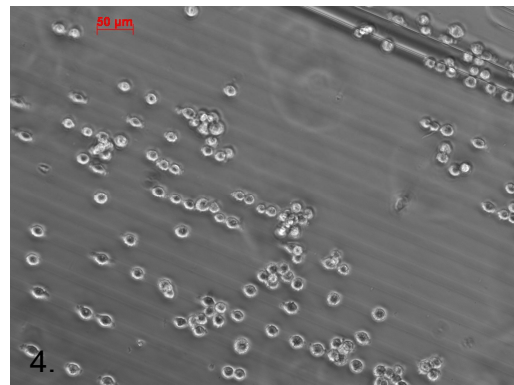
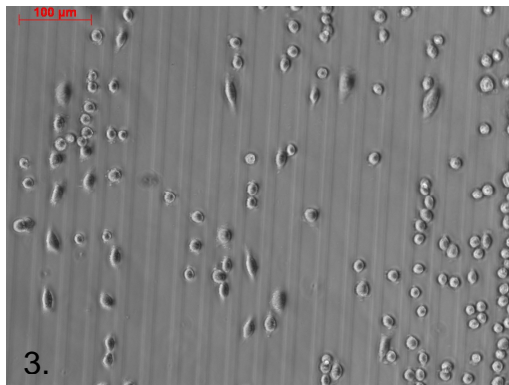
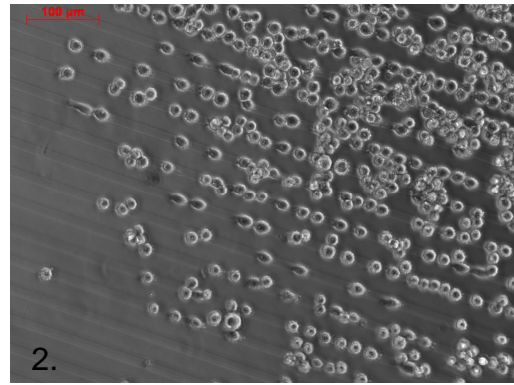
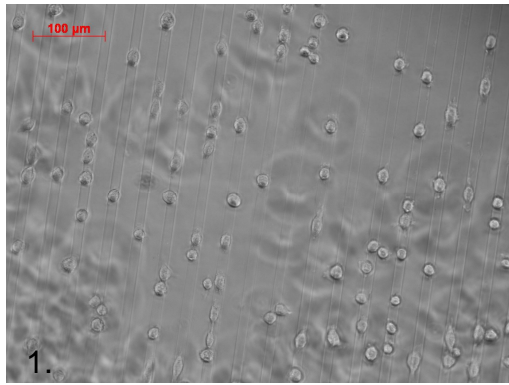


Fig. 18: Optical microscope images (1., 2., 3., 4.) and FESEM images after staining (5., 6., 7., 8.) of 24 hours adhering cells on the "Pattern of Elasticity" samples. 1. 10_20_5 sample; 2. 20_10_5 sample; 3. 10_50_5 sample; 4., 20_10_5 sample; 5. 10_20_5 sample; 6. 10_20_5 sample; 7. 10_20_5 sample; 8. 10_20_5 sample.

Looking at the images there are many round-shaped cells that do not adhere after 24 hours. Considering the morphology of adherent cells they seem to be not so strongly attached to the substratum and migrating because they do not show pronounced protrusion. In any case, considering spreading cells, they were dominantly adhering and spreading on the stiffer lines (1/10 PEG) in an aligned fashion on all samples and only some cell parts or round cells were present on the softer lines.

Conclusions

After testing smooth star PEG for cell migration substrata, a new type of substratum based on the phenomenon of durotaxis was studied. A technique for its production with PEG was developed and tested. Preliminary cell adhesion experiments were carried out showing that this idea can be useful. A campaign of cell migration experiments is needed to understand how the migration of cells occurs. The study of collagen production on these substrata should also be investigated in further studies.

References

- [1] Fairclough JPA and Norman AI. Structure and rheology of aqueous gels. *Annual Reports on the Progress of Chemistry, Section C: Physical Chemistry*. 2003;99:243-276.
- [2] Hennink WE, van Nostrum CF. Novel crosslinking methods to design hydrogels. *Advanced Drug Delivery Reviews*. 2002;54(1):13-36.
- [3] Kopecek J. Hydrogel biomaterials: A smart future? *Biomaterials*. 2007;28:5185-5192.
- [4] Lensen MC, Mela P, Mourran A, Groll J, Heuts J, Rong HT, Moller M. Micro- and nanopatterned star poly(ethylene glycol) (PEG) materials prepared by UV-based imprint lithography. *Langmuir*. 2007;23(14):7841-7846.
- [5] Lensen MC, Schulte VA, Salber J, Diez M, Menges F, Moller M. Cellular responses to novel, micropatterned biomaterials. *Pure and Applied Chemistry*. 2008;80(11):2479-2487.
- [6] Sakai T, Matsunaga T, Yamamoto Y, Ito C, Yoshida R, Suzuki S, Sasaki N, Shibayama M, Chung UI. Design and fabrication of a high-strength hydrogel with ideally homogeneous network structure from tetrahedron-like macromonomers. *Macromolecules*. 2008;41(14):5379-5384.

- [7] Schulte VA, Diez M, Moller M, Lensen MC. Surface Topography Induces Fibroblast Adhesion on Intrinsically Nonadhesive Poly(ethylene glycol) Substrates. *Biomacromolecules*. 2009;10(10):2795-2801.
- [8] Wang JHC, Jia FY, Gilbert TW, Woo SLY. Cell orientation determines the alignment of cell-produced collagenous matrix. *Journal of Biomechanics*. 2003;(1):97-102.

APPENDIX

The script used to solve the model presented in chapter 3 are reported:

TRAIETTORIE (main script)

```
% Salvataggio Traiettorie
clc
close all
clear all

N=10;           % Number of cells
beta=0.15;      % [h^-1]
alpha=23.2;     % [micron^2*h^-3]
Tdim=24;        % [h] Tempo Dimensionale

for simu=1:N
    close all
    x0=[465 250]; % posizione in cui si trova la cellula [micron]
    %[X]=MODELLO(alpha,beta,Tdim,x0); % DOMINIO ISOTROPO
    [X]=BIFASICO(alpha,beta,Tdim,x0); % DOMINIO BIFASICO

    s = ['C:\Documents and Settings\Filippo\Desktop\traiettorielosanna\Cell'
int2str(simu) '.txt']
    save( s, 'X', '-ascii');
end
```

MODELLO (function for the isotropic domain)

```
function [x]=MODELLO(alpha,beta,Tdim,x0)
%-----
%   Rectangular Grid MAIN
%   Plane stress analysis of a square grid using isoparametric four-node
%   elements
%   Griglia Omogenea
%   bcdof = a vector containing dofs associated with boundary conditions
%   bcval = a vector containing boundary condition values associated with
%   the dofs in 'bcdof'
%   ATTENZIONE
%   Function derivata dallo script PIPPOMAINCIMUOVIAMO_GEN con variabile
%   d'ingresso beta
%-----
%
%
%clc
%clear all
close all
```

```

% profile on
%
global L H nline ncolumn sdof phi B Prig
%
% -----
% Parametri temporali
% -----
TF=Tdim*beta; % Maximum time Adimensional
dtdim=0.5; % Time Step (9 min)
dt=dtdim*beta; % TIME STEP
ADIMENSIONALE
Q=length(0:dt:TF); % Numero di time steps nella simulazione
AD=sqrt(alpha/beta^3); % Lunghezza Adimensionale
phi=25; % diametro della cellula corrispondente a 25 micron
nline=100; % number of lines in the grid
ncolumn=100; % number of column in the grid
L=800; % length of the grid
H=800; % height of the grid
passo=pi/6; % passo delle forze
%x0=[L/2 H/2]; % posizione in cui si trova la cellula
v0=[0 0]; % velocità iniziale
x=[x0;zeros(Q,2)]; % inizializzazione posizioni
xadim=[x0./AD;zeros(Q,2)]; % inizializzazione posizioni adimensionali
v=[v0;zeros(Q,2)]; % inizializzazione velocità
theta=(0:passo:2*pi)'; % angolo piatto suddiviso
sfas=passo/2; % sfasamento dei punti di misura
F=1e-3; % modulo della forza [microN]
a=L/ncolumn; % dimensione x elemento
b=H/nline; % dimensione y elemento
rag=phi/2; % raggio della cellula
showmethpoints = 0;
%
%
%
%
*****
%
% P R E P R O C E S S O R E
%
%*****
%
% -----
% Definizione parametri mesh
% -----
nnel=4; % number of nodes per element
ndof=2; % number of dofs per node
nel=nline*ncolumn; % number of elements
nnodeline=ncolumn+1; % number of nodes per line
nnodecolumn=nline+1; % number of nodes per column
nnode=nnodeline*nnodecolumn; % total number of nodes in system
sdof=nnode*ndof; % total system dofs
edof=nnel*ndof; % degrees of freedom per element
T = length(theta)-1;

%
% -----
% Definizione parametri del materiale
% -----
%emodule=1; % elastic modulus
%poisson=0.3; % Poisson's ratio

```

```

%planeopt=1;                % Plane stress, plane strain, axisymmetric, 3D

E1=1000;
E2=1;
n=0.3;
G12=E1/2/(1+n);
%
% -----
% Inizializzazione matrici notevoli
% -----
%kk=sparse(sdof,sdof);      % system matrix as a SPARSE matrix
%UV=zeros(sdof,1);         % system displacement vector
%eldisp=zeros(edof,1);     % element displacement vector
%index=zeros(edof,1);      % index vector
%matmtx=zeros(3,3);        % constitutive matrix
%
% -----
% Definizione condizioni al contorno
% -----
Ulft=(1:2:(nline+1)*2)';
Vlft=(2:2:(nline+1)*2)';
Urit=(((ncolumn*(nline+1))+1)*2)-1:2:((ncolumn+1)*(nline+1))*2)';
Vrit=(((ncolumn*(nline+1))+1)*2):2:((ncolumn+1)*(nline+1))*2)';
Ubot=(1:(nline+1)*2:((nline+1)*ncolumn+1)*2-1)';
Vbot=(2:(nline+1)*2:((nline+1)*ncolumn+1)*2)';
Utop=((nline+1)*2-1:(nline+1)*2:((nline+1)*(ncolumn+1)*2-1))';
Vtop=((nline+1)*2:(nline+1)*2:((nline+1)*(ncolumn+1)*2))';
bcdof=[Utop;Ubot;Vtop;Vbot;Ulft;Urit;Vlft;Vrit];% LATI INCASTRATI
bcval=zeros(length(bcdof),1); dofs constrained whose described values are 0
clear Ulft Vlft Urit Vrit Ubot Vbot Utop Vtop;
%
% -----
% Matrice di rigidezza dell'elemento (quadrato a 4 nodi)
% -----

matmtx=femataniso(E1,E2,n,G12);      % compute constitutive matrix
% matmtx=fematiso(planeopt,emodule,poisson);
% Matrici S

S11=b/(6*a)*[2 -2 -1 1;-2 2 1 -1;-1 1 2 -2;1 -1 -2 2];
S12=1/4*[1 1 -1 -1;-1 -1 1 1;-1 -1 1 1;1 1 -1 -1];
S22=a/(6*b)*[2 1 -1 -2;1 2 -2 -1;-1 -2 2 1;-2 -1 1 2];

% Matrici K da permutare

K11=matmtx(1,1)*S11+matmtx(3,3)*S22;
K12=matmtx(1,2)*S12+matmtx(3,3)*S12';
K22=matmtx(3,3)*S11+matmtx(2,2)*S22;

% Matrice di permutazione

Pk=zeros(8,8);
Pk(1,1)=1;
Pk(2,3)=1;
Pk(3,5)=1;
Pk(4,7)=1;
Pk(5,2)=1;
Pk(6,4)=1;
Pk(7,6)=1;

```

```

Pk(8,8)=1;

% Matrice di rigidezza dell'elemento
k=Pk'*[K11 K12;K12' K22]*Pk;

%-----
% Assemblaggio della matrice di rigidezza del sistema
%-----
%
kk=manassemblygenret(k);    % MATRICE DI RIGIDEZZA DELLA GRIGLIA
% -----
% Definizione dei punti d'applicazione delle
% forze e dei punti di valutazione dello
% spostamento
% -----
%
for j=1:Q
ff=zeros(sdof,1);% Inizializzazione della forza all'interno del ciclo
% temporale!!!!!!!!!!!!!!!!!! (ci ho perso un giorno)
P=zeros(T,2);
EP=zeros(T,3);
M=P;
EM=EP;
%
for i=1:T
    P(i,:)=[x(j,1)+rag*cos(theta(i)) x(j,2)+rag*sin(theta(i))];
% coordinate globali adimensionali dei punti P
    EP(i,:)=EL(P(i,:));
% Elementi dei punti P di applicazione della forza, e loro coordinate
locali
    M(i,:)=[x(j,1)+rag*cos(theta(i)+sfas) x(j,2)+rag*sin(theta(i)+sfas)];
% coordinate globali dei punti M
    EM(i,:)=EL(M(i,:));
% Elementi dei punti M di misura dello spostamento, e loro coordinate
locali
end
%
if showmethpoints
    figure
    plot(P(:,1),P(:,2),'.',M(:,1),M(:,2),'+')
    set(gca,'XTick',0:L/nline:L)
    set(gca,'YTick',0:H/ncolumn:H)
    axis equal
    xlim([0 L])
    ylim([0 H])
    grid on
end
%
% -----
% Definizione carichi esterni applicati
% -----
for i=1:T
    nodes = NODESINELEM(EP(i,1));
    FVx=-F*cos(theta(i));
    FVy=-F*sin(theta(i));
    WA1=PSI1(EP(i,2:3),a,b);
    WA2=PSI2(EP(i,2:3),a,b);
    WA3=PSI3(EP(i,2:3),a,b);
    WA4=PSI4(EP(i,2:3),a,b);
    ff(2*nodes(1)-1)=ff(2*nodes(1)-1)+FVx*WA1;

```

```

ff(2*nodes(1))=ff(2*nodes(1))+FVy*WA1;
ff(2*nodes(2)-1)=ff(2*nodes(2)-1)+FVx*WA2;
ff(2*nodes(2))=ff(2*nodes(2))+FVy*WA2;
ff(2*nodes(3)-1)=ff(2*nodes(3)-1)+FVx*WA3;
ff(2*nodes(3))=ff(2*nodes(3))+FVy*WA3;
ff(2*nodes(4)-1)=ff(2*nodes(4)-1)+FVx*WA4;
ff(2*nodes(4))=ff(2*nodes(4))+FVy*WA4;
end
% -----
% Imposizione delle condizioni al contorno
% -----
[kk,ff]=applybc2(kk,ff,bcdof,bcval);
UV=kk\ff;          % vettore degli spostamenti nodali
%
%
%
% *****
%
% P O S T P R O C E S S O R E
%
% *****
%
uM=zeros(T,2);
UsumM=zeros(T,1);
for i=1:T
    nodes = NODESINELEM(EM(i,1));
    uM(i,:)=[UV(2*nodes(1)-1)*PSI1(EM(i,2:3),a,b)+UV(2*nodes(2)-
1)*PSI2(EM(i,2:3),a,b)+ ...
            UV(2*nodes(3)-1)*PSI3(EM(i,2:3),a,b)+UV(2*nodes(4)-
1)*PSI4(EM(i,2:3),a,b) UV(2*nodes(1))*PSI1(EM(i,2:3),a,b)+...

UV(2*nodes(2))*PSI2(EM(i,2:3),a,b)+UV(2*nodes(3))*PSI3(EM(i,2:3),a,b)+UV(2*
nodes(4))*PSI4(EM(i,2:3),a,b)];          % spostamento dei punti M
    UsumM(i)=norm(uM(i,:));          % Calcolo del modulo del
vettore spostamento nei punti di misura
    %proiezuM(i)=-uM(i,:)*[cos(theta(i)+sfas);sin(theta(i)+sfas)];
end
%UsumM=proiezuM';

thetaI=[theta(1)-3*sfas; theta(1)-sfas; theta+sfas;
theta(length(theta))+3*sfas];
UsumMI=[UsumM(length(UsumM)-1); UsumM(length(UsumM)); UsumM; UsumM(1);
UsumM(2)];
deltaint=pi/180;
thetaint=0:deltaint:2*pi;
% suddivido l'intervallo fra 0 e 180 gradi in sottointervalli di 1 grado
rig=interp1(thetaI(1:length(UsumMI)),1./UsumMI,thetaint,'spline','extrap');
% Rigidezza, interpolata con delle spline, in funzione dell'angolo (0-180)
A=deltaint*((rig(1)+rig(length(thetaint)))/2 + sum(rig(2:length(thetaint)-
1)));          % Integrale della funzione "rig" valutato con la regola dei
trapezi
Prig=rig/A;
%figure
%subplot(2,1,1)
%plot(thetaint*180/pi,Prig,'b')%,thetaI(1:length(UsumMI))*180/pi,1./UsumMI/
A,'o')
%xlim([0 360])
%ylim([0 1])

```

```

%hold on
B=deltaint*((Prig(1)+Prig(length(thetaint)))/2 +
sum(Prig(2:(length(thetaint)-1)))); % condizione di normalizzazione
(Integrale della distribuzione di probabilità = 1)

SIM(1)=Prig(1)*deltaint;
for i=2:length(thetaint)-1
SIM(i)=Prig(i)*deltaint+SIM(i-1);
end

%CHARLIE=[0 SIM];
%figure
%subplot(2,1,2)
%plot(SIM,thetaint(1:length(SIM)),SIM,2*pi*SIM,'r')
%xlim([0 1])
%ylim([0 2*pi])
DIR=interp1(SIM,thetaint(1:length(SIM)),rand,'linear','extrap'); %
Angolo in radianti
%DIRdeg(j)=DIR*180/pi % Angolo scelto (gradi)

% -----
% Calcolo della velocità utilizzando l'equazione di Langevin
% -----
W=randn(1,2);
r=norm(W);
KL=[r*cos(DIR) r*sin(DIR)];

% EQUAZIONE ADIMENSIONALIZZATA
s=1;
v(j+1,:)=v(j,:)*(1-dt)+s*sqrt(dt)*KL;
xadim(j+1,:)=xadim(j,:)+dt*v(j+1,:); % X adimensionale
x(j+1,:)=xadim(j+1,:)*AD; % x dimensionale

% Condizioni sui bordi

tol=0.001; % tolleranza per non far stare la cellula sul bordo

if x(j+1,1)>=(L-phi/2)
x(j+1,1)=L-phi/2-tol;
elseif x(j+1,1)<=phi/2
x(j+1,1)=phi/2+tol;
end

if x(j+1,2)>=(H-phi/2)
x(j+1,2)=H-phi/2-tol;
elseif x(j+1,2)<=phi/2
x(j+1,2)=phi/2+tol;
end

end

```

BIFASICO (function for the biphasic domain)

```
function [x]=BIFASICO(alpha,beta,Tdim,x0)
```

```

%-----
%   Rectangular Grid MAIN
%   Plane stress analysis of a square grid using isoparametric
%   four-node elements
%   Griglia Omogenea%
%   bcdof = a vector containing dofs associated with boundary conditions
%   bcval = a vector containing boundary condition values associated with
%           the dofs in 'bcdof'
%
%-----
%
%clc
%clear all
%close all
%
%profile on
%
global L H nline ncolumn sdof phi a b
%
% -----
% Parametri temporali
% -----
TF=Tdim*beta;                % Maximum time Adimensional
dtdim=0.15;                 % Time Step [9 min]
dt=dtdim*beta;             % TIME STEP ADIMENSIONALE
Q=length(0:dt:TF);         % Numero di time steps nella simulazione
AD=sqrt(alpha/beta^3);     % Lunghezza Adimensionale
phi=25;                    % diametro della cellula [micron]
nline=70;                  % number of lines in the grid
ncolumn=70;               % number of column in the grid
L=700;                    % length of the grid [micron]
H=500;                    % height of the grid [micron]
passo=pi/6;               % passo delle forze
%x0=[L/2 H/2];            % posizione in cui si trova la cellula [micron]
v0=[0 0];                 % velocità iniziale [micron/h]
x=[x0;zeros(Q,2)];        % inizializzazione posizioni [micron]
v=[v0;zeros(Q,2)];        % inizializzazione velocità [micron/h]
xadim=[x0./AD;zeros(Q,2)]; % inizializzazione posizioni adimensionali
theta=(0:passo:2*pi)';    % angolo piatto suddiviso
sfas=passo/2;             % sfasamento dei punti di misura
F=1e-3;                   % modulo della forza [microN]
a=L/ncolumn;              % dimensione x elemento [micron]
b=H/nline;                % dimensione y elemento [micron]
rag=phi/2;                % raggio della cellula [micron]
showmethpoints = 0;
%
%
%
%
*****
%
% P R E P R O C E S S O R E
%
%*****
%
% -----
% Definizione parametri mesh
% -----
nnel=4;                    % number of nodes per element

```

```

ndof=2; % number of dofs per node
nel=nline*ncolumn; % number of elements
nnodeline=ncolumn+1; % number of nodes per line
nnodecolumn=nline+1; % number of nodes per column
nnode=nnodeline*nnodecolumn; % total number of nodes in system
sdof=nnode*ndof; % total system dofs
edof=nnel*ndof; % degrees of freedom per element
T = length(theta)-1;
%
% -----
% Definizione parametri del materiale
% -----
%emodule=1; % elastic modulus
%poisson=0.3; % Poisson's ratio
%planeopt=1; % Plane stress, plane strain, axisymmetric, 3D

% PROPRIETA' MATERIALE 1 MAT=(E1,E2,n,G12)

MAT1=[0.8 0.8 0.3 0.8/2/(1+0.2)]; % 1e3/2/(1+0.2) [MPa MPa - MPa ]
%E1=1e1;
%E2=1e6;
%n=0.4;
%G12=1e2;%E1/2/(1+n);

% PROPRIETA' MATERIALE 2

MAT2=[0.2 0.2 0.3 0.2/2/(1+0.2)]; % [MPa MPa - MPa ]
%
% -----
% Inizializzazione matrici notevoli
% -----
kk=sparse(sdof,sdof); % system matrix as a SPARSE matrix
%UV=zeros(sdof,1); % system displacement vector
%eldisp=zeros(edof,1); % element displacement vector
%index=zeros(edof,1); % index vector
%matmtx=zeros(3,3); % constitutive matrix
%
% -----
% Definizione condizioni al contorno
% -----
Ulft=(1:2:(nline+1)*2)';
Vlft=(2:2:(nline+1)*2)';
Urit=(((ncolumn*(nline+1))+1)*2)-1:2:((ncolumn+1)*(nline+1))*2)';
Vrit=(((ncolumn*(nline+1))+1)*2):2:((ncolumn+1)*(nline+1))*2)';
Ubot=(1:(nline+1)*2:((nline+1)*ncolumn)+1)*2-1)';
Vbot=(2:(nline+1)*2:((nline+1)*ncolumn)+1)*2)';
Utop=((nline+1)*2-1:(nline+1)*2:((nline+1)*(ncolumn+1)*2-1))';
Vtop=((nline+1)*2:(nline+1)*2:((nline+1)*(ncolumn+1)*2))';
bcdof=[Urit; Ulft; Vrit; Vlft;Utop;Ubot;Vtop;Vbot]; % LATI INCASTRATI
bcval=zeros(length(bcdof),1);%dofs constrained whose described values are 0
clear Ulft Vlft Urit Vrit Ubot Vbot Utop Vtop;
%
%
k1=RIGEL(MAT1);
k2=RIGEL(MAT2);
%
% -----
% Assemblaggio della matrice di rigidezza del sistema
% -----
%

```

```

kk1=ASSDSSXDX(k1);
save('RIG1','kk1');
clear kk1

kk2=ASSDSSXDX(k2);
save('RIG2','kk2');
clear kk2

kk3=ASSDSCC(k1,k2) % MATRICE DI RIGIDEZZA DELLA FILA CONDIVISA
save('RIG3','kk3');
clear kk3

load('RIG1')
kk(1:2*(nline+1)*(ncolumn/2),1:2*(nline+1)*(ncolumn/2))=kk1(1:2*(nline+1)*
ncolumn/2,1:2*(nline+1)*(ncolumn/2));
kk(2*((nline+1)*(ncolumn/2)-nline)-
1:2*(nline+1)*(ncolumn/2),2*((nline+1)*(ncolumn/2)+1)-
1:2*(nline+1)*(ncolumn/2+1))=kk1(2*(nline+2)-
1:2*(nline+1)*2,2*((nline+1)*2+1)-1:2*((nline+1)*3));
clear kk1
load('RIG3')
kk((2*((nline+1)*ncolumn/2)+1)-
1:2*((nline+1)*ncolumn/2)+nline+1),2*((nline+1)*(ncolumn/2-1)+1)-
1:2*((nline+1)*(ncolumn/2+2)))=kk3(2*(nline+2)-1:2*((nline+2)+nline),:);
clear kk3
load('RIG2')
kk((2*((nline+1)*ncolumn/2)+nline+2))-
1:sdof,(2*((nline+1)*ncolumn/2)+nline+2))-1:sdof)=kk2(2*(nline+2)-
1:2*(nline+1)*(ncolumn/2+1),2*(nline+2)-1:2*(nline+1)*(ncolumn/2+1));
kk(2*((nline+1)*(ncolumn/2+1)+1)-
1:2*(nline+1)*(ncolumn/2+2),2*((nline+1)*(ncolumn/2)+1)-
1:2*(nline+1)*(ncolumn/2+1))=kk2(2*(nline+2)-
1:2*(nline+1)*2,1:2*(nline+1));
clear kk2

% -----
% Definizione dei punti d'applicazione delle
% forze e dei punti di valutazione dello
% spostamento
% -----

for j=1:Q
ff=zeros(sdof,1); % system force vector !!!!!!!!!!!!!!!!!!!!!!!!!!!!!!!!!!!!!!!
P=zeros(T,2);
EP=zeros(T,3);
M=P;
EM=EP;

for i=1:T
P(i,:)=[x(j,1)+rag*cos(theta(i)) x(j,2)+rag*sin(theta(i))];
% coordinate globali dei punti P
EP(i,:)=EL(P(i,:));
% Elementi dei punti P di applicazione della forza, e loro coordinate
locali
M(i,:)=[x(j,1)+rag*cos(theta(i)+sfas) x(j,2)+rag*sin(theta(i)+sfas)];
% coordinate globali dei punti M
EM(i,:)=EL(M(i,:));
% Elementi dei punti M di misura dello spostamento, e loro coordinate
locali

```

```

end

if showmethpoints
    figure
    plot(P(:,1),P(:,2),'.',M(:,1),M(:,2),'+')
    set(gca,'XTick',0:L/ncolumn:L)
    set(gca,'YTick',0:H/nline:H)
    axis equal
    xlim([0 L])
    ylim([0 H])
    grid on
end

% -----
% Definizione carichi esterni applicati
% -----
for i=1:T
    nodes = NODESINELEM(EP(i,1));
    FVx=-F*cos(theta(i));
    FVy=-F*sin(theta(i));
    WA1=PSI1(EP(i,2:3),a,b);
    WA2=PSI2(EP(i,2:3),a,b);
    WA3=PSI3(EP(i,2:3),a,b);
    WA4=PSI4(EP(i,2:3),a,b);
    ff(2*nodes(1)-1)=ff(2*nodes(1)-1)+FVx*WA1;
    ff(2*nodes(1))=ff(2*nodes(1))+FVy*WA1;
    ff(2*nodes(2)-1)=ff(2*nodes(2)-1)+FVx*WA2;
    ff(2*nodes(2))=ff(2*nodes(2))+FVy*WA2;
    ff(2*nodes(3)-1)=ff(2*nodes(3)-1)+FVx*WA3;
    ff(2*nodes(3))=ff(2*nodes(3))+FVy*WA3;
    ff(2*nodes(4)-1)=ff(2*nodes(4)-1)+FVx*WA4;
    ff(2*nodes(4))=ff(2*nodes(4))+FVy*WA4;
end
% -----
% Imposizione delle condizioni al contorno
% -----
[kk,ff]=applybc2(kk,ff,bcdof,bcval);

UV=kk\ff;           % vettore degli spostamenti nodali

%
% *****
%
% P O S T P R O C E S S O R E
%
% *****
%
%
uM=zeros(T,2);
UsumM=zeros(T,1);
for i=1:T
    nodes = NODESINELEM(EM(i,1));
    uM(i,:)=[UV(2*nodes(1)-1)*PSI1(EM(i,2:3),a,b)+UV(2*nodes(2)-
1)*PSI2(EM(i,2:3),a,b)+ ...

```

```

UV(2*nodes(3)-1)*PSI3(EM(i,2:3),a,b)+UV(2*nodes(4)-
1)*PSI4(EM(i,2:3),a,b) UV(2*nodes(1))*PSI1(EM(i,2:3),a,b)+...

UV(2*nodes(2))*PSI2(EM(i,2:3),a,b)+UV(2*nodes(3))*PSI3(EM(i,2:3),a,b)+UV(2*
nodes(4))*PSI4(EM(i,2:3),a,b)]; % spostamento dei punti M
UsumM(i)=norm(uM(i,:));
%proiezuM(i)=-uM(i,:)*[cos(theta(i)+sfas);sin(theta(i)+sfas)];
end
% UsumM=proiezuM';

% CALCOLO DEL MODULO DEL VETTORE SPOSTAMENTO NEI PUNTI DI MISURA

thetaI=[theta(1)-3*sfas; theta(1)-sfas; theta+sfas;
theta(length(theta))+3*sfas]; % Completamento del vettore theta per
effettuare l'interpolazione
UsumMI=[UsumM(length(UsumM)-1); UsumM(length(UsumM)); UsumM; UsumM(1);
UsumM(2)];
deltaint=pi/180;
thetaint=0:deltaint:2*pi;
% suddivido l'intervallo fra 0 e 180 gradi in sottointervalli di 1 grado
rig=interp1(thetaI,1./UsumMI,thetaint,'linear','extrap');
% Rigidezza, interpolata con delle spline, in funzione dell'angolo (0-180)
A=deltaint*((rig(1)+rig(length(thetaint)))/2 + sum(rig(2:length(thetaint)-
1))); % Integrale della funzione "rig" valutato con la regola dei trapezi
% A=sum(rig*(pi/180));
% Valutazione dell'integrale della funzione interpolata, calcolato con la
regola dei trapezi
Prig=rig/A;
% subplot(2,1,1);
% plot(thetaint*180/pi,Prig,'b',thetaI*180/pi,1./UsumMI/A,'o')
% hold on
% xlim([0 360])
% ylim([0 1])
% B=deltaint*((Prig(1)+Prig(length(thetaint)))/2 +
sum(Prig(2:(length(thetaint)-1)))); % condizione di normalizzazione
(Integrale della distribuzione di probabilità = 1)
% B=sum(Prig*(2*pi/360)); % condizione di normalizzazione (Integrale
della distribuzione di probabilità = 1)
% figure

SIM(1)=Prig(1)*deltaint;
for i=2:length(thetaint)-1
SIM(i)=Prig(i)*deltaint+SIM(i-1);
end

DIR=interp1(SIM,thetaint(1:length(SIM)),rand,'linear','extrap');
% Angolo in radianti
DIRdeg=DIR*360/(2*pi);

% -----
% Calcolo della velocità utilizzando l'equazione di Langevin
% -----
W=randn(1,2); % [h^1/2]
r=norm(W);
KL=[r*cos(DIR) r*sin(DIR)]; % componente della forza dovuta alla rigidezza del
% substrato [h^1/2]

```

```

s=1;
v(j+1,:)=v(j,:)*(1-dt)+s*sqrt(dt)*KL;
xadim(j+1,:)=xadim(j,:)+dt*v(j+1,:);           % X adimensionale
x(j+1,:)=xadim(j+1,:)*AD;                       % x dimensionale

% Condizioni sui bordi
tol=0.001;   % tolleranza per non far stare la cellula sul bordo

if x(j+1,1)>=(L-phi/2)
    x(j+1,1)=L-phi/2-tol;
elseif x(j+1,1)<=phi/2
    x(j+1,1)=phi/2+tol;
end

if x(j+1,2)>=(H-phi/2)
    x(j+1,2)=H-phi/2-tol;
elseif x(j+1,2)<=phi/2
    x(j+1,2)=phi/2+tol;
end

end

```

FEMATISO

```

function [matmtrx]=fematiso(iopt,elastic,poisson)

%-----
% Purpose:
%   determine the constitutive equation for isotropic material
%
% Synopsis:
%   [matmtrx]=fematiso(iopt,elastic,poisson)
%
% Variable Description:
%   elastic - elastic modulus
%   poisson - Poisson's ratio
%   iopt=1 - plane stress analysis
%   iopt=2 - plane strain analysis
%   iopt=3 - axisymmetric analysis
%   iopt=4 - three dimensional analysis
%-----

if iopt==1           % plane stress
    matmtrx= elastic/(1-poisson*poisson)* ...
    [1 poisson 0; ...
    poisson 1 0; ...
    0 0 (1-poisson)/2];

elseif iopt==2      % plane strain
    matmtrx= elastic/((1+poisson)*(1-2*poisson))* ...
    [(1-poisson) poisson 0;
    poisson (1-poisson) 0;
    0 0 (1-2*poisson)/2];

```

```

elseif iopt==3      % axisymmetry
    matmtrx= elastic/((1+poisson)*(1-2*poisson))* ...
    [(1-poisson) poisson poisson 0;
    poisson (1-poisson) poisson 0;
    poisson poisson (1-poisson) 0;
    0 0 0 (1-2*poisson)/2];

else      % three-dimension
    matmtrx= elastic/((1+poisson)*(1-2*poisson))* ...
    [(1-poisson) poisson poisson 0 0 0;
    poisson (1-poisson) poisson 0 0 0;
    poisson poisson (1-poisson) 0 0 0;
    0 0 0 (1-2*poisson)/2 0 0;
    0 0 0 0 (1-2*poisson)/2 0;
    0 0 0 0 0 (1-2*poisson)/2];

end

```

MANASSEMBLYGENRET

```

% -----
% Assemblaggio a mano della matrice di rigidezza
% per una griglia omogenea di elementi quadrati
% Griglia quadrata o rettangolare
% -----

function out=manassemblygenret(k)

global nline ncolumn sdof

S=nline*2;      % Dalla prima colonna alla prima colonna della seconda banda
%kmin=min((min(abs(k))));      % valore assoluto minimo degli elementi di k

% Coefficienti Nodi Centrali

A=(k(1,1)+k(3,3)+k(5,5)+k(7,7));
B=(k(2,2)+k(4,4)+k(6,6)+k(8,8));
C=(k(3,5)+k(1,7));
D=(k(4,6)+k(2,8));
E=k(7,3);
F=k(7,4);
G=k(8,3);
H=k(8,4);
I=(k(7,5)+k(1,3));
L=(k(8,6)+k(2,4));
M=k(1,5);
N=k(1,6);
O=k(2,5);
P=k(2,6);

```

```

kk=sparse(1:2:sdof,1:2:sdof,A/2,sdof,sdof) +
sparse(2:2:sdof,2:2:sdof,B/2,sdof,sdof) + sparse(1:2:sdof-
2,3:2:sdof,C,sdof,sdof) + ...
    sparse(2:2:sdof-2,4:2:sdof,D,sdof,sdof) + sparse(2:2:sdof-
S,S+1:2:sdof,F,sdof,sdof) + ...
    sparse(1:2:sdof-S,S+1:2:sdof,E,sdof,sdof)+ sparse(2:2:sdof-
S,S+2:2:sdof,H,sdof,sdof) + sparse(1:2:sdof-S-1,S+2:2:sdof,G,sdof,sdof) +
...
    sparse(1:2:sdof-S-2,S+3:2:sdof,I,sdof,sdof) + sparse(2:2:sdof-S-
2,S+4:2:sdof,L,sdof,sdof) +...
    sparse(2:2:sdof-S-4,S+5:2:sdof,O,sdof,sdof) + sparse(1:2:sdof-S-
4,S+5:2:sdof,M,sdof,sdof)+ sparse(2:2:sdof-S-4,S+6:2:sdof,P,sdof,sdof) +
...
    sparse(1:2:sdof-S-5,S+6:2:sdof,N,sdof,sdof);
kk=kk+kk';

```

```

% Lato sinistro

```

```

%P1=[4 -1 72 0 4 1;1 -22 0 72 -1 -22];
%P2=[-18 13 -44 0 -18 -13;13 -18 0 8 -13 -18];
P1=[k(7,1) k(7,2) k(7,7)+k(1,1) k(7,8)+k(1,2) k(1,7) k(1,8);k(8,1) k(8,2)
k(8,7)+k(2,1) k(8,8)+k(2,2) k(2,7) k(2,8)];
P2=[k(7,3) k(7,4) k(7,5)+k(1,3) k(7,6)+k(1,4) k(1,5) k(1,6);k(8,3) k(8,4)
k(7,6)+k(1,4) k(8,6)+k(2,4) k(1,6) k(2,6)];
for i=3:2:(nline*2)-1 % Sarebbe da sistemare!!!
    kk(i:i+1,i-2:i+3)=P1;
    kk(i:i+1,i+S:i+S+5)=P2;
end

```

```

% Lato destro

```

```

%P1=[-18 -13 -44 0 -18 13;-13 -18 0 8 13 -18];
%P2=[4 1 72 0 4 -1;-1 -22 0 72 1 -22];
P1=[k(5,1) k(5,2) k(5,7)+k(3,1) k(5,8)+k(3,2) k(3,7) k(3,8);k(6,1) k(6,2)
k(6,7)+k(4,1) k(6,8)+k(4,2) k(4,7) k(4,8)];
P2=[k(5,3) k(5,4) k(5,5)+k(3,3) k(5,6)+k(3,4) k(3,5) k(3,6);k(6,3) k(6,4)
k(6,5)+k(4,3) k(6,6)+k(4,4) k(4,5) k(4,6)];
for i=((nline+1)*ncolumn+2)*2-1:2:((nline+1)*(ncolumn+1)-1)*2-1
    kk(i:i+1,i-2:i+3)=P2;
    kk(i:i+1,i-S-4:i-S+1)=P1;
end

```

```

% Lato inferiore

```

```

%P1=[-22 1 -18 13;-1 4 13 -18];
%P2=[72 0 8 0;0 72 0 -44];
%P3=[-22 -1 -18 -13;1 4 -13 -18];
P1=[k(3,1) k(3,2) k(3,7) k(3,8);k(4,1) k(4,2) k(4,7) k(4,8)];
P2=[k(3,3)+k(1,1) k(3,4)+k(1,2) k(3,5)+k(1,7) k(3,6)+k(1,8);k(4,3)+k(2,1)
k(4,4)+k(2,2) k(4,5)+k(2,7) k(4,6)+k(2,8)];
P3=[k(1,3) k(1,4) k(1,5) k(1,6);k(2,3) k(2,4) k(2,5) k(2,6)];

```

```

% S=nline*2!!!

```

```

for i=(nline+2)*2-1:(nline+1)*2:((nline+2)+(nline+1)*(ncolumn-2))*2-1;
    if i==(nline+2)*2-1
        kk(i:i+1,i-2:i-1)=zeros(2,2);
    end
end

```

```

        kk(i:i+1,i+S:i+S+1)=zeros(2,2);
    else
        kk(i:i+1,i-S-4:i-S-3)=zeros(2,2);
        kk(i:i+1,i-2:i-1)=zeros(2,2);
        kk(i:i+1,i+S:i+S+1)=zeros(2,2);
    end

    kk(i:i+1,i-(nline+1)*2:i-(nline+1)*2+3)=P1;
    kk(i:i+1,i:i+3)=P2;
    kk(i:i+1,i+(nline+1)*2:i+(nline+1)*2+3)=P3;
end

% Lato superiore

P1=[-18 -13 -22 -1;-13 -18 1 4];
P2=[8 0 72 0;0 -44 0 72];
P3=[-18 13 -22 1;13 -18 -1 4];
P1=[k(5,1) k(5,2) k(5,7) k(5,8);k(6,1) k(6,2) k(6,7) k(6,8)];
P2=[k(5,3)+k(7,1) k(7,2)+k(5,4) k(5,5)+k(7,7) k(5,6)+k(7,8); k(6,3)+k(8,1)
k(6,4)+k(8,2) k(6,5)+k(8,7) k(6,6)+k(8,8)];
P3=[k(7,3) k(7,4) k(7,5) k(7,6);k(8,3) k(8,4) k(8,5) k(8,6)];

for i=((nline+1)*2)*2-1:(nline+1)*2:(((nline+1)*2)+(nline+1)*(ncolumn-
2))*2-1
    if i~=((nline+1)*2)+(nline+1)*(ncolumn-2))*2-1
        kk(i:i+1,i-S:i-S+1)=zeros(2,2);
        kk(i:i+1,i+2:i+3)=zeros(2,2);
        kk(i:i+1,i+S+4:i+S+5)=zeros(2,2);
    else
        kk(i:i+1,i-S:i-S+1)=zeros(2,2);
        kk(i:i+1,i+2:i+3)=zeros(2,2);
    end

    kk(i:i+1,i-(nline+2)*2:i-(nline+2)*2+3)=P1;
    kk(i:i+1,i-2:i+1)=P2;
    kk(i:i+1,i+nline*2:i+nline*2+3)=P3;
end

%Vertice inferiore sinistro
P1=[36 13 4 1;13 36 -1 -22];
P2=[-22 -1 -18 -13;1 4 -13 -18];
P1=[k(1,1) k(1,2) k(1,7) k(1,8);k(2,1) k(2,2) k(2,7) k(2,8)];
P2=[k(1,3) k(1,4) k(1,5) k(1,6);k(2,3) k(2,4) k(2,5) k(2,6)];

kk(1:2,:)=zeros(2,sdof);
kk(1:2,1:4)=P1;
kk(1:2,(1+nline+1)*2-1:(1+nline+1)*2+2)=P2;

% Vertice superiore destro
P1=[-18 -13 -22 -1;-13 -18 1 4];
P2=[4 1 36 13;-1 -22 13 36];
P1=[k(5,1) k(5,2) k(5,7) k(5,8);k(6,1) k(6,2) k(6,7) k(6,8)];
P2=[k(5,3) k(5,4) k(5,5) k(5,6);k(6,3) k(6,4) k(6,5) k(6,6)];

kk(sdof-1:sdof,:)=zeros(2,sdof);

```

```

kk(s dof-1:sdof,((nline+1)*(ncolumn+1)-(nline+2))*2-
1:((nline+1)*(ncolumn+1)-(nline+2))*2+2)=P1;
kk(s dof-1:sdof,s dof-3:sdof)=P2;

% Vertice superiore sinistro
%P1=[4 -1 36 -13;1 -22 -13 36];
%P2=[-18 13 -22 1;13 -18 -1 4];
P1=[k(7,1) k(7,2) k(7,7) k(7,8);k(8,1) k(8,2) k(8,7) k(8,8)];
P2=[k(7,3) k(7,4) k(7,5) k(7,6);k(8,3) k(8,4) k(8,5) k(8,6)];

kk((nline+1)*2-1:(nline+1)*2,:)=zeros(2,s dof);
kk((nline+1)*2-1:(nline+1)*2,nline*2-1:nline*2+2)=P1;
kk((nline+1)*2-1:(nline+1)*2,(2*nline+1)*2-1:(2*nline+1)*2+2)=P2;

% Vertice inferiore destro
%P1=[-22 1 -18 13;-1 4 13 -18];
%P2=[36 -13 4 -1;-13 36 1 -22];
P1=[k(3,1) k(3,2) k(3,7) k(3,8);k(4,1) k(4,2) k(4,7) k(4,8)];
P2=[k(3,3) k(3,4) k(3,5) k(3,6);k(4,3) k(4,4) k(4,5) k(4,6)];

kk(((nline+1)*ncolumn+1)*2-1:((nline+1)*ncolumn+1)*2,:)=zeros(2,s dof);
kk(((nline+1)*ncolumn+1)*2-1:((nline+1)*ncolumn+1)*2,((nline+1)*(ncolumn-
1)+1)*2-1:((nline+1)*(ncolumn-1)+1)*2+2)=P1;
kk(((nline+1)*ncolumn+1)*2-
1:((nline+1)*ncolumn+1)*2,((nline+1)*ncolumn+1)*2-
1:((nline+1)*ncolumn+1)*2+2)=P2;

out=kk;

%k11=k(1:2,1:2);
%k21=k(3:4,1:2);
%k31=k(5:6,1:2);
%k41=k(7:8,1:2);

%k12=k21 %k(1:2,3:4); %sym
%k22=k(3:4,3:4);
%k32=k(5:6,3:4);
%k42=k(7:8,3:4);

%k13=k31 %k(1:2,5:6); %sym
%k23=k32 %k(3:4,5:6); %sym
%k33=k(5:6,5:6);
%k43=k(7:8,5:6);

%k14=k41 %k(1:2,7:8); %sym
%k24=k42 %k(3:4,7:8); %sym
%k34=k43 %k(5:6,7:8); %sym
%k44=k(7:8,7:8);

```

NODESINEL

```
function out = NODESINELEM(nel);
```

```

% returns a row vector with the nodes contained in the element nel

global nline ncolumn

addme = floor((nel-1)/nline);

out = addme + nel + [0, nline + 1, nline + 2, 1];

```

RIGEL

```

%-----
% Matrice di rigidezza dell'elemento (quadrato a 4 nodi)
%-----

function out=RIGEL(MAT)

% MAT=[E1,E2,n,G12]

global a b

matmtx=femataniso(MAT(1),MAT(2),MAT(3),MAT(4));           % compute
%constitutive matrix
%matmtx=fematiso(planeopt,emodule,poisson);

% Matrici S

S11=b/(6*a)*[2 -2 -1 1;-2 2 1 -1;-1 1 2 -2;1 -1 -2 2];
S12=1/4*[1 1 -1 -1;-1 -1 1 1;-1 -1 1 1;1 1 -1 -1];
S22=a/(6*b)*[2 1 -1 -2;1 2 -2 -1;-1 -2 2 1;-2 -1 1 2];

% Matrici K da permutare

K11=matmtx(1,1)*S11+matmtx(3,3)*S22;
K12=matmtx(1,2)*S12+matmtx(3,3)*S12';
K22=matmtx(3,3)*S11+matmtx(2,2)*S22;

% Matrice di permutazione

P=zeros(8,8);
P(1,1)=1;
P(2,3)=1;
P(3,5)=1;
P(4,7)=1;
P(5,2)=1;
P(6,4)=1;
P(7,6)=1;
P(8,8)=1;

```

```
% Matrice di rigidezza dell'elemento
```

```
out=P'*[K11 K12;K12' K22]*P;
```

ASSDSSXDX

```
% -----  
% Assemblaggio a mano della matrice di rigidezza  
% per una griglia omogenea di elementi quadrati  
% Griglia quadrata o rettangolare  
% -----  
  
function out=ASSDSSXDX(k)  
  
global nline ncolumn sdof  
  
% H > L  
% nline = Linee della griglia globale  
% ncolumn = Colonne della griglia globale  
  
lin=nline; % linee di metà griglia  
col=ncolumn/2; % colonne di metà griglia  
dimkkSX=(lin+1)*(col+1)*2; % dimensioni matrice  
  
% Blocchi della matrice di rigidezza dell'elemento  
  
k11=k(1:2,1:2);  
k21=k(3:4,1:2);  
k31=k(5:6,1:2);  
k41=k(7:8,1:2);  
  
k12=k(1:2,3:4);  
k22=k(3:4,3:4);  
k32=k(5:6,3:4);  
k42=k(7:8,3:4);  
  
k13=k(1:2,5:6);  
k23=k(3:4,5:6);  
k33=k(5:6,5:6);  
k43=k(7:8,5:6);  
  
k14=k(1:2,7:8);  
k24=k(3:4,7:8);  
k34=k(5:6,7:8);  
k44=k(7:8,7:8);  
  
% NODI CENTRALI  
kkSX=sparse(dimkkSX,dimkkSX); % system matrix as a SPARSE matrix
```

```

% i = numero nodo della colonna centrale
for j=1:(col-1)
for i=(lin+1)*j+2:((lin+1)*(1+j)-1)
kkSX((i*2)-1:(i*2),(i-lin-2)*2-1:(i-lin-2)*2)=k31;
kkSX((i*2)-1:(i*2),(i-lin-1)*2-1:(i-lin-1)*2)=k34+k21;
kkSX((i*2)-1:(i*2),(i-1)*2-1:(i-1)*2)=k32+k41;
kkSX((i*2)-1:(i*2),(i*2)-1:(i*2))=k33+k44+k11+k22;
kkSX((i*2)-1:(i*2),(i-lin)*2-1:(i-lin)*2)=k24;
kkSX((i*2)-1:(i*2),(i+1)*2-1:(i+1)*2)=k23+k14;
kkSX((i*2)-1:(i*2),(i+lin+2)*2-1:(i+lin+2)*2)=k13;
kkSX((i*2)-1:(i*2),(i+lin+1)*2-1:(i+lin+1)*2)=k12+k43;
kkSX((i*2)-1:(i*2),(i+lin)*2-1:(i+lin)*2)=k42;
end
end

```

```

% LATO INFERIORE

```

```

for i=lin+2:(lin+1):(lin+1)*(col-1)+1
kkSX(2*i-1:2*i,(i-lin-1)*2-1:(i-lin-1)*2)=k21;
kkSX(2*i-1:2*i,(i-lin)*2-1:(i-lin)*2)=k24;
kkSX(2*i-1:2*i,2*i-1:2*i)=k22+k11;
kkSX(2*i-1:2*i,2*(i+1)-1:2*(i+1))=k23+k14;
kkSX(2*i-1:2*i,(i+lin+1)*2-1:(i+lin+1)*2)=k12;
kkSX(2*i-1:2*i,(i+lin+2)*2-1:(i+lin+2)*2)=k13;
end

```

```

% LATO SUPERIORE

```

```

for i=(lin+1)*2:(lin+1):(lin+1)*col
kkSX(2*i-1:2*i,(i-lin-1)*2-1:(i-lin-1)*2)=k34;
kkSX(2*i-1:2*i,(i-lin-2)*2-1:(i-lin-2)*2)=k31;
kkSX(2*i-1:2*i,2*i-1:2*i)=k33+k44;
kkSX(2*i-1:2*i,2*(i-1)-1:2*(i-1))=k32+k41;
kkSX(2*i-1:2*i,(i+lin+1)*2-1:(i+lin+1)*2)=k43;
kkSX(2*i-1:2*i,(i+lin)*2-1:(i+lin)*2)=k42;
end

```

```

% LATO SINISTRO

```

```

for i=2:lin
kkSX(2*i-1:2*i,2*(i-1)-1:2*(i-1))=k41;
kkSX(2*i-1:2*i,2*i-1:2*i)=k44+k11;
kkSX(2*i-1:2*i,2*(i+1)-1:2*(i+1))=k14;
kkSX(2*i-1:2*i,2*(i+lin)-1:2*(i+lin))=k42;
kkSX(2*i-1:2*i,2*(i+lin+1)-1:2*(i+lin+1))=k43+k12;
kkSX(2*i-1:2*i,2*(i+lin+2)-1:2*(i+lin+2))=k13;
end

```

```

%LATO DESTRO

```

```

for i=(lin+1)*col+2:(lin+1)*col+lin
kkSX(2*i-1:2*i,2*(i-lin-2)-1:2*(i-lin-2))=k31;
kkSX(2*i-1:2*i,2*(i-lin-1)-1:2*(i-lin-1))=k34+k21;
kkSX(2*i-1:2*i,2*(i-lin)-1:2*(i-lin))=k24;
kkSX(2*i-1:2*i,2*(i-1)-1:2*(i-1))=k32;
kkSX(2*i-1:2*i,2*i-1:2*i)=k33+k22;
kkSX(2*i-1:2*i,2*(i+1)-1:2*(i+1))=k23;
end

```

```

% VERTICE INFERIORE SINISTRO

VIS=1;

kkSX(2*VIS-1:2*VIS,2*VIS-1:2*VIS)=k11;
kkSX(2*VIS-1:2*VIS,2*(VIS+1)-1:2*(VIS+1))=k14;
kkSX(2*VIS-1:2*VIS,2*(VIS+lin+1)-1:2*(VIS+lin+1))=k12;
kkSX(2*VIS-1:2*VIS,2*(VIS+lin+2)-1:2*(VIS+lin+2))=k13;

% VERTICE SUPERIORE SINISTRO

VSS=lin+1;

kkSX(2*VSS-1:2*VSS,2*(VSS-1)-1:2*(VSS-1))=k41;
kkSX(2*VSS-1:2*VSS,2*VSS-1:2*VSS)=k44;
kkSX(2*VSS-1:2*VSS,2*(VSS+lin)-1:2*(VSS+lin))=k42;
kkSX(2*VSS-1:2*VSS,2*(VSS+lin+1)-1:2*(VSS+lin+1))=k43;

% VERTICE INFERIORE DESTRO

VID=(lin+1)*col+1;

kkSX(2*VID-1:2*VID,2*(VID-lin-1)-1:2*(VID-lin-1))=k21;
kkSX(2*VID-1:2*VID,2*(VID-lin)-1:2*(VID-lin))=k24;
kkSX(2*VID-1:2*VID,2*VID-1:2*VID)=k22;
kkSX(2*VID-1:2*VID,2*(VID+1)-1:2*(VID+1))=k23;

% VERTICE SUPERIORE DESTRO

VSD=(lin+1)*(col+1);

kkSX(2*VSD-1:2*VSD,2*(VSD-lin-2)-1:2*(VSD-lin-2))=k31;
kkSX(2*VSD-1:2*VSD,2*(VSD-lin-1)-1:2*(VSD-lin-1))=k34;
kkSX(2*VSD-1:2*VSD,2*(VSD-1)-1:2*(VSD-1))=k32;
kkSX(2*VSD-1:2*VSD,2*VSD-1:2*VSD)=k33;

out=kkSX;

```

ASSDSCC

```

% -----
% Assemblaggio a mano della matrice di rigidezza
% per una griglia omogenea di elementi quadrati
% Griglia quadrata o rettangolare
% -----

function out=ASSDSCC(k1,k2)

global nline ncolumn sdof

```

```

L=nline;
C=2;

% Blocchi prima matrice

k111=k1(1:2,1:2);
k121=k1(3:4,1:2);
k131=k1(5:6,1:2);
k141=k1(7:8,1:2);

k112=k1(1:2,3:4);
k122=k1(3:4,3:4);
k132=k1(5:6,3:4);
k142=k1(7:8,3:4);

k113=k1(1:2,5:6);
k123=k1(3:4,5:6);
k133=k1(5:6,5:6);
k143=k1(7:8,5:6);

k114=k1(1:2,7:8);
k124=k1(3:4,7:8);
k134=k1(5:6,7:8);
k144=k1(7:8,7:8);

%Blocchi seconda matrice

k211=k2(1:2,1:2);
k221=k2(3:4,1:2);
k231=k2(5:6,1:2);
k241=k2(7:8,1:2);

k212=k2(1:2,3:4);
k222=k2(3:4,3:4);
k232=k2(5:6,3:4);
k242=k2(7:8,3:4);

k213=k2(1:2,5:6);
k223=k2(3:4,5:6);
k233=k2(5:6,5:6);
k243=k2(7:8,5:6);

k214=k2(1:2,7:8);
k224=k2(3:4,7:8);
k234=k2(5:6,7:8);
k244=k2(7:8,7:8);

% NODI CENTRALI
kkDS=sparse((L+1)*(C+1)*2,(L+1)*(C+1)*2); % system matrix as a SPARSE
matrix

% i = numero nodo della colonna centrale

for i=((L+1)*(C/2))+2:(L+1)*C/2+L
kkDS((i*2)-1:(i*2),(i-L-2)*2-1:(i-L-2)*2)=k131;
kkDS((i*2)-1:(i*2),(i-L-1)*2-1:(i-L-1)*2)=k134+k121;
kkDS((i*2)-1:(i*2),(i-1)*2-1:(i-1)*2)=k132+k241;

```

```

kkDS((i*2)-1:(i*2),(i*2)-1:(i*2))=k133+k244+k211+k122;
kkDS((i*2)-1:(i*2),(i-L)*2-1:(i-L)*2)=k124;
kkDS((i*2)-1:(i*2),(i+1)*2-1:(i+1)*2)=k123+k214;
kkDS((i*2)-1:(i*2),(i+L+2)*2-1:(i+L+2)*2)=k213;
kkDS((i*2)-1:(i*2),(i+L+1)*2-1:(i+L+1)*2)=k212+k243;
kkDS((i*2)-1:(i*2),(i+L)*2-1:(i+L)*2)=k242;
end

% NODO INFERIORE della colonna centrale

NI=((L+1)*(C/2)+1);

kkDS(2*NI-1:2*NI,(NI-L-1)*2-1:(NI-L-1)*2)=k121;
kkDS(2*NI-1:2*NI,(NI-L)*2-1:(NI-L)*2)=k124;
kkDS(2*NI-1:2*NI,2*NI-1:2*NI)=k122+k211;
kkDS(2*NI-1:2*NI,2*(NI+1)-1:2*(NI+1))=k123+k214;
kkDS(2*NI-1:2*NI,(NI+L+1)*2-1:(NI+L+1)*2)=k212;
kkDS(2*NI-1:2*NI,(NI+L+2)*2-1:(NI+L+2)*2)=k213;

% NODO SUPERIORE della colonna centrale

NS=(L+1)*(C/2+1);

kkDS(2*NS-1:2*NS,(NS-L-1)*2-1:(NS-L-1)*2)=k134;
kkDS(2*NS-1:2*NS,(NS-L-2)*2-1:(NS-L-2)*2)=k131;
kkDS(2*NS-1:2*NS,2*NS-1:2*NS)=k133+k244;
kkDS(2*NS-1:2*NS,2*(NS-1)-1:2*(NS-1))=k132+k241;
kkDS(2*NS-1:2*NS,(NS+L+1)*2-1:(NS+L+1)*2)=k243;
kkDS(2*NS-1:2*NS,(NS+L)*2-1:(NS+L)*2)=k242;

%kkDS((nline+1)*ncolumn/2+(nline+2))*2-1:sdof,:)=zeros(sdof-
(nline+1)*(ncolumn/2+1)*2,sdof); % Completamento di kk3 per renderla
quadrata

out=kkDS;

```

The script used to evaluate the parameters of cell migration (MSD, angles) are reported:

MSD_ANGLE_3

```

close all
clear all
clc

[FileName,PathName]=uigetfile({'*.txt;*.log','Path coordinates (*.txt,
*.log)';'*.*', 'All Files (*.*)'},'Choose file(s)', 'MultiSelect', 'on');
FL=sort(FileName);
M=size(FL,2);

for j=1:M
    b(:, :, j)=load(FL{j});

```

```

end

prompt = {'Enter time interval [min]:','Enter objective lens (4 or 10):'};
dlg_title = 'Input';
num_lines = 1;
def = {'10','4'};
answer = inputdlg(prompt,dlg_title,num_lines,def);
Deltat=str2num(answer{1});

if answer{2}=='10';
    scalefactor=0.97;
elseif answer{2}=='4';
    scalefactor=2.28;
else
    scalefactor=1;
end

b=scalefactor*(b);
clear scalefactor;

Sz=size(b);
N=Sz(1);
n=Sz(2);

clear j

sispx=[];
sispy=[];

for j=1:M;
    for i=1:N-1;
        for k=1:N-i;
            dispk(k)=(b(k+i,1,j)-b(k,1,j));
            dispyk(k)=(b(k+i,2,j)-b(k,2,j));

            end
            Disp(i,j)=(1/(N-i))*sum(dispk);
            Dispy(i,j)=(1/(N-i))*sum(dispyk);

            Sisp(i,j)=(1/(i*Deltat))*Disp(i,j);
            Sisy(i,j)=(1/(i*Deltat))*Dispy(i,j);

            clear dispk;
            clear dispyk;

        end
    end

end

sispx=mean(Sisp,1);
sispy=mean(Sisy,1);

hx=ttest(sispx)';
hy=ttest(sispy)';

if hx==0
    Sbiasx=0;
else

```

```

        Sbiasx=mean(sispx);
        clear hx;
    end

if hy==0
    Sbiasy=0;
else
    Sbiasy=mean(sispy);
    clear hy;
end

for j=1:M;
    for i=1:N-1;
        for k=1:N-i;
            dk(k)=(b(k+i,1,j)-i*Deltat*Sbiasx-b(k,1,j))^2+(b(k+i,2,j)-
i*Deltat*Sbiasy-b(k,2,j))^2);
            dkk(k)=(b(k+i,1,j)-b(k,1,j))^2+(b(k+i,2,j)-b(k,2,j))^2);
        end
        Dk(i,j)=(1/(N-i))*sum(dk);
        Dkk(i,j)=(1/(N-i))*sum(dkk);
        Sk(i,j)=(Dk(i,j))/(Deltat*i)^2)^0.5;
        Skk(i,j)=(Dkk(i,j))/(Deltat*i)^2)^0.5;
        clear dk;
        clear dkk;
    end
end

%attenzione alla definizione di Sk. Mi sembra più un contributo random...

clear i
clear j
clear k

CumSk=cumsum(Sk.^2);

for j=1:M;
for i=1:N-1;
    Zk(i,j)=Dk(i,j)/(n*CumSk(i,j));
end
end

Di=mean(Dk,2);
StDi=std(Dk,0,2);

Si=mean(Sk,2);
StSi=std(Sk,0,2);

Stoti=mean(Skk,2);
StStoti=std(Skk,0,2);

Diplus=Di+StDi;
Dimenus=Di-StDi;

Siplus=Si+StSi;
Simenus=Si-StSi;

```

```

Stotiplus=Stoti+StStoti;
Stotimenu=Stoti-StStoti;

Zi=mean(Zk,2);
StZi=std(Zk,0,2);

Ziplus=Zi+StZi;
Zimenu=Zi-StZi;

for j=1:M;
    l(j)=norm(b(N,:,j)-b(1,:,j));
    for i=1:N-1
        disp(i,j)=norm(b(i+1,:,j)-b(i,:,j));
    end
    cumdisp=cumsum(disp);
    J(j)=l(j)/((cumdisp(N-1,j)));
end

clear i
clear j

I=1
%A=floor((N-1)/I);
A=N-I;
v=[1 0];

for j=1:M;
    for k=1:A;
        %h=1+I*(k-1);
        %g=I*k+1;
        %u(k,:)=(b(g,:,j)-b(h,:,j));
        u(k,:)=(b(k+I,:,j)-b(k,:,j));
        %clear h
        %clear g
    end

    for h=1:A-1;

alpha(h,j)=acosd(dot(u(h,:),u(h+1,:))/(norm(u(h,:))*norm(u(h+1,:))));
    phi(h,j)=acosd(dot(u(h,:),v)/(norm(u(h,:))*norm(v)));
    end
    clear u
end

clear j

pimezzi=0:10:170;
h=size(pimezzi,2);
W=alpha(:,1);
Q=phi(:,1);

for i=2:M
    W=[W; alpha(:,i)];
    Q=[Q; phi(:,i)];
end

[nalpha xalpha]=hist(W,h);

```

```

[nphi yphi]=hist(Q,h);

Ax=1/(trapz(xalpha,nalpha));
Ay=1/(trapz(yphi,nphi));

%%%%%%%%%%%%%%
%% PICTURES %%
%%%%%%%%%%%%%%
%
% figure
% hist(W,pimezzi)
% title('angle between adjacent vectors')
% xlim([0 180]);
%
% figure
% hist(Q,pimezzi)
% title('angle resp vert axis')
% xlim([0 180]);

% [nw,xw]=hist(W,pimezzi);
% [nq,xq]=hist(Q,pimezzi);
%
% nw=nw/M;
% nq=nq/M;

tln=input('   inserire nome esperimento   ')

figure
AA=bar(pimezzi,Ax*nalpha)
title('angle between consecutive steps')
xlim([0 180]); ylim([0 0.05]);

figure
AV=bar(pimezzi,Ay*nphi,'r')
title('angle resp x axis')
xlim([0 180]); ylim([0 0.01]);

figure
plot(1:N-1,Di,'o',1:N-1,Diplus,1:N-1,Dimenus)
title('msd')

figure
hold on
for j=1:M
    loglog(1:N-1,Dk(:,j))
    lbl=FL{j};
    text(N-1,Dk(N-1,j),lbl);
    clear lbl
end
title('mean squared displacement')
hold off

figure
hold on
for j=1:M
    plot(b(:,1,j),b(:,2,j))
    lbl=FL{j};

```

```

    text(b(N,1,j),b(N,2,j),lbl);
    clear lbl
end
hold off

figure
hold on
for j=1:M
    PATH=plot(b(:,1,j)-b(1,1,j),b(:,2,j)-b(1,2,j));
end
xlim([-300 300])
ylim([-300 300])
hold off

figure
plot(1:N-1,Si,'x',1:N-1,Siplus,1:N-1,Simenus)
title('speed')

speedmeanres=Si(I)
speedstdres=StSi(I)

speedTOTmeanres=Stoti(I)
speedTOTstdres=StStoti(I)

%disp(' J ')
Jmeanres=(mean(J))
Jstdres=(std(J))

%disp(' Sbiasx ')
Sbiasx

%disp(' Sbiasy ')
Sbiasy

RES=[];

RES(1)=speedTOTmeanres';
RES(2)=speedTOTstdres';
RES(3)=Sbiasx';
RES(4)=Sbiasy';
RES(5)=Jmeanres';
RES(6)=Jstdres';

I=num2str(I)
res='res_';
flnm=strcat(res,'@',I,tln);
xlswrite(flnm, RES)

tlnAA=strcat('AA_',I,'_',tln);
saveas(AA,tlnAA,'m');
saveas(AA,tlnAA,'bmp');

tlnAV=strcat('AV_',I,'_',tln);
saveas(AV,tlnAV,'m');
saveas(AV,tlnAV,'bmp');

```

```
tlnPATH=strcat('Path','_',tln);  
saveas(PATH,tlnPATH,'m');  
saveas(PATH,tlnPATH,'bmp');
```